Searches for third-generation scalar leptoquarks in s√s = 13 TeV *pp* collisions with the ATLAS detector

Aaboud, M., Aad, G., Abbott, B., Abbot, D. C., Abdinbov, O., Abhayasinghe, D. K., … Zwalinksi, L.

2019.

Published for SISSA by Springer

Received: *February 22, 2019*
Revised: *June 11, 2019*
Accepted: *June 17, 2019*
Published: *June 28, 2019*

Searches for third-generation scalar leptoquarks in $\sqrt{s} = 13$ TeV pp collisions with the ATLAS detector

The ATLAS collaboration

E-mail: atlas.publications@cern.ch

Abstract: Limits are set on the pair production of scalar leptoquarks, where all possible decays of the leptoquark into a quark (t, b) and a lepton (τ, ν) of the third generation are considered. The limits are presented as a function of the leptoquark mass and the branching ratio into charged leptons for up-type ($\mathrm{LQ}_3^{\mathrm{u}} \to t\nu/b\tau$) and down-type ($\mathrm{LQ}_3^{\mathrm{d}} \to b\nu/t\tau$) leptoquarks. Many results are reinterpretations of previously published ATLAS searches. In all cases, LHC proton-proton collision data at a centre-of-mass energy of $\sqrt{s} = 13$ TeV recorded by the ATLAS detector in 2015 and 2016 are used, corresponding to an integrated luminosity of 36.1 fb^{-1}. Masses below 800 GeV are excluded for both $\mathrm{LQ}_3^{\mathrm{u}}$ and $\mathrm{LQ}_3^{\mathrm{d}}$ independently of the branching ratio, with masses below about 1 TeV being excluded for the limiting cases of branching ratios equal to zero or unity.

Keywords: Hadron-Hadron scattering (experiments)

ArXiv ePrint: 1902.08103

https://doi.org/10.1007/JHEP06(2019)144

JHEP06(2019)144

Contents

1 Introduction 1

2 ATLAS detector 3

3 Signal simulation 3

4 The $b\tau b\tau$ channel 4

5 The tt plus $E_{\mathrm{T}}^{\mathrm{miss}}$ channel with one lepton 13

6 The tt plus $E_{\mathrm{T}}^{\mathrm{miss}}$ channel with zero leptons 16

7 The $\tau\tau b$ plus $E_{\mathrm{T}}^{\mathrm{miss}}$ channel 17

8 The bb plus $E_{\mathrm{T}}^{\mathrm{miss}}$ channel 22

9 Limits on the LQ mass as a function of B 25

10 Conclusion 27

The ATLAS collaboration 31

JHEP06(2019)144

1 Introduction

Leptoquarks (LQ) are predicted by many extensions [1–7] of the Standard Model (SM) and provide a connection between the quark and lepton sectors, which exhibit a similar structure in the SM. Also, recent hints of a potential violation of lepton universality in measurements of B-meson decays can be attributed, if confirmed, to the exchange of LQs [8–14]. LQs are bosons carrying colour and fractional electrical charge. They possess non-zero baryon and lepton numbers and decay into a quark-lepton pair. Leptoquarks can be scalar or vector bosons and can be produced singly or in pairs in proton-proton collisions.

This analysis focuses on the pair-production of third-generation scalar leptoquarks, i.e. LQs that decay into third-generation SM particles. The assumption that LQs can only interact with leptons and quarks of the same family follows the minimal Buchmüller-Rückl-Wyler model [15], which is the benchmark model used in this analysis. The LQs couple to the quark-lepton pair via a Yukawa interaction. The couplings are determined by two parameters: a model parameter β and the coupling parameter λ. The coupling to the charged lepton (τ) is given by $\sqrt{\beta}\lambda$, and the coupling to the τ-neutrino ν by $\sqrt{1-\beta}\lambda$. The search is carried out for an up-type ($\mathrm{LQ}_3^{\mathrm{u}} \to t\nu/b\tau$) and a down-type ($\mathrm{LQ}_3^{\mathrm{d}} \to b\nu/t\tau$) leptoquark.

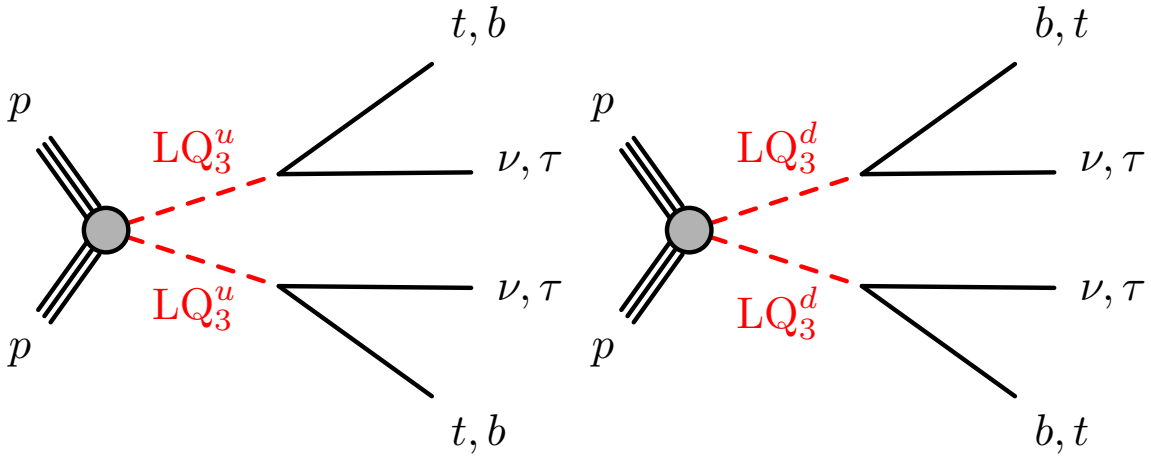

Figure 1. Pair production and decay of $\mathrm{LQ}_3^{\mathrm{u}}$ and $\mathrm{LQ}_3^{\mathrm{d}}$.

The LQ model is identical to the one used for a recent ATLAS search for first- and second-generation scalar LQs using the dataset from 2015 and 2016, consisting of 36.1 fb^{-1} of data taken at $\sqrt{s} = 13\,\mathrm{TeV}$ [16]. In the following, the third-generation results are presented for that same dataset, where all possible decays of the pair-produced $\mathrm{LQ}_3^{\mathrm{u}}$ and $\mathrm{LQ}_3^{\mathrm{d}}$ into a quark (t, b) and a lepton (τ, ν) of the third generation are considered. The results are presented as a function of the leptoquark mass and the branching ratio (B) into charged leptons, in contrast to using mass and β as done for the first and second generations. This is due to the fact that β is not equal to the branching ratio for third-generation LQs due to the sizeable top-quark mass. Previous ATLAS results for third-generation LQs for the case $B = 0$ for both $\mathrm{LQ}_3^{\mathrm{u}}$ and $\mathrm{LQ}_3^{\mathrm{d}}$ used the $\sqrt{s} = 8\,\mathrm{TeV}$ dataset from 2012 [17]. The most recent CMS results are based on the 2016 dataset targeting $B = 0$ for both $\mathrm{LQ}_3^{\mathrm{u}}$ and $\mathrm{LQ}_3^{\mathrm{d}}$ [18] as well as $B = 1$ for $\mathrm{LQ}_3^{\mathrm{u}}$ [19] and $\mathrm{LQ}_3^{\mathrm{d}}$ [20].

The results presented here are from a dedicated LQ search based on a search for pair-produced Higgs bosons decaying into two b-jets and two τ-leptons [21], where the search is optimized for the $\mathrm{LQ}_3^{\mathrm{u}}$ pair production with $B \approx 1$, and four reinterpretations of ATLAS searches for supersymmetric particles. Supersymmetric particles can have similar or even identical experimental signatures and very similar kinematics to pair-produced LQs. Pair production of the supersymmetric partner of the top (bottom) quark, known as the top (bottom) squark, has the same experimental signature of a $t\bar{t}$-pair ($b\bar{b}$-pair) and missing transverse momentum as $\mathrm{LQ}_3^{\mathrm{u}}$ ($\mathrm{LQ}_3^{\mathrm{d}}$) pair production with $B = 0$ (see figure 1). Hence, the ATLAS searches for top squarks in final states with one [22] or zero [23] leptons and for bottom squarks [24] are optimal when searching for $\mathrm{LQ}_3^{\mathrm{u}}$ and $\mathrm{LQ}_3^{\mathrm{d}}$ with $B = 0$, respectively. The final state of two τ-leptons, b-jets, and missing transverse momentum is targeted in another top-squark pair-production search [25] and is expected to be sensitive to medium and high branching ratios into charged leptons. For all analyses, the results are presented as a function of B and the leptoquark mass for both $\mathrm{LQ}_3^{\mathrm{u}}$ and $\mathrm{LQ}_3^{\mathrm{d}}$.

The paper is structured as follows. After a brief description of the ATLAS detector, the Monte Carlo (MC) simulations of LQ pair production are discussed. This is followed by

JHEP06(2019)144

a description of the five analyses, starting with the dedicated search for two b-jets and two τ-leptons. Four brief sections describe the reinterpretations of searches for supersymmetric particles, as the published analyses are not modified for this reinterpretation. Each of the five analysis sections finish with cross-section and mass limits for a fixed value of B to which the analysis is particularly sensitive. Finally, the results of all analyses are presented as a function of B and leptoquark mass.

2 ATLAS detector

The ATLAS detector [26] is a multipurpose particle detector at the LHC with nearly 4π coverage around the collision point.[1] Closest to the beam is the inner detector, which provides charged-particle tracking in the range $|\eta| < 2.5$. During the LHC shutdown between Run 1 and Run 2, a new innermost layer of silicon pixels was added, which improves the track impact parameter resolution and vertex position resolution [27–29]. The inner detector is surrounded by a superconducting solenoid providing a 2 T axial magnetic field, followed by a lead/liquid-argon electromagnetic sampling calorimeter and a steel/scintillator-tile hadronic calorimeter. The endcap and forward regions are instrumented with liquid-argon calorimeters for both the electromagnetic and hadronic energy measurements up to $|\eta| = 4.9$. The outer part of the detector consists of a muon spectrometer with high-precision tracking chambers for coverage up to $|\eta| = 2.7$, fast detectors for triggering over $|\eta| < 2.4$, and three large superconducting toroidal magnets with eight coils each. Events are selected by a two-level trigger system consisting of a hardware-based trigger for the first level and a software-based system for the second level [30].

3 Signal simulation

Signal samples were generated at next-to-leading order (NLO) in QCD with MadGraph5_aMC@NLO 2.4.3 [31], using the LQ model of ref. [32] that adds parton showers to previous fixed-order NLO OCD calculations [33], and the NNPDF 3.0 NLO [34] parton distribution functions (PDF), interfaced with Pythia 8.212 [35] using the A14 set of tuned parameters [36] for the parton shower and hadronization. The leptoquark signal production cross-sections are taken from calculations [37] of direct top-squark pair production, as both are massive, coloured, scalar particles with the same production modes. The calculations are at NLO plus next-to-leading-logarithm accuracy, with uncertainties determined by variations of factorization and renormalization scales, α_s, and PDF variations.

Madspin [38] was used for the decay of the LQ. The parameter λ was set to 0.3, resulting in a LQ width of about 0.2% of its mass [15, 39]. The samples were produced for a model parameter of $\beta = 0.5$, where desired branching ratios B were obtained by

[1] ATLAS uses a right-handed coordinate system with its origin at the nominal interaction point (IP) in the centre of the detector and the z-axis along the beam pipe. The x-axis points from the IP to the centre of the LHC ring, and the y-axis points upward. Cylindrical coordinates (r,ϕ) are used in the transverse plane, ϕ being the azimuthal angle around the beam pipe. The pseudorapidity is defined in terms of the polar angle θ as $\eta = -\ln\tan(\theta/2)$. Angular distance is measured in units of $\Delta R = \sqrt{(\Delta\eta)^2 + (\Delta\phi)^2}$.

JHEP06(2019)144

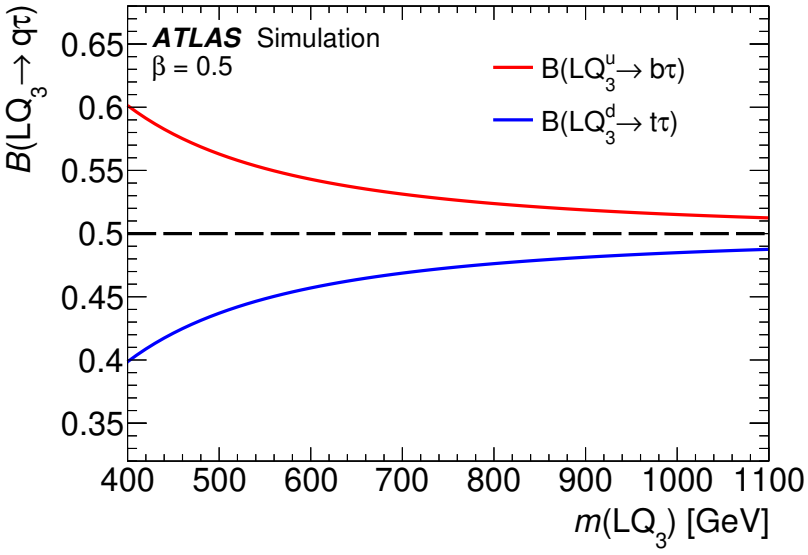

Figure 2. Branching ratio into charged leptons for $\beta = 0.5$ and different LQ masses for $\mathrm{LQ}_3^{\mathrm{u}} \to b\tau/t\nu$ and $\mathrm{LQ}_3^{\mathrm{d}} \to t\tau/b\nu$.

reweighting the samples based on generator information. Additional samples for $\beta = 1$ are used in the analysis of the final state with two b-jets and two τ-leptons.

Due to the difference between the model parameter β and B for third-generation LQs, the branching ratio $\hat{B}$ in the simulated sample with $\beta = 0.5$ can either be calculated from the given parameter λ and the resulting decay width or be taken from the generator information of the MC sample. It is shown in figure 2 as a function of the leptoquark mass. The reweighting is based on the number of charged leptons n_{cl} at generator level originating directly from the decaying leptoquarks for each event. The weight w depends on the $\hat{B}$ of the produced MC sample and on the B of the decay channel and is

$$w(B) = \left(\frac{B}{\hat{B}}\right)^{n_{\mathrm{cl}}} \times \left(\frac{1-B}{1-\hat{B}}\right)^{(2-n_{\mathrm{cl}})}.$$

4 The $b\tau b\tau$ channel

To search for pair-produced scalar leptoquarks decaying into $b\tau b\tau$, final states in which one τ-lepton decays leptonically and the other hadronically ($\tau_\ell\tau_{\mathrm{had}}$), as well as the case in which both τ-leptons decay hadronically ($\tau_{\mathrm{had}}\tau_{\mathrm{had}}$), are considered. This analysis utilizes the same analysis strategy employed by the ATLAS search for pair-produced Higgs bosons decaying into $bb\tau\tau$ final states [21] but optimized for a leptoquark signal with decays into $b\tau b\tau$.

Object reconstruction in the detector (electrons, muons, τ-leptons, jets, and b-jets) employed for $\tau_\ell\tau_{\mathrm{had}}$ and $\tau_{\mathrm{had}}\tau_{\mathrm{had}}$ channels is the same as in ref. [21]. The data were collected through three triggers, a single-lepton (electron or muon) trigger (SLT), a single-τ-lepton trigger (STT), and a di-τ-lepton trigger (DTT). The offline selection is dependent on the trigger and is summarized in table 1. Events in each channel must pass the associated trigger or else the event is discarded. The selection criteria are chosen to optimize the

JHEP06(2019)144

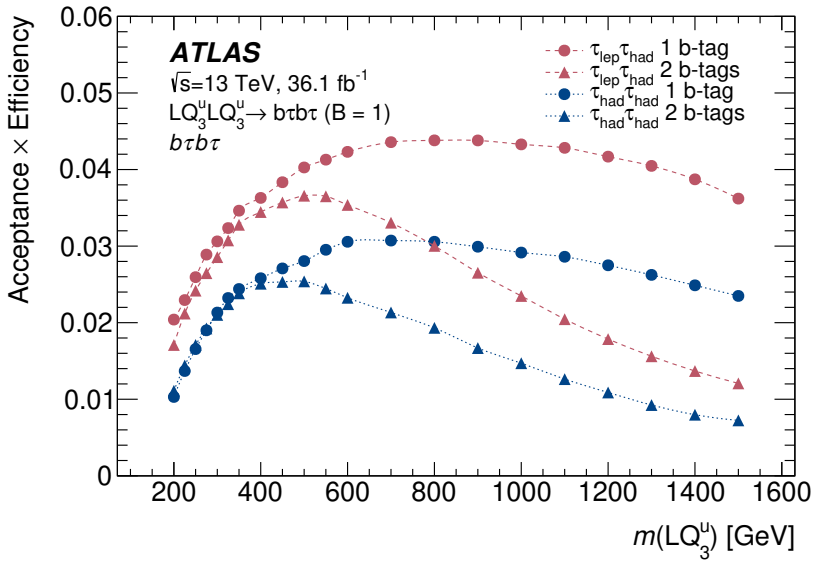

Figure 3. The acceptance times efficiency for the up-type leptoquark signal is shown for the $\tau_\ell\tau_{\text{had}}$ and $\tau_{\text{had}}\tau_{\text{had}}$ channels as a function of the leptoquark mass. The offline selection is summarized in table 1. The results are given separately for selected events with one and two b-tagged jets.

trigger efficiency for the associated data samples. Events are split into categories according to the multiplicity of b-tagged jets. Events with one or two b-tagged jets are considered signal-like events (1-tag and 2-tag events), which form two separate signal regions. In events with one b-tag, the highest-p_{T} non-tagged jet is considered for leptoquark event reconstruction. The acceptance times efficiency for the LQ_3^{u} signal is shown in figure 3 for $\tau_\ell\tau_{\text{had}}$ and $\tau_{\text{had}}\tau_{\text{had}}$ channels as a function of the leptoquark mass with $B = 1$. The decrease in acceptance times efficiency with leptoquark mass is driven by a combination of reduced b-tagging effiency and the efficiency in pairing the bottom quark and τ-lepton. After applying the selection criteria, boosted decision trees (BDTs) are used to improve discrimination between signal and background. The BDTs are only trained on the up-type leptoquark signal. The sensitivity to the down-type leptoquark decay channel is due to the final state $t\tau t\tau \to Wb\tau Wb\tau$, where the W bosons decay into jets. Because this analysis does not veto additional jets, it is sensitive to this decay chain, although it is not optimal.

BDTs are trained to separate the signal from the expected backgrounds, and the BDT score distributions are used as the final discriminant to test for the presence of a signal. The BDTs utilize several input variables, shown in the list below, including those derived from a mass-pairing strategy which extracts the most likely $b\tau$ pairs by minimizing the mass difference between the leptoquark candidates:

- s_{T}: the scalar sum of missing transverse momentum ($E_{\text{T}}^{\text{miss}}$), the p_{T} of any reconstructed τ-lepton(s), the p_{T} of the two highest-p_{T} jets, and the p_{T} of the lepton in $\tau_\ell\tau_{\text{had}}$ events

- $m_{\tau,\text{jet}}$: the invariant mass between the leading τ-lepton and its mass-paired jet

JHEP06(2019)144

$\tau_\ell\tau_{\text{had}}$(SLT)	• Exactly one e passing 'tight' identification criteria or one μ passing 'medium' identification criteria [40, 41]. Events containing additional electrons or muons with 'loose' identification criteria and $p_{\text{T}} > 7\,\text{GeV}$ are vetoed. • Exactly one hadronically decaying τ-lepton with transverse momentum (p_{T}) $> 25\,\text{GeV}$ and $\lvert\eta\rvert < 2.3$. • Opposite-sign charge between the τ-lepton and the light lepton (e/μ). • At least two central jets in the event with $p_{\text{T}} > 60$ (20) GeV for the leading (subleading) jet.
$\tau_{\text{had}}\tau_{\text{had}}$(STT)	• Events containing electrons or muons with 'loose' identification criteria and $p_{\text{T}} > 7\,\text{GeV}$ are vetoed. • Exactly two hadronically decaying τ-leptons with $\lvert\eta\rvert < 2.3$. The leading τ-lepton must have $p_{\text{T}} > 100$, 140, or 180 GeV for data periods where the trigger p_{T} threshold was 80, 125, or 160 GeV respectively. The subleading τ-lepton is required to have $p_{\text{T}} > 20\,\text{GeV}$. • The two τ-leptons must have opposite-sign charge. • At least two jets in the event with $p_{\text{T}} > 45$ (20) GeV for the leading (subleading) jet.
$\tau_{\text{had}}\tau_{\text{had}}$(DTT)	• Selected events from STT are vetoed as are events containing electrons or muons with 'loose' identification criteria and $p_{\text{T}} > 7\,\text{GeV}$. • Exactly two hadronically decaying τ-leptons with $\lvert\eta\rvert < 2.3$. The leading (subleading) τ-lepton must have $p_{\text{T}} > 60$ (30) GeV. • The two τ-leptons must have opposite-sign charge. • At least two jets in the event with $p_{\text{T}} > 80$ (20) GeV for the leading (subleading) jet.

Table 1. Summary of applied event selection for the $\tau_\ell\tau_{\text{had}}$ and $\tau_{\text{had}}\tau_{\text{had}}$ channels.

- $m_{\ell,\text{jet}}$: the invariant mass between the lepton and its matching jet from the mass-pairing strategy ($\tau_\ell\tau_{\text{had}}$ only)
- $\Delta R(\text{lep}, \text{jet})$: the ΔR between the electron or muon (leading τ-lepton) and jet in $\tau_\ell\tau_{\text{had}}$ ($\tau_{\text{had}}\tau_{\text{had}}$)
- $E_{\text{T}}^{\text{miss}}$ ϕ centrality: quantifies the ϕ separation between the $E_{\text{T}}^{\text{miss}}$ and τ-lepton(s). Full definition is in ref. [21]
- p_{T}^{τ}: the p_{T} of the leading τ-lepton
- $\Delta\phi(\text{lep}, E_{\text{T}}^{\text{miss}})$: the opening angle between the lepton and $E_{\text{T}}^{\text{miss}}$ ($\tau_\ell\tau_{\text{had}}$ only)

Kinematic distributions for $\tau_\ell\tau_{\text{had}}$ and $\tau_{\text{had}}\tau_{\text{had}}$ signal regions in 2-tag events are shown in figure 4. Separate BDTs are trained for $\tau_\ell\tau_{\text{had}}$ and $\tau_{\text{had}}\tau_{\text{had}}$ categories for each mass point of the LQ_3^{u} MC sample and for each b-tag signal region. The signal samples used in the training include events with a small range of leptoquark masses around the given mass point to ensure the BDT is sensitive to signals that have masses between the hypotheses simulated. In the $\tau_\ell\tau_{\text{had}}$ channel the training is performed against the dominant $t\bar{t}$ background only. BDTs for the $\tau_{\text{had}}\tau_{\text{had}}$ channel are trained against simulated $t\bar{t}$ and $Z \to \tau\tau$ events and multi-jet events from data.

JHEP06(2019)144

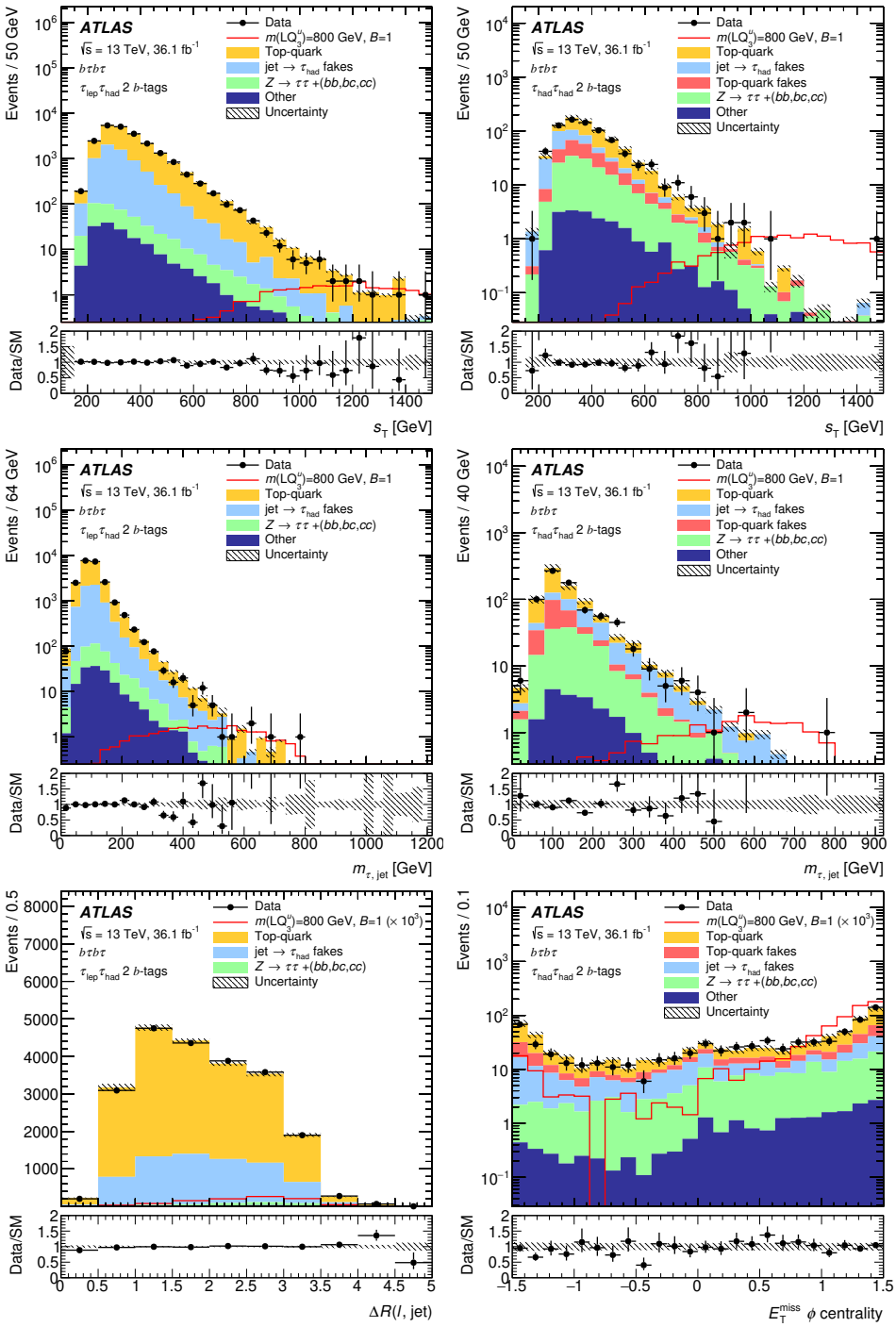

Figure 4. Kinematic distributions for $\tau_\ell\tau_{\text{had}}$ (left) and $\tau_{\text{had}}\tau_{\text{had}}$ (right) signal regions in 2-tag events after performing the combined channel fit. The ratio of the data to the sum of the backgrounds is shown in the lower panel. The hatched bands indicate the combined statistical and systematic uncertainties in the background. Distributions include the scalar sum of transverse momentum of reconstructed objects in the event (s_{T}), the invariant mass between the leading τ-lepton and its mass-paired jet ($m_{\tau,\text{jet}}$), the invariant mass between the lepton and its matching jet from the mass-pairing strategy ($m_{\ell,\text{jet}}$), the ΔR between the leading τ-lepton and jet ($\Delta R(\text{lep},\text{jet})$), and the $E_{\text{T}}^{\text{miss}}$ ϕ centrality, which quantifies the ϕ separation between the $E_{\text{T}}^{\text{miss}}$ and τ-lepton(s).

JHEP06(2019)144

The background estimation techniques in this analysis are the same as used in ref. [21] and are summarized here. In both channels, background processes containing true τ-leptons are taken from simulation. The dominant background processes are $t\bar{t}$ and $Z/\gamma^* \to \tau\tau$ produced in association with jets originating from heavy-flavour quarks (bb, bc, cc). The $t\bar{t}$ events are normalized using events with low BDT output score in the $\tau_\ell\tau_{\text{had}}$ category. Events from $Z/\gamma^* \to \tau\tau$ plus heavy-flavour jets are normalized using a control region of events that include two muons with combined invariant mass consistent with that of a Z boson. Backgrounds in which quark- or gluon-initiated jets are misidentified as hadronically decaying τ-leptons are estimated using data-driven methods. In both channels, $t\bar{t}$ events are estimated separately from other background sources if one or more reconstructed τ-lepton decays are mis-reconstructed jets (so-called 'fake τ-leptons'). In the $\tau_\ell\tau_{\text{had}}$ channel all fake-τ-lepton contributions from $t\bar{t}$, W+jets, and multi-jet processes are estimated using an inclusive fake-factor method, described in ref. [21]. Theory uncertainties in the modeling of the $t\bar{t}$ and Z+jets background containing true τ_{had} are assessed by varying the matrix element generator and the parton shower model, and by adjusting the factorization and renormalization scales along with the amount of additional radiation. The resulting variations in the BDT distributions are included as shape uncertainties in the final fit.

In the $\tau_{\text{had}}\tau_{\text{had}}$ channel, the fake-τ-lepton $t\bar{t}$ component is estimated as follows: the probability for a jet from a hadronic W-boson decay to be reconstructed as a hadronically decaying τ-lepton is measured in data. This is used then to correct the MC prediction, after subtracting the predicted number of true τ-leptons from the MC. Three control regions are defined for both $\tau_\ell\tau_{\text{had}}$ and $\tau_{\text{had}}\tau_{\text{had}}$: these include 1-$b$-tag and 2-$b$-tag same-sign lepton events that are mostly events with fake τ-leptons and a $t\bar{t}$ control region as defined in ref. [21]. The uncertainty in the modeling is estimated by varying the fake-factors and fake-rates within their statistical uncertainties and varying the amount of true τ_{had} background subtracted. Systematic uncertainties on the extrapolation of the fake τ_{had} backgrounds from the control regions, where they are derived, to the signal regions are estimated by varying the control region definition; an uncertainty due to the difference in the flavour composition of the jet faking the τ_{had} is also assigned based on simulation.

The BDT responses in the 2-tag same-sign and top-quark control regions are shown in figure 5. The background modeling was checked in these control regions, which validates the signal-sensitive region at high BDT score. The 1-tag and 2-tag $\tau_\ell\tau_{\text{had}}$ and $\tau_{\text{had}}\tau_{\text{had}}$ signal regions are shown in figures 6 and 7 for up-type samples with a mass of 400 GeV ($B = 1$) and down-type leptoquark samples with a mass of 800 GeV ($B = 1$). The binning choice differs between the figures as this follows an algorithm depending on the number of signal (in the case of the signal region only) and background events in each bin. Yield tables are shown for both 1-tag and 2-tag regions in table 2, where the numbers quoted are after performing the combined fit, described below.

Systematic uncertainties are considered and propagated through the full analysis. The uncertainties in the luminosity, background modeling, and detector modeling are calculated as in ref. [21]. The impact of varying the renormalization/factorization scales and choice of PDF on the signal acceptance was also investigated.

JHEP06(2019)144

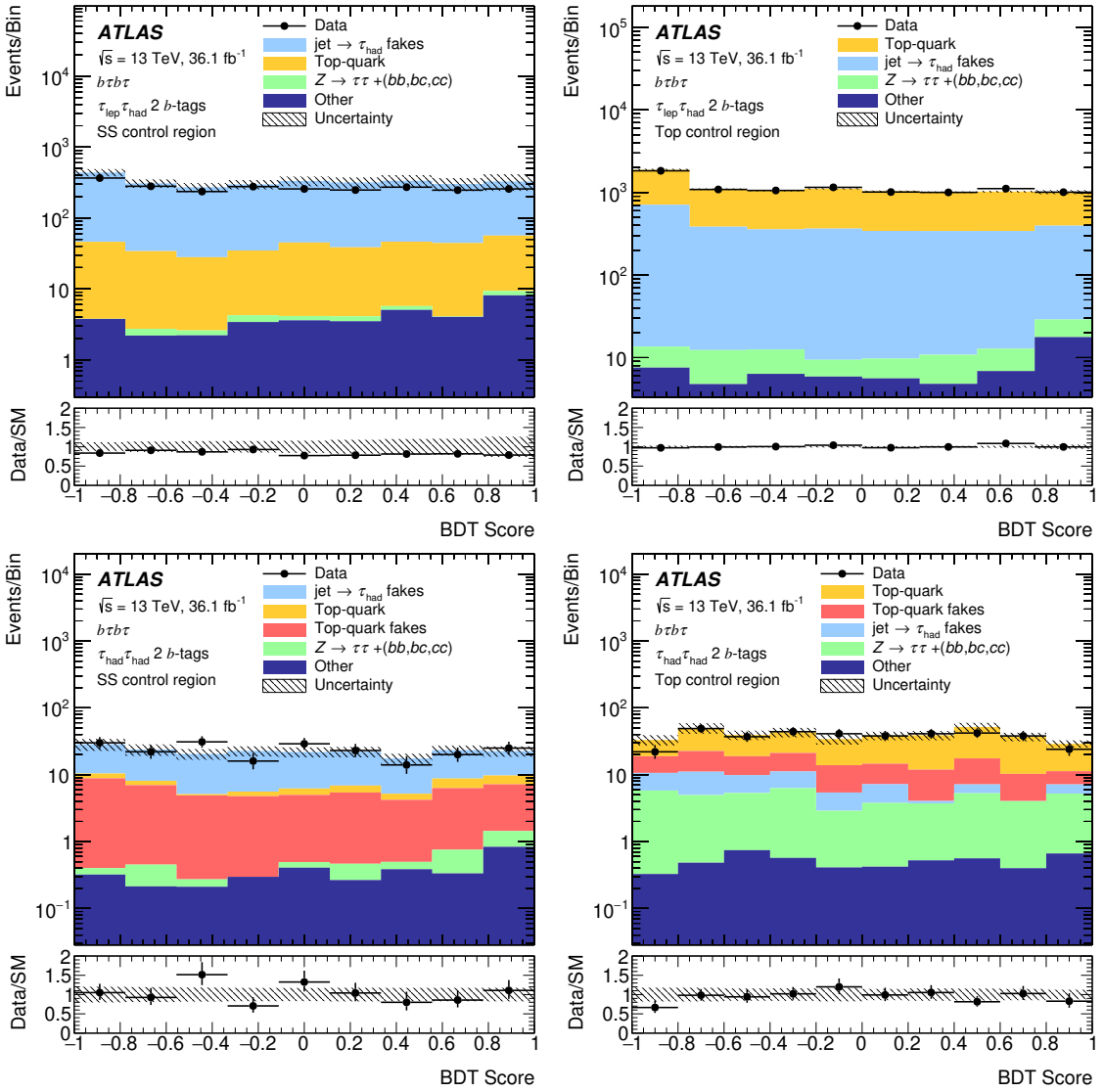

Figure 5. BDT score distributions for $\tau_\ell\tau_{\text{had}}$ (top) and $\tau_{\text{had}}\tau_{\text{had}}$ (bottom) 2-tag channels in the same-sign (left) and top-quark (right) control regions after performing the combined fit to all channels. The ratio of the data to the sum of the backgrounds is shown in the lower panel. The hatched bands indicate the combined statistical and systematic uncertainties in the background.

The fit strategy follows that in ref. [21]. The BDT output score is the discriminating variable for all channels and signals in a single combined fit of all signal and control regions. A CL_s method [42] based on one-sided profile-likelihood test statistics is used to test the signal hypothesis. In the profile-likelihood function, Gaussian constraints are used for shape systematic uncertainties and log-normal constraints for normalization uncertainties. The binning in the BDT output categories at high BDT output score is modified to ensure sufficient statistics. The Standard Model predictions are consistent with the data. Figure 8 shows the expected and observed 95% confidence level (CL) upper limits on the cross-section for scalar up-type and down-type leptoquark pair production as a function of

JHEP06(2019)144

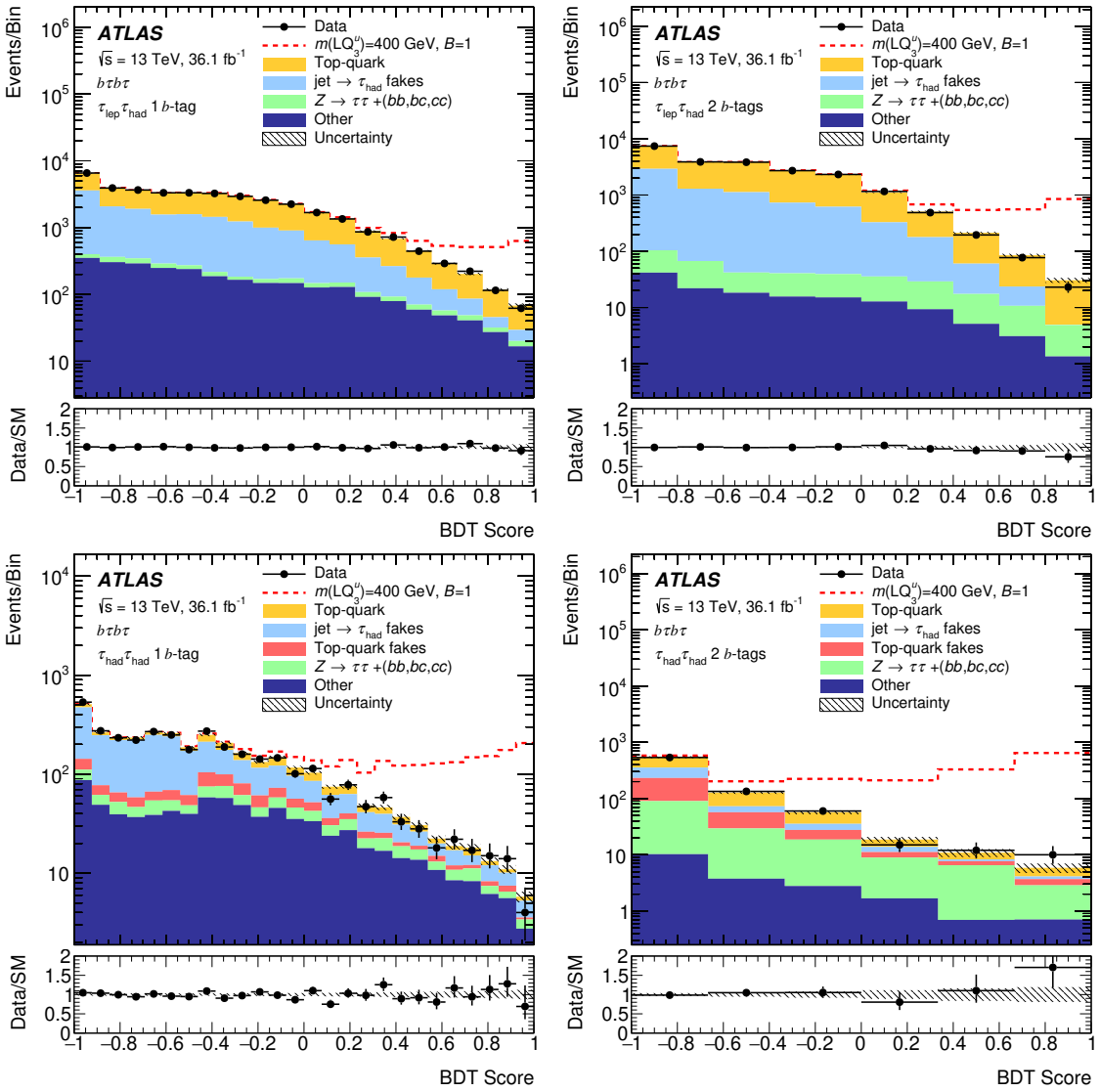

Figure 6. BDT score distributions for $\tau_\ell\tau_{\rm had}$ (top) and $\tau_{\rm had}\tau_{\rm had}$ (bottom) channels in the 1-tag (left) and 2-tag (right) regions after performing the combined channel fit. The stacked histograms show the various SM background contributions, which are normalized to the expected cross-section. The hatched band indicates the total statistical and systematic uncertainty in the SM background. The error bars on the black data points represent the statistical uncertainty in the data yields. The dashed histogram shows the expected additional yields from a leptoquark signal model for a up-type leptoquark sample with a mass of 400 GeV ($B = 1$) added on top of the SM prediction. The ratio of the data to the sum of the backgrounds is shown in the lower panel.

JHEP06(2019)144

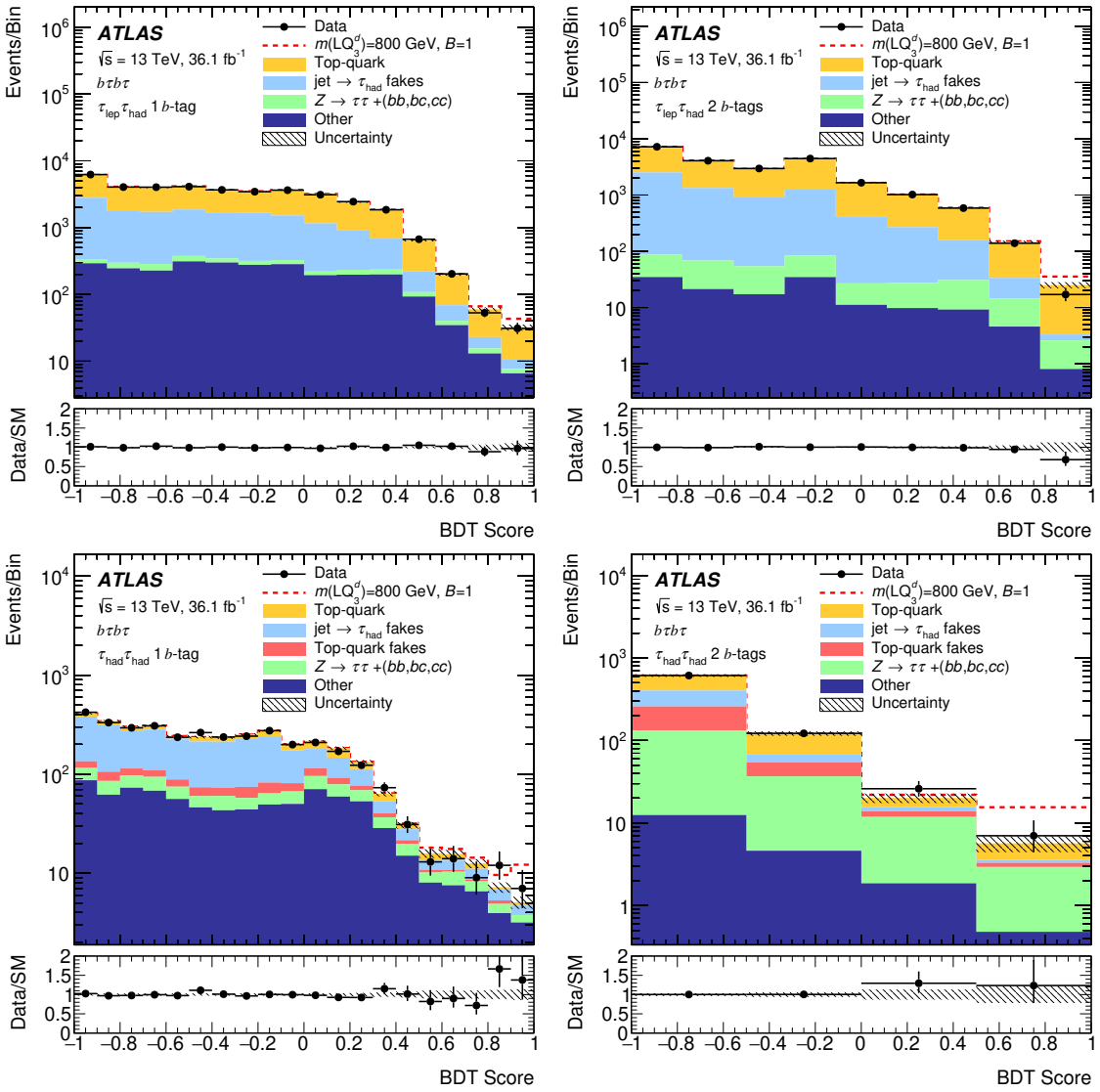

Figure 7. BDT score distributions for $\tau_\ell\tau_{\text{had}}$ (top) and $\tau_{\text{had}}\tau_{\text{had}}$ (bottom) channels in the 1-tag (left) and 2-tag (right) regions after performing the combined channel fit. The stacked histograms show the various SM background contributions, which are normalized to the expected cross-section. The hatched band indicates the total statistical and systematic uncertainty in the SM background. The error bars on the black data points represent the statistical uncertainty in the data yields. The dashed histogram shows the expected additional yields from a leptoquark signal model for a down-type leptoquark sample with a mass of 800 GeV ($B = 1$) added on top of the SM prediction. The ratio of the data to the sum of the backgrounds is shown in the lower panel.

JHEP06(2019)144

Sample	Post-fit yield			
	$\tau_\ell\tau_{\text{had}}$		$\tau_{\text{had}}\tau_{\text{had}}$	
	1-tag	2-tag	1-tag	2-tag
$t\bar{t}$	17800 ± 1500	14460 ± 980	285 ± 83	238 ± 69
Single top	2500 ± 180	863 ± 73	63 ± 8	27 ± 3
QCD fake-τ	–	–	1860 ± 110	173 ± 34
$t\bar{t}$ fake-τ	–	–	200 ± 110	142 ± 79
Fake-τ	13900 ± 1700	6400 ± 1000	–	–
$Z \to \tau\tau + (bb, bc, cc)$	520 ± 160	285 ± 83	258 ± 64	156 ± 36
Other	2785 ± 270	158 ± 26	817 ± 95	21 ± 4
Total Background	37510 ± 220	22120 ± 160	3482 ± 59	756 ± 27
Data	37527	22117	3469	768
$m(\text{LQ}_3^{\text{u}}) = 400\,\text{GeV}$	2140 ± 140	1950 ± 160	1430 ± 190	1430 ± 200
$m(\text{LQ}_3^{\text{d}}) = 400\,\text{GeV}$	1420 ± 170	1096 ± 82	850 ± 110	672 ± 88
$m(\text{LQ}_3^{\text{u}}) = 800\,\text{GeV}$	39.1 ± 2.8	25.2 ± 2.3	25.6 ± 3.9	16.8 ± 2.7
$m(\text{LQ}_3^{\text{d}}) = 800\,\text{GeV}$	23 ± 2.3	16.6 ± 1.4	17.8 ± 2.8	12.4 ± 2.2
$m(\text{LQ}_3^{\text{u}}) = 1500\,\text{GeV}$	0.25 ± 0.02	0.08 ± 0.01	0.16 ± 0.03	0.05 ± 0.01

Table 2. Post-fit expected numbers of signal and background events, determined from a background-only fit, compared to the observed number of data events after applying the selection criteria and requiring at least one b-tagged jet. Both the up-type and down-type leptoquark samples here use $B = 1$. In the $\tau_\ell\tau_{\text{had}}$ channel, the fake-τ-lepton background includes all processes in which a jet is misidentified as a τ-lepton, while in the $\tau_{\text{had}}\tau_{\text{had}}$ case the fake background from QCD multi-jet processes and $t\bar{t}$ production are derived separately. The $t\bar{t}$ background includes events with true τ_{had} and the very small contribution from leptons misidentified as τ_{had}. The 'Other' category includes contributions from W+jets, Z+jets, and diboson processes. The total background is not identical to the sum of the individual components since the latter are rounded for presentation, while the sum is calculated with the full precision before being rounded. The uncertainty in the total background is smaller than that in the $t\bar{t}$ and multi-jet backgrounds due to these being strongly anti-correlated.

leptoquark mass for the combined $\tau_\ell\tau_{\text{had}}$ + $\tau_{\text{had}}\tau_{\text{had}}$ channels. The theoretical prediction for the cross-section of scalar leptoquark pair production is shown by the solid line, along with the uncertainties. These limits are used to set upper limits on the leptoquark branching ratio $B(\text{LQ} \to q\tau)$ as a function of the leptoquark mass. From the data, masses below 1030 GeV and 930 GeV are excluded for LQ_3^{u} and LQ_3^{d} respectively, at 95% CL for the case of B equal to unity. The expected exclusion ranges are 1030 GeV and 930 GeV, respectively.

JHEP06(2019)144

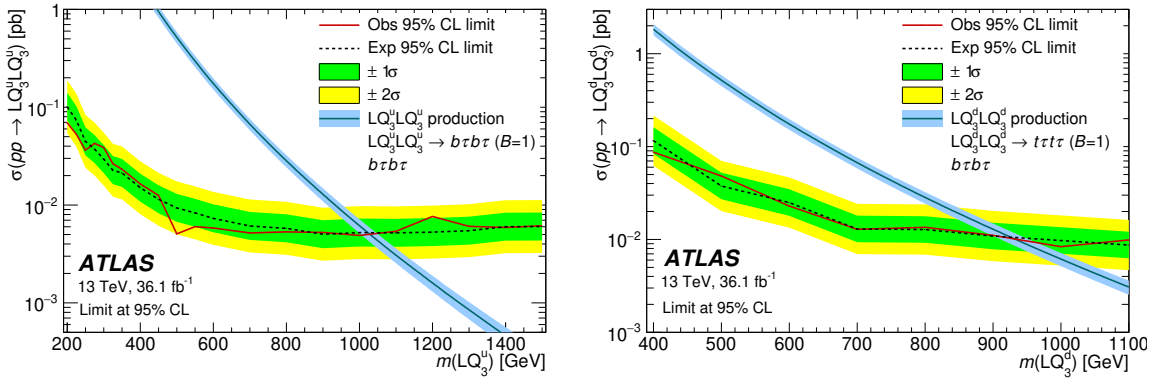

Figure 8. Expected and observed 95% CL upper limits on the cross-section for up-type (left) and down-type (right) scalar leptoquark pair production with $B = 1$ as a function of leptoquark mass for the combined $\tau_\ell\tau_{\text{had}}$ and $\tau_{\text{had}}\tau_{\text{had}}$ channels. The observed limit is shown as the solid line. The thickness of the theory curve represents the theoretical uncertainty from PDFs, renormalization and factorization scales, and the strong coupling constant α_s.

5 The tt plus $E_{\text{T}}^{\text{miss}}$ channel with one lepton

In this section, the LQ reinterpretation of a dedicated search for top-squark pair production [22] in final states with one lepton is described. Events where both LQs decay into a top quark and a neutrino are targeted, where one top quark decays hadronically and the other one semileptonically. Events containing one isolated lepton, jets, and missing transverse momentum in the final state are considered. Two signal regions (SR) of the top-squark search [22], tN_med and tN_high, have optimal sensitivity for medium (∼600 GeV) and high (∼1 TeV) masses of the leptoquark. The tN_med SR is additionally binned in $E_{\text{T}}^{\text{miss}}$, while the tN_high SR is taken as a single-bin cut-and-count experiment. Both signal regions require at least four jets, at least one b-tagged jet, exactly one isolated electron or muon, and high $E_{\text{T}}^{\text{miss}}$. Variables sensitive to the direction of the $E_{\text{T}}^{\text{miss}}$ are used, e.g. the transverse mass of the lepton and $E_{\text{T}}^{\text{miss}}$, denoted by m_{T},[2] and am_{T2} [43], which targets pair-produced heavy objects that each decay into a different number of measured and unmeasured particles in the detector. The hadronically decaying top quark is reconstructed using jet reclustering, where several jets are combined using the anti-k_t algorithm [44] with a large radius parameter that is initially set to 3.0 and then adjusted in an iterative process [22].

The various backgrounds are estimated using simulated data. The dominant background consists of $t\bar{t}$ events, which, due to the high m_{T} requirements, are mainly from dileptonic $t\bar{t}$ decays in which one lepton is not reconstructed ($t\bar{t}$ 2L), even though this decay topology is strongly suppressed by requiring am_{T2} to be above the top-quark mass. Other major backgrounds are due to the production of a W boson in association with one or more jets (W+jets) and the production of a $t\bar{t}$ pair in association with a vector boson ($t\bar{t}+V$), where the latter is dominated by contributions from $t\bar{t}+Z(\to \nu\nu)$. For each SR, a

[2]The transverse mass m_{T} is defined as $m_{\text{T}} = \sqrt{2p_{\text{T}}^{\text{lep}} E_{\text{T}}^{\text{miss}}[1-\cos(\Delta\phi)]}$, where $\Delta\phi$ is the azimuthal angle between the lepton and the missing transverse momentum direction and $p_{\text{T}}^{\text{lep}}$ is the transverse momentum of the charged lepton.

JHEP06(2019)144

Observed events		8	
Total SM	3.8	±	1.0
$m(\mathrm{LQ}_3^{\mathrm{u}}) = 800$ GeV	11.9	±	1.8
$m(\mathrm{LQ}_3^{\mathrm{u}}) = 900$ GeV	9.5	±	1.2
$m(\mathrm{LQ}_3^{\mathrm{u}}) = 1000$ GeV	6.7	±	0.7
$m(\mathrm{LQ}_3^{\mathrm{u}}) = 1100$ GeV	3.7	±	0.3

Table 3. The number of observed events in the cut-and-count SR tN_high, together with the expected number of background events including their total uncertainties, taken from ref. [22]. Additionally, the expected number of signal events are given for $B = 0$ for up-type LQs of different masses with statistical uncertainties.

set of dedicated single-bin CRs is defined in order to control the background normalization. The $t\bar{t}$ 2L CR is defined at high m_{T} and with a veto on hadronically decaying top-quark candidates, while the W+jets CR is defined at low m_{T} and with a veto on hadronically decaying top-quark candidates. The top-quark candidate veto is fulfilled if either no top-quark candidate is found or if the mass is lower than the SR threshold. Additionally, a CR for semileptonic $t\bar{t}$ events ($t\bar{t}$ 1L) is defined, as these events contribute strongly to the other CRs. A CR for single-top events is defined similarly to the W+jets CR, but with at least two b-jets. The $t\bar{t} + Z$ background is estimated with a three-lepton selection.

The statistical analysis for a SR is based on a simultaneous likelihood fit to the observed events in the CRs and the SR, where the background samples and a signal sample are included in all regions. The fit determines at the same time the background normalization as well as a potential signal contribution. For each SR, a set of validation regions is defined in addition to the CRs. The validation regions are not part of the fit but are used to validate the background normalization in this second set of disjunct regions. Systematic uncertainties are included as nuisance parameters in the profile-likelihood estimate. The test statistic is the profile log-likelihood ratio and its distribution is calculated using the asymptotic approximation [45].

The number of observed events in the data in each SR and the expected number of background events as calculated in a fit to only the CRs while neglecting a potential signal contamination are taken from ref. [22] and shown in tables 3 and 4. In addition, the expected number of signal events for different leptoquark masses is shown for each SR. The contamination from the leptoquark signal in the CRs is below 10% in all cases. Figure 9 shows the $E_{\mathrm{T}}^{\mathrm{miss}}$ distribution in the tN_med SR.

The combination of the exclusion limits for the SRs is obtained by selecting the signal region with the better expected limit for each mass point. For LQ masses of 950, 1000, and 1100 GeV, the limit of the tN_high signal region is selected, otherwise the limit of the tN_med signal region is selected. The expected and observed exclusion limits are shown in figure 10. The theoretical prediction for the cross-section of scalar leptoquark pair production is shown by the solid line along with the uncertainties. Pair-produced third-generation scalar leptoquarks decaying into $t\nu t\bar{\nu}$ are excluded at 95% CL for $m_{\mathrm{LQ}} < 930$ GeV. The expected exclusion range is $m_{\mathrm{LQ}} < 1020$ GeV.

JHEP06(2019)144

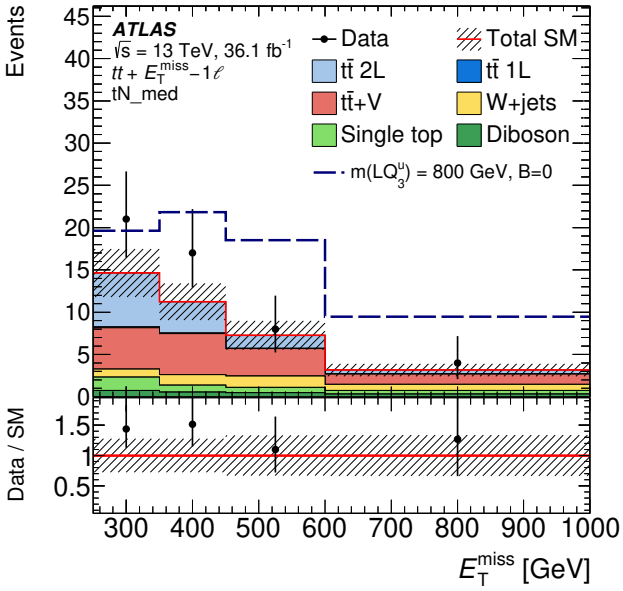

Figure 9. Observed and expected $E_{\mathrm{T}}^{\mathrm{miss}}$ distributions are shown in the tN_med signal region, as is their ratio. The error band includes statistical and systematic uncertainties. The expected SM backgrounds are normalized to the values determined in the fit. The expected number of signal events for an up-type LQ with $m_{\mathrm{LQ}} = 800\,\mathrm{GeV}$ and $B = 0$ is added on top of the SM prediction. The last bin contains the overflow events.

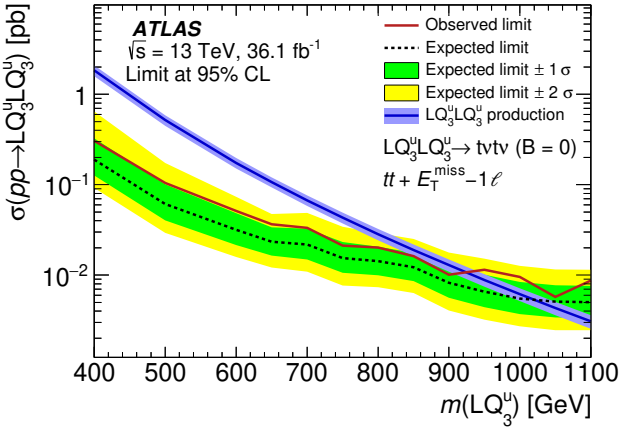

Figure 10. Observed and expected 95% CL upper limit on the cross-section for up-type LQ pair production with $B = 0$ as a function of the LQ mass. The $\pm 1(2)\sigma$ uncertainty bands around the expected limit represent all sources of statistical and systematic uncertainties. The thickness of the theory curve represents the theoretical uncertainty from PDFs, renormalization and factorization scales, and the strong coupling constant α_{s}.

JHEP06(2019)144

$E_{\mathrm{T}}^{\mathrm{miss}}$	[250, 350] GeV	[350, 450] GeV	[450, 600] GeV	> 600 GeV
Observed events	21	17	8	4
Total SM	14.6 ± 2.8	11.2 ± 2.2	7.3 ± 1.7	3.16 ± 0.74
$m(\mathrm{LQ}_3^{\mathrm{u}}) = 400$ GeV	166 ± 44	58 ± 32	11 ± 11	5.7 ± 5.7
$m(\mathrm{LQ}_3^{\mathrm{u}}) = 600$ GeV	21.0 ± 5.6	49.6 ± 8.8	31.8 ± 5.5	1.4 ± 2.1
$m(\mathrm{LQ}_3^{\mathrm{u}}) = 800$ GeV	5.0 ± 1.5	10.6 ± 1.7	11.2 ± 2.0	6.3 ± 1.4
$m(\mathrm{LQ}_3^{\mathrm{u}}) = 1000$ GeV	0.46 ± 0.14	1.18 ± 0.24	2.92 ± 0.49	4.61 ± 0.64

Table 4. The number of observed events in the shape-fit SR tN_med, together with the expected number of background events including their total uncertainties, taken from ref. [22]. Additionally, the expected number of signal events are given for $B = 0$ for up-type LQs of different masses with statistical uncertainties. The numbers are given for the four bins characterized by an interval of the $E_{\mathrm{T}}^{\mathrm{miss}}$ variable.

6 The tt plus $E_{\mathrm{T}}^{\mathrm{miss}}$ channel with zero leptons

In this section, the LQ reinterpretation of the ATLAS analysis optimized for the search of top-squark pair production [23] in final states with zero leptons is discussed. The signature targeted is two hadronically decaying top quarks and invisible particles, closely matching the signature where both LQs decay into a top quark and a neutrino. Three signal regions (SRA, SRB, SRD) of the top-squark search [23] have the greatest sensitivity to the LQ signal models. SRA is optimal for high LQ masses, e.g. $m_{\mathrm{LQ}} \approx 1\,\mathrm{TeV}$, which typically results in high $E_{\mathrm{T}}^{\mathrm{miss}}$ and top quarks with a significant boost. SRB is sensitive to medium LQ masses, which tend to have a softer $E_{\mathrm{T}}^{\mathrm{miss}}$ spectrum and less-boosted top quarks. SRD targets a resonance decaying into a b-quark and an invisible particle, giving sensitivity to $\mathrm{LQ}_3^{\mathrm{d}} \to b\nu$ events.

A common preselection is defined for all signal regions. At least four jets are required, of which at least one must be b-tagged. The four leading jets (ordered in p_{T}) must satisfy $p_{\mathrm{T}} > 80, 80, 40, 40\,\mathrm{GeV}$, respectively, due to the tendency for signal events to have higher-energy jets than background events. Events containing reconstructed electrons or muons are vetoed. The $E_{\mathrm{T}}^{\mathrm{miss}}$ trigger threshold motivates the $E_{\mathrm{T}}^{\mathrm{miss}} > 250\,\mathrm{GeV}$ requirement and rejects most of the background from multi-jet and all-hadronic $t\bar{t}$ events.

Similarly to the tt+$E_{\mathrm{T}}^{\mathrm{miss}}-1\ell$ analysis in section 5, hadronically decaying top quarks are reconstructed using jet reclustering. SRA and SRB require the presence of two reclustered $R = 1.2$ jets. Both SRA and SRB are divided into three orthogonal, one-bin subregions, which are combined for maximal signal sensitivity. The categorization in subregions is based on the mass of the subleading (ordered in p_{T}) reclustered jet ($m^1_{\mathrm{jet},R=1.2}$). In all subregions it is required that the leading reclustered $R = 1.2$ jet has a mass ($m^0_{\mathrm{jet},R=1.2}$) of at least 120 GeV. The subregions are denoted by TT, TW, and T0 corresponding to requirements of $m^1_{\mathrm{jet},R=1.2} > 120\,\mathrm{GeV}$, $60 < m^1_{\mathrm{jet},R=1.2} < 120\,\mathrm{GeV}$, and $m^1_{\mathrm{jet},R=1.2} < 60\,\mathrm{GeV}$, respectively. In addition to the $R = 1.2$ reclustered jet mass, one of the most discriminating variables in SRA is $E_{\mathrm{T}}^{\mathrm{miss}}$, which has to be above 400 GeV or higher depending on the subregion. In SRB, the $E_{\mathrm{T}}^{\mathrm{miss}}$ requirement is looser ($E_{\mathrm{T}}^{\mathrm{miss}} > 250\,\mathrm{GeV}$) than in SRA since the signals that SRB is targeting tend to have softer $E_{\mathrm{T}}^{\mathrm{miss}}$ spectra.

JHEP06(2019)144

Two SRD subregions, SRD-low and SRD-high, are defined for which at least five jets are required, two of which must be b-tagged. Requirements are made on the transverse momenta of the jets as well as on the scalar sum of the transverse momenta of the two b-tagged jets, which needs to be above 400 GeV for SRD-high and above 300 GeV for SRD-low. Tight requirements are also applied to the m_{T} calculated from $E_{\mathrm{T}}^{\mathrm{miss}}$ and the b-tagged jet that has the smallest ($m_{\mathrm{T}}^{b,\mathrm{min}}$) and largest ($m_{\mathrm{T}}^{b,\mathrm{max}}$) $\Delta\phi$ relative to the $E_{\mathrm{T}}^{\mathrm{miss}}$ direction.

The dominant background processes are $Z \to \nu\nu$ in association with b-jets, semileptonic $t\bar{t}$ where one of the W bosons decays into $\tau\nu$, and $t\bar{t} + Z(\to \nu\nu)$. To estimate the normalization of these backgrounds, control regions are designed to be as close as possible to individual signal regions while being strongly enhanced in the background of interest. For the $Z \to \nu\nu$ background, $Z \to \ell\ell$ control regions are used where the leptons are removed to mimic the $E_{\mathrm{T}}^{\mathrm{miss}}$ produced by the $Z \to \nu\nu$ process. To estimate the $t\bar{t}$ background, a set of one-lepton control regions is used. Finally, the $t\bar{t}+Z(\to \nu\nu)$ background is estimated using a $t\bar{t}+\gamma$ control region where the photon p_{T} is used to approximate $E_{\mathrm{T}}^{\mathrm{miss}}$. Several normalizations for the subdominant backgrounds, such as single-top and W+jets production, are also estimated using control regions. The normalizations are calculated using a simultaneous binned profile-likelihood fit. Signal contamination in the control regions, specifically regions used to estimate the normalization of $t\bar{t}$, single top, and W+jets, is negligible.

The statistical analysis is done similarly to the one described in section 5. Here the signal yields are extracted during a simultaneous fit to all control regions plus SRD or the three subregion categories of either SRA or SRB. The two subregions of SRD are not orthogonal and are not statistically combined. The combined limits use the best expected limit among all signal regions.

Figure 11 shows observed and expected $E_{\mathrm{T}}^{\mathrm{miss}}$ distributions in SRA, $\Delta R\,(b,b)$ distributions in SRB, and $m_{\mathrm{T}}^{b,\mathrm{max}}$ distributions in SRD-low and SRD-high. In addition, examples of signal distributions with different LQ masses and branching ratios are added on top of the SM prediction. These examples are chosen such that these signals are close to being excluded. The expected and observed numbers of events as well as the expected number of events for the example signals are shown in table 5 for each region.

The expected and observed exclusion limits on the cross-section for $\mathrm{LQ}_3^{\mathrm{u}}$ and $\mathrm{LQ}_3^{\mathrm{d}}$ for $B = 0$ are shown as a function of the leptoquark mass in figure 12. The theoretical prediction for the cross-section of scalar leptoquark pair-production is shown by the solid line along with the uncertainties. As expected, there is better sensitivity to $\mathrm{LQ}_3^{\mathrm{u}}$ than to $\mathrm{LQ}_3^{\mathrm{d}}$, excluding pair-produced $\mathrm{LQ}_3^{\mathrm{u}}$ decaying into $t\nu t\bar{\nu}$ for masses smaller than 1000 GeV at 95% CL. The expected limit is $m_{\mathrm{LQ}} < 1020$ GeV.

7 The $\tau\tau b$ plus $E_{\mathrm{T}}^{\mathrm{miss}}$ channel

The ATLAS search for top-squark pair production with decays via τ-sleptons [25] selects events containing two τ-leptons, at least two jets, of which at least one must be b-tagged, and missing transverse momentum. Its reinterpretation is expected to have good sensitivity for all B except at very low values, with the maximum sensitivity at intermediate values.

JHEP06(2019)144

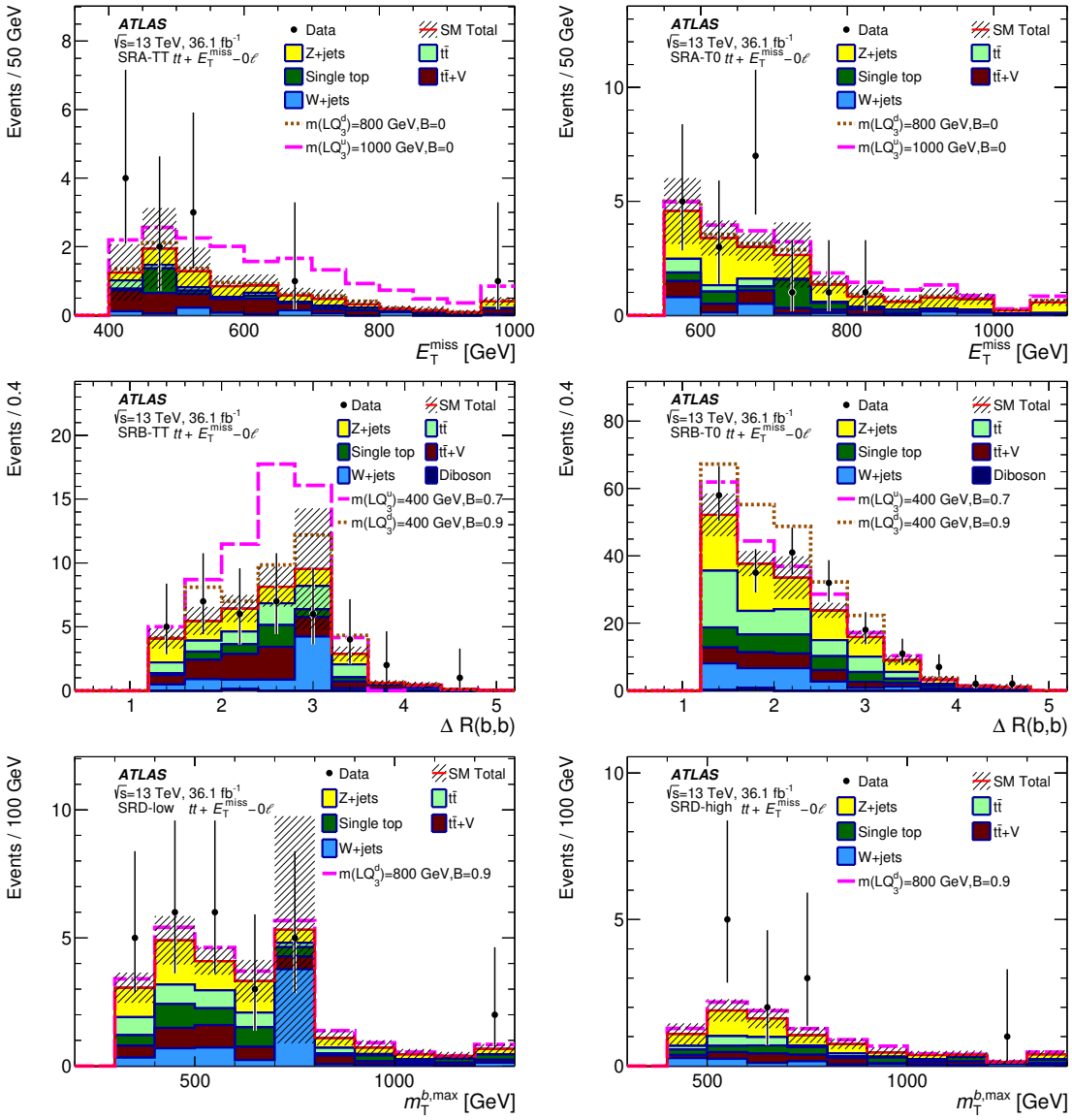

Figure 11. Distributions of $E_{\mathrm{T}}^{\mathrm{miss}}$ in SRA (upper panels) and $\Delta R\,(b,b)$ in SRB (middle panels) separately for the individual top reconstruction categories TT and T0 and the $m_{\mathrm{T}}^{b,\mathrm{max}}$ distribution in SRD-low and SRD-high (lower panels). The expected SM backgrounds are normalized to the values determined in the fit. The expected number of signal events for different LQ masses and branching ratios B is added on top of the SM prediction. The last bin contains the overflow events.

JHEP06(2019)144

SR		TT	TW	T0	low	high
A	Observed	11	9	18	-	-
	SM Total	8.6 ± 2.1	9.3 ± 2.2	18.7 ± 2.7		
	$m(\mathrm{LQ}_3^{\mathrm{u}}) = 1000\,\mathrm{GeV},\ B = 0$	8.5 ± 0.7	4.8 ± 0.6	5.0 ± 0.7		
	$m(\mathrm{LQ}_3^{\mathrm{d}}) = 800\,\mathrm{GeV},\ B = 0$	3.1 ± 1.1	3.7 ± 1.2	15.5 ± 2.5		
B	Observed	38	53	206	-	-
	SM Total	39 ± 8	52 ± 7	179 ± 26		
	$m(\mathrm{LQ}_3^{\mathrm{u}}) = 400\,\mathrm{GeV},\ B = 0.7$	26 ± 7	18 ± 8	27 ± 9		
	$m(\mathrm{LQ}_3^{\mathrm{d}}) = 400\,\mathrm{GeV},\ B = 0.9$	9 ± 4	18 ± 9	63 ± 9		
D	Observed	-			27	11
	SM Total	-			25 ± 6	8.5 ± 1.5
	$m(\mathrm{LQ}_3^{\mathrm{d}}) = 800\,\mathrm{GeV},\ B = 0.9$	-			2.87 ± 0.35	1.45 ± 0.23

Table 5. Number of observed events in SRA, SRB, and SRD, together with the number of fitted background events including their total uncertainty, taken from ref. [23] (CR background-only fit). Additionally, the expected number of signal events for different branching ratios and LQ masses close to the exclusion limits are given with statistical uncertainties.

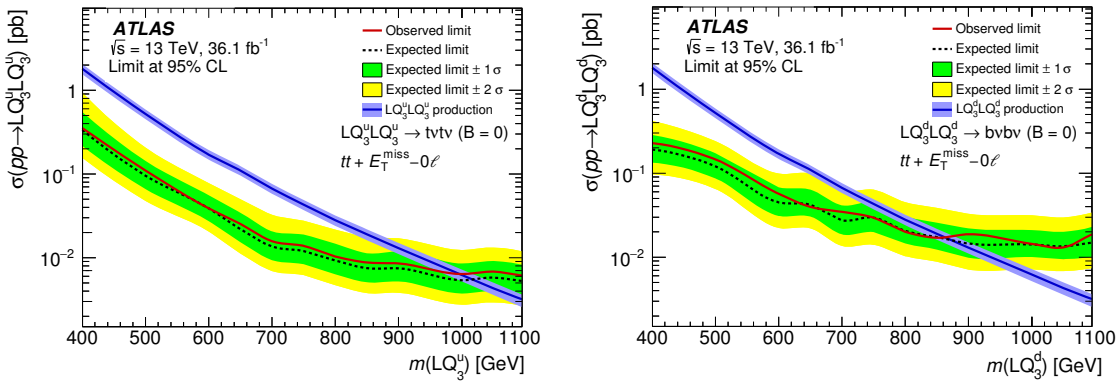

Figure 12. Observed and expected 95% CL upper limits on the cross-section for up-type (left panel) and down-type (right panel) LQ pair production with $B = 0$ as a function of the LQ mass. The $\pm 1(2)\sigma$ uncertainty bands around the expected limit represent all sources of statistical and systematic uncertainties. In the right panel the expected limit has an undulated behaviour due to the use of different signal regions for different mass points and the statistical uncertainties of the background MC in SRD. The thickness of the theory curve represents the theoretical uncertainty from PDFs, renormalization and factorization scales, and the strong coupling constant α_{s}.

Events are classified according to the decay of the τ-leptons. Both the $\tau_{\mathrm{had}}\tau_{\mathrm{had}}$ and the $\tau_\ell\tau_{\mathrm{had}}$ channels are considered. Two signal selections are defined, one for the $\tau_\ell\tau_{\mathrm{had}}$ channel (SR LH) and another one for the $\tau_{\mathrm{had}}\tau_{\mathrm{had}}$ channel (SR HH). Both signal selections require the two leptons to have opposite electric charge. The main discriminating variables are $E_{\mathrm{T}}^{\mathrm{miss}}$ and the stransverse mass m_{T2}, which is a generalization of the transverse mass for final states with two invisible particles [46–48] and computed from the selected lepton pair and $E_{\mathrm{T}}^{\mathrm{miss}}$.

JHEP06(2019)144

The dominant background process with the targeted final-state signature is pair production of top quarks. As in the original analysis, two types of contributions are discriminated, depending on whether the identified hadronically decaying τ-lepton(s) in the selected event are real or candidate particles (typically jets, electrons, or, in rare cases, muons), which are misidentified as hadronically decaying τ-leptons (fake τ-leptons).

In the $\tau_\ell\tau_{\text{had}}$ channel, the contribution of events with fake τ-leptons is estimated using a data-driven method, which is based on a measurement of the number of hadronically decaying τ-leptons satisfying loose identification criteria that also pass the tighter analysis selection (fake-factor method). The contribution of events with true τ-leptons is estimated from simulation, using a dedicated control-region selection to normalize the overall contribution to the level observed in data. In the $\tau_{\text{had}}\tau_{\text{had}}$ channel, both the contributions with fake and with true τ-leptons are estimated from simulation with data-driven normalization factors obtained from two dedicated control regions. A requirement on the transverse mass computed from the transverse momentum of the leading τ-lepton and the missing transverse momentum is used to discriminate between events with true and fake τ-leptons. The requirement of opposite electric charge is not used for the control region targeting events with fake τ-leptons, since in that case the charges of the two τ-leptons are not correlated. Two additional control regions common to both channels are used to obtain data-driven normalization factors for the background contributions from diboson production and production of top-quark pairs in association with an additional W or Z boson. For these control regions, events that pass a single-lepton trigger and contain at least two signal leptons and two jets are used. The remaining definitions of these control regions and further details of the background estimation and its validation are in ref. [25]. Good agreement between data and predicted background yields is found in validation regions when the normalization factors derived in the control regions are applied.

The statistical analysis is done similarly to the one described in section 5. However, the signal regions are independent and can therefore be statistically combined in the fit. The expected number of events from the background-only fit and the number of observed events in the signal regions are shown in table 6 for the two analysis channels, together with the predicted event yields for a number of leptoquark signals. The number of observed events agrees with the predicted Standard Model background. Figure 13 shows the distribution of $m_{\text{T2}}(\ell, \tau_{\text{had}})$, one of the main discriminating variables, after applying all selection requirements of the signal region SR LH except for the one on $m_{\text{T2}}(\ell, \tau_{\text{had}})$, which is indicated by the vertical line and arrow instead. The stacked histograms in the plot are the expected Standard Model backgrounds. In addition, the stacked dashed histogram shows the predicted distribution of a benchmark signal model for up-type leptoquarks with a mass of 750 GeV and branching ratio $B = 0.5$. As no significant excess in the signal regions is observed in the data, upper limits are set on the production cross-section. Figure 14 shows the expected and observed cross-section limits as a function of the leptoquark mass both for up- and down-type leptoquarks. Leptoquark masses up to 780 GeV and 800 GeV are excluded for $B = 0.5$ at 95% confidence level for pair-produced up- and down-type leptoquarks, respectively.

JHEP06(2019)144

		SR HH	SR LH
Observed events		2	3
Total SM		1.9 ± 1.0	2.2 ± 0.6
$m(\mathrm{LQ}_3^{\mathrm{u}}) = 500$ GeV	$B = 0.5$	10.8 ± 3.4	27 ± 7
$m(\mathrm{LQ}_3^{\mathrm{u}}) = 750$ GeV	$B = 0$	< 0.1	1.0 ± 0.3
$m(\mathrm{LQ}_3^{\mathrm{u}}) = 750$ GeV	$B = 0.5$	2.6 ± 0.8	7.3 ± 1.5
$m(\mathrm{LQ}_3^{\mathrm{u}}) = 750$ GeV	$B = 1$	2.6 ± 0.9	0.33 ± 0.1
$m(\mathrm{LQ}_3^{\mathrm{u}}) = 1000$ GeV	$B = 0.5$	0.3 ± 0.09	1.1 ± 0.3
$m(\mathrm{LQ}_3^{\mathrm{d}}) = 500$ GeV	$B = 0.5$	25 ± 7	49 ± 11
$m(\mathrm{LQ}_3^{\mathrm{d}}) = 750$ GeV	$B = 0$	< 0.1	< 0.1
$m(\mathrm{LQ}_3^{\mathrm{d}}) = 750$ GeV	$B = 0.5$	1.9 ± 0.5	6.2 ± 1.5
$m(\mathrm{LQ}_3^{\mathrm{d}}) = 750$ GeV	$B = 1$	2.4 ± 1.1	2.5 ± 1.0
$m(\mathrm{LQ}_3^{\mathrm{d}}) = 1000$ GeV	$B = 0.5$	0.53 ± 0.16	1.6 ± 0.4

Table 6. The expected number of SM background events obtained from the background fit and the number of observed events in SR HH and SR LH, together with the expected number of signal events for different mass hypotheses m, leptoquark types, and branching ratios B into charged leptons.

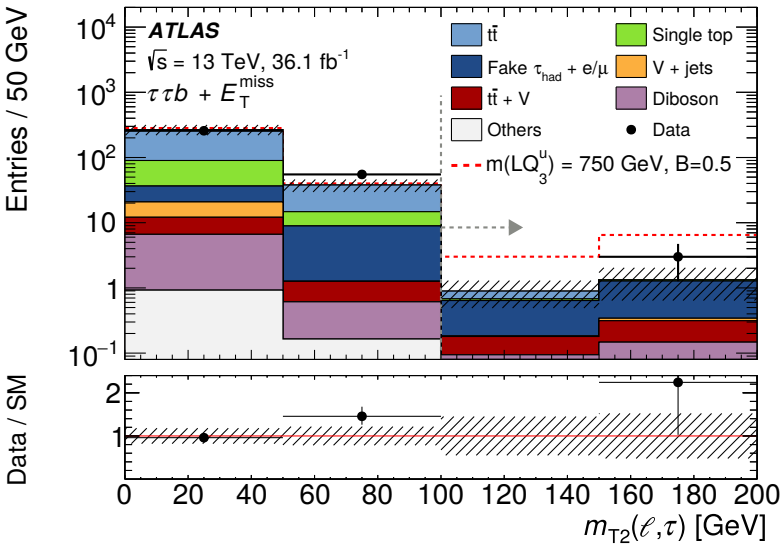

Figure 13. Distribution of the stransverse mass $m_{\mathrm{T2}}(\ell, \tau_{\mathrm{had}})$ [46–48] in the signal region of the $\tau_\ell\tau_{\mathrm{had}}$ channel before applying the selection requirement on $m_{\mathrm{T2}}(\ell, \tau_{\mathrm{had}})$, which is indicated by the dashed vertical line and arrow. The stacked histograms show the various SM background contributions, which are normalized to the values determined in the fit. The hatched band indicates the total statistical and systematic uncertainty in the SM background. The error bars on the black data points represent the statistical uncertainty in the data yields. The dashed histogram shows the expected additional yields from a leptoquark signal model $\mathrm{LQ}_3^{\mathrm{u}}$ with $m_{\mathrm{LQ}} = 750\,\mathrm{GeV}$ and $B = 0.5$ added on top of the SM prediction. The rightmost bin includes the overflow.

JHEP06(2019)144

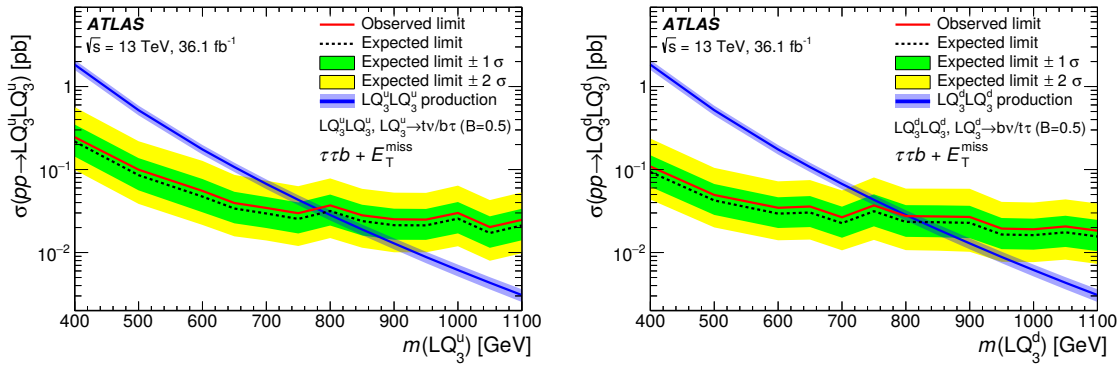

Figure 14. Expected cross-section limits, their combined statistical and systematic uncertainties excluding the theoretical cross-section uncertainty, and observed cross-sections limits at 95% CL for $B = 0.5$ as a function of the leptoquark mass. The two channels, $\tau_{\mathrm{had}}\tau_{\mathrm{had}}$ and $\tau_{\ell}\tau_{\mathrm{had}}$, are combined for the $\mathrm{LQ}_3^{\mathrm{u}}$ model (left) and $\mathrm{LQ}_3^{\mathrm{d}}$ model (right). Statistical fluctuations are present in the expected limits because of the low number of simulated signal events passing the comparably tight signal-region selections. The thickness of the band around the theoretical cross-section curve represents the uncertainty from PDFs, renormalization and factorization scales, and the strong coupling constant α_{s}.

For low leptoquark masses and high branching ratios into charged leptons, a non-negligible number of simulated signal events pass the control-region selections. This leads to the background normalization factors being biased towards lower values when obtained from the exclusion fits instead of the background-only fits, and drives the nuisance parameters for the systematic uncertainties away from their nominal values. Several tests were performed to check the validity of the fit procedure used to derive the exclusion. Signal-injection tests confirmed that the fit reliably reproduces the input signal yield. In addition, it was shown that artificially reducing the input signal yield for excluded phase-space regions with a high signal contamination in the control regions, thereby reducing the signal contamination, would still allow to exclude the leptoquark signal.

8 The bb plus $E_{\mathrm{T}}^{\mathrm{miss}}$ channel

The search for direct bottom-squark pair production in either the zero- or one-lepton channel [24] is reinterpreted in the context of LQ production. The analysis in the zero-lepton channel targets LQs which both decay into a bottom quark and a neutrino, i.e. $\mathrm{LQ}_3^{\mathrm{d}}$ production with $B = 0$. The one-lepton channel, also requiring two b-tagged jets and $E_{\mathrm{T}}^{\mathrm{miss}}$, is expected to provide sensitivity to $\mathrm{LQ}_3^{\mathrm{d}}$ production at intermediate values of B, as well as to small and intermediate values of B for $\mathrm{LQ}_3^{\mathrm{u}}$ production.

For the zero-lepton SRs (denoted by b0L), events with two high-p_{T} b-tagged jets, zero leptons, and a large amount of $E_{\mathrm{T}}^{\mathrm{miss}}$ are selected. An exclusive jet selection (requiring 2–4 jets) is applied, preventing sizeable sensitivities to $\mathrm{LQ}_3^{\mathrm{u}}$ production in this SR. Events with large $E_{\mathrm{T}}^{\mathrm{miss}}$ arising from mismeasured jets are rejected using a selection of $\left|\Delta\phi\left(\mathrm{jet}^{i}, E_{\mathrm{T}}^{\mathrm{miss}}\right)\right|_{(i=1\ldots4)} > 0.4$. The two b-jets are required to be the two leading jets in the event and their invariant mass must be greater than 200 GeV. After these baseline

JHEP06(2019)144

selections, three SRs are constructed using increasingly tighter selections on the contransverse mass m_{CT} [49], which targets pair-produced heavy objects that each decay in an identical way into a visible and an invisible particle. It is the main discriminating variable in the zero-lepton channel, with overlapping selections of $m_{\mathrm{CT}} > 350$, 450, and 550 GeV distinguishing the SRs.

For the one-lepton SRs (denoted by b1L), events with two b-tagged jets, one lepton (e/μ) with $p_{\mathrm{T}} > 27$ GeV, and large $E_{\mathrm{T}}^{\mathrm{miss}}$ are selected. Unlike the zero-lepton regions, an inclusive jet selection is used, with any two of the jets being tagged as b-jets. A selection of $\left|\Delta\phi\left(\mathrm{jet}^{i}, E_{\mathrm{T}}^{\mathrm{miss}}\right)\right| > 0.4$ for the four leading jets is used to reject events with large $E_{\mathrm{T}}^{\mathrm{miss}}$ from mismeasured jets. Selections on the minimum invariant mass of the lepton and one of the two b-jets, $m_{b,\ell}^{\mathrm{min}}$, and on am_{T2} are used to reduce the $t\bar{t}$ background, while a selection on m_{T} is used to reject W+jets events. After applying the previously introduced selections, two overlapping SRs are designed using m_{eff}, the scalar sum of the p_{T} of the jets and the $E_{\mathrm{T}}^{\mathrm{miss}}$, as the main discriminating variable. The SRs are designed with selections of either $m_{\mathrm{eff}} > 600$ or 750 GeV.

The dominant backgrounds in the analysis are dependent upon the lepton multiplicity of the SR under consideration. For the zero-lepton SRs, the main SM background is Z-boson production ($Z \to \nu\nu$) in association with b-jets. Other significant sources of background arise from $t\bar{t}$ pair production, single-top Wt production, and W-boson production in association with b-jets. Control regions are defined to constrain each of the aforementioned SM backgrounds, which are designed to be kinematically close, yet orthogonal, to the SRs and also mutually orthogonal to each other. A two-lepton CR is used to constrain the Z+jets process, where the invariant mass of the leptons is required to be near the Z-boson mass. The leptons are removed from the $E_{\mathrm{T}}^{\mathrm{miss}}$ calculation to mimic the expected $E_{\mathrm{T}}^{\mathrm{miss}}$ from the $Z \to \nu\nu$ process. The $t\bar{t}$, single-top, and W+jets processes are constrained in three one-lepton CRs: one CR with an inverted (relative to the SR) am_{T2} selection to create a region dominated by $t\bar{t}$; a region with an inverted m_{T} selection to constrain W+jets; and a final region with an inverted $m_{b,\ell}^{\mathrm{min}}$ selection to constrain single-top production. For the one-lepton SRs, the main SM backgrounds are $t\bar{t}$ pair production and single-top production. A one-lepton CR is designed to constrain the $t\bar{t}$ background by inverting the SR am_{T2} selection. The single-top background is constrained using the same CR as used for the zero-lepton single-top background. Signal contamination in these CRs is below 10% in all regions.

The statistical analysis is done in full analogy to the one described in section 5. The number of observed events in data for each SR and the expected post-fit SM background yields are presented in table 7. Two example LQ signal sample yields with $m_{\mathrm{LQ}} = 750$ GeV are presented for comparison, with various assumptions about the branching ratio. Figure 15 presents the distributions of four key kinematic variables in the SRs, with two signal samples added on top of the SM background. The top row shows the m_{CT} and $E_{\mathrm{T}}^{\mathrm{miss}}$ in the zero-lepton b0L_SRA350 region. The bottom row shows the am_{T2} and m_{eff} in the one-lepton b1L_SRA600 region.

JHEP06(2019)144

SR selection	b0L_SRA350	b0L_SRA450	b0L_SRA550	b1L_SRA600	b1L_SRA750
Observed events	81	24	10	21	13
Fitted bkg events	70.1 ± 13.0	21.4 ± 4.5	7.2 ± 1.5	23.0 ± 5.4	14.4 ± 3.6
$m_{\mathrm{LQ}} = 750\,\mathrm{GeV}$					
$B(\mathrm{LQ}_3^{\mathrm{d}} \to t\tau) = 1.0$	< 0.1	< 0.1	< 0.1	0.4 ± 0.2	0.4 ± 0.2
$B(\mathrm{LQ}_3^{\mathrm{d}} \to t\tau) = 0.5$	28.4 ± 1.7	18.1 ± 1.5	7.6 ± 0.9	5.1 ± 0.8	5.0 ± 0.9
$B(\mathrm{LQ}_3^{\mathrm{d}} \to t\tau) = 0.0$	107.1 ± 6.7	68.3 ± 5.8	29.6 ± 3.7	0.3 ± 0.2	0.3 ± 0.2
$B(\mathrm{LQ}_3^{\mathrm{u}} \to b\tau) = 1.0$	1.3 ± 0.6	0.8 ± 0.5	0.2 ± 0.2	0.6 ± 0.4	0.6 ± 0.3
$B(\mathrm{LQ}_3^{\mathrm{u}} \to b\tau) = 0.5$	2.4 ± 0.4	1.5 ± 0.3	0.3 ± 0.1	10.2 ± 1.1	9.6 ± 0.1
$B(\mathrm{LQ}_3^{\mathrm{u}} \to b\tau) = 0.0$	2.6 ± 1.0	1.7 ± 0.6	0.4 ± 0.3	16.7 ± 3.3	14.7 ± 0.3

Table 7. Number of observed events and background-only fit results in the SRs. The uncertainties contain both the statistical and systematic uncertainties. Two example LQ signal samples are also shown for comparison, with various assumptions about $B(\mathrm{LQ} \to q\tau)$.

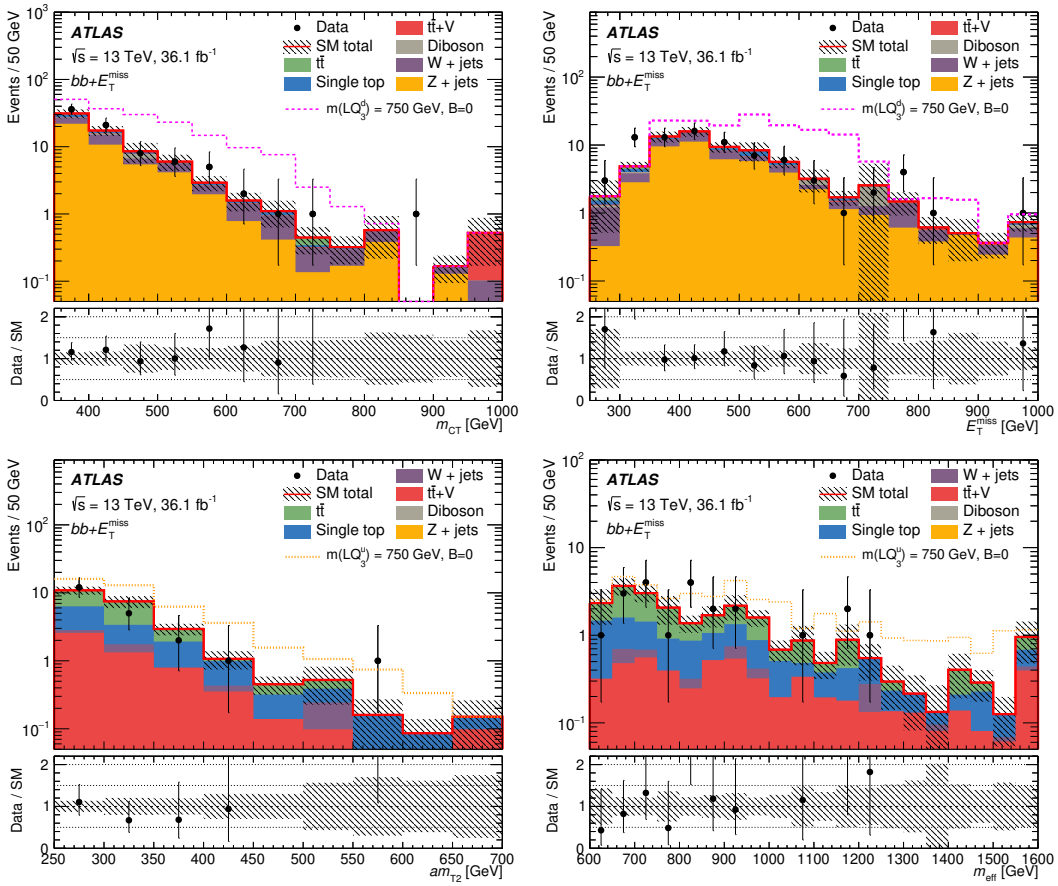

Figure 15. Distributions for key kinematic variables in the zero- and one-lepton SR selections for the contransverse mass, m_{CT} [49] and $E_{\mathrm{T}}^{\mathrm{miss}}$ in the zero-lepton SR (top) and am_{T2} [43] and m_{eff} in the one-lepton SRs (bottom). Two example LQ signal samples are added on top of the SM background, $\mathrm{LQ}_3^{\mathrm{d}}$ (dashed lines top plots) and $\mathrm{LQ}_3^{\mathrm{u}}$ (dashed lines bottom plots). The assumed $B(\mathrm{LQ} \to q\tau)$ for both signal samples is zero, and m_{LQ} is 750 GeV. The expected SM backgrounds are normalized to the values determined in the fit. The last bin contains the overflow events.

JHEP06(2019)144

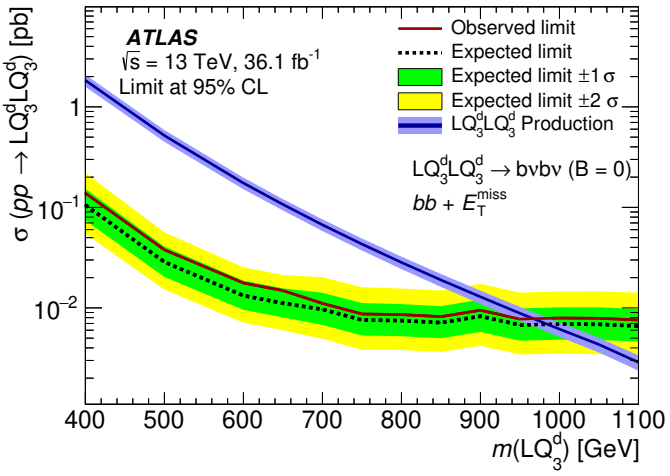

Figure 16. Observed and expected 95% CL upper limits on the cross-section for down-type LQ pair production with $B = 0$ as a function of the LQ mass. The $\pm 1(2)\sigma$ uncertainty bands around the expected limit represent all sources of statistical and systematic uncertainties. The thickness of the theory curve represents the theoretical uncertainty from PDFs, renormalization and factorization scales, and the strong coupling constant α_s.

The combination of the exclusion limits for the SRs is obtained by selecting the signal region with the best expected limit for each mass point. The expected and observed exclusion limits on the cross-section for $\mathrm{LQ}_3^{\mathrm{d}}$ and $B = 0$ are shown in figure 16 as a function of the leptoquark mass. Also shown is the theoretical prediction for the cross-section of scalar leptoquark pair production including the uncertainties. The expected and observed 95% CL lower limits on the mass of a down-type LQ decaying into $b\nu\bar{b}\bar{\nu}$ are 980 GeV and 970 GeV, respectively.

9 Limits on the LQ mass as a function of B

The limits on cross-section and mass for a fixed value of B that is expected to have the highest sensitivity for the respective analysis, are presented in the previous five sections. Here, figure 17 shows the limits on the LQ mass as a function of B for all five analyses for $\mathrm{LQ}_3^{\mathrm{u}}$ and $\mathrm{LQ}_3^{\mathrm{d}}$ pair production. The region to the left of the contour lines is excluded at 95% confidence level.

The strongest limits in terms of mass exclusion are for $\mathrm{LQ}_3^{\mathrm{u}}$ for $B = 1$ and $B = 0$ in the $b\tau b\tau$ and tt+$E_{\mathrm{T}}^{\mathrm{miss}}$ channel, respectively, and for $\mathrm{LQ}_3^{\mathrm{d}}$ for $B = 0$ in the bb+$E_{\mathrm{T}}^{\mathrm{miss}}$ channel. These are the cases where the channels are optimized ($b\tau b\tau$) or optimal (tt+$E_{\mathrm{T}}^{\mathrm{miss}}$, bb+$E_{\mathrm{T}}^{\mathrm{miss}}$), as discussed in the introduction. However, as can be seen from figure 17, all channels exhibit good sensitivities to both types of LQs and to a larger range of B values, except for the tt+$E_{\mathrm{T}}^{\mathrm{miss}}-1\ell$ channel, which is not sensitive to $\mathrm{LQ}_3^{\mathrm{d}}$ mainly due to the requirement of exactly one lepton.

Therefore, good sensitivity to both types of LQs at all values of B is obtained, excluding masses below 800 GeV for both $\mathrm{LQ}_3^{\mathrm{u}}$ and $\mathrm{LQ}_3^{\mathrm{d}}$ independently of the branching ratio, with masses below 1000 GeV and 1030 GeV (970 GeV and 920 GeV) being excluded for the limiting cases of B equal to zero and unity for $\mathrm{LQ}_3^{\mathrm{u}}$ ($\mathrm{LQ}_3^{\mathrm{d}}$).

JHEP06(2019)144

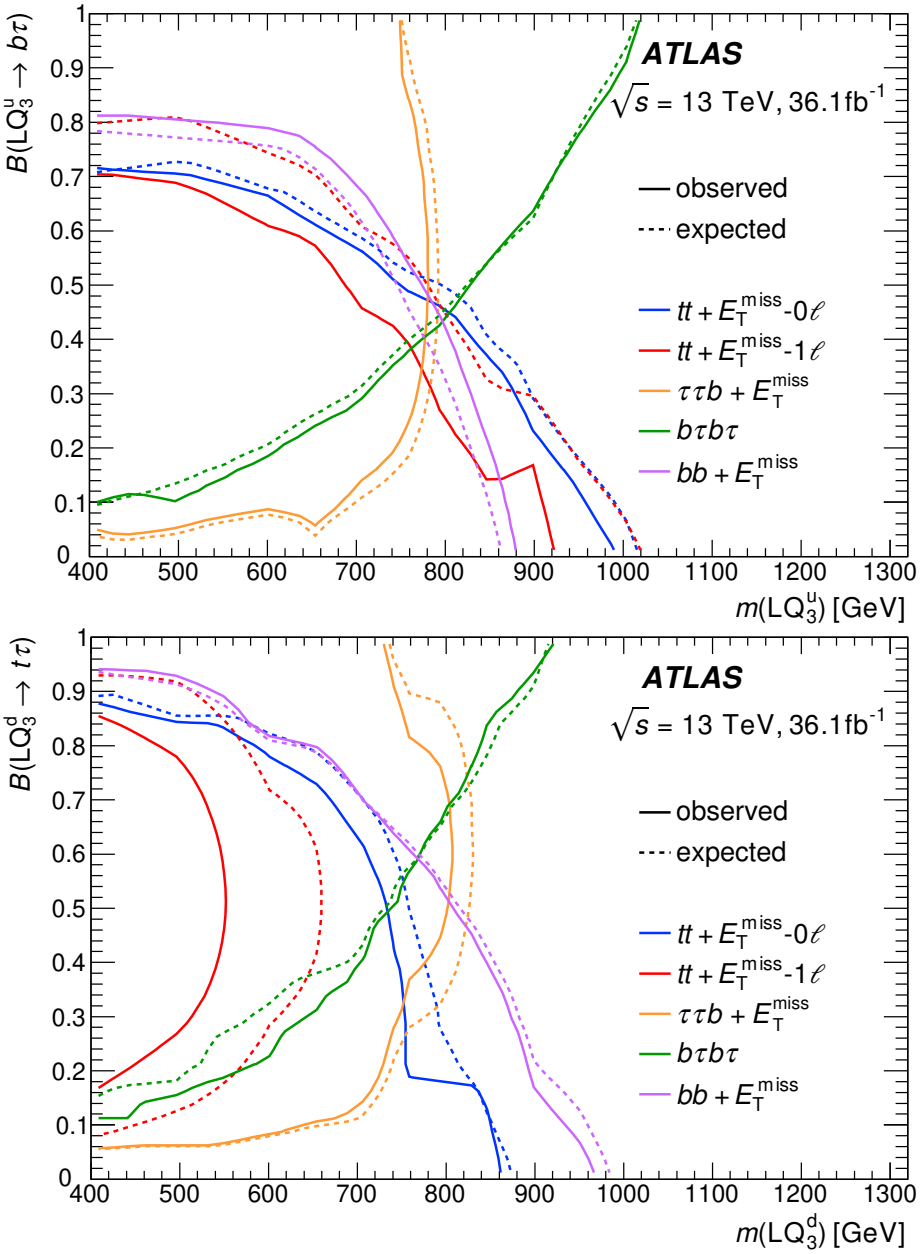

Figure 17. Limits on the branching ratio into charged leptons for scalar third-generation up-type (upper panel) leptoquark pair production ($LQ_3^u \to b\tau/t\nu$) and down-type (lower panel) leptoquark pair production ($LQ_3^d \to t\tau/b\nu$) as a function of the leptoquark mass. The limits are based on a dedicated LQ search for two b-jets and two τ-leptons ($b\tau b\tau$), and reinterpretations of the search for bottom-squark pair production (bb+E_T^{miss}) [24], for top-squark pair production with one (tt+E_T^{miss}-1ℓ) [22] or zero leptons (tt+E_T^{miss}-0ℓ) [23] in the final state, and for top squarks decaying via τ-sleptons ($\tau\tau b$+E_T^{miss}) [25]. The region to the left of the contour lines is excluded at 95% confidence level.

JHEP06(2019)144

10 Conclusion

Pair production of scalar third-generation leptoquarks is investigated for all possible decays of the leptoquarks into a quark (t, b) and a lepton (τ, ν) of the third generation. LHC proton-proton collision data recorded by the ATLAS detector in 2015 and 2016 at a centre-of-mass energy of $\sqrt{s} = 13\,\text{TeV}$ are used, with an integrated luminosity of $36.1\,\text{fb}^{-1}$. The results are based on reinterpretations of previously published ATLAS results as well as a dedicated search, where no significant excess above the SM background expectation is observed.

Upper limits on the LQ pair-production cross-section as a function of the LQ mass are reported for both the up-type ($\text{LQ}_3^{\text{u}} \to t\nu/b\tau$) and down-type ($\text{LQ}_3^{\text{d}} \to b\nu/t\tau$) leptoquarks for branching ratios into charged leptons equal to zero, 0.5, or unity. Based on the theoretical prediction for the LQ pair-production cross-section, these upper limits on the cross-section can be converted to lower limits on the mass, excluding leptoquarks with masses below about 1 TeV for both LQ types and for both limiting cases of branching ratios into charged leptons of zero or unity.

In addition, mass limits are shown as a function of the branching ratio into charged leptons for both the up- and down-type leptoquarks. Even for intermediate values of the branching ratio, masses below at least 800 GeV are excluded. These mass limits quickly increase to about 1 TeV for small and large branching ratios.

Acknowledgments

We thank CERN for the very successful operation of the LHC, as well as the support staff from our institutions without whom ATLAS could not be operated efficiently.

We acknowledge the support of ANPCyT, Argentina; YerPhI, Armenia; ARC, Australia; BMWFW and FWF, Austria; ANAS, Azerbaijan; SSTC, Belarus; CNPq and FAPESP, Brazil; NSERC, NRC and CFI, Canada; CERN; CONICYT, Chile; CAS, MOST and NSFC, China; COLCIENCIAS, Colombia; MSMT CR, MPO CR and VSC CR, Czech Republic; DNRF and DNSRC, Denmark; IN2P3-CNRS, CEA-DRF/IRFU, France; SRNSFG, Georgia; BMBF, HGF, and MPG, Germany; GSRT, Greece; RGC, Hong Kong SAR, China; ISF and Benoziyo Center, Israel; INFN, Italy; MEXT and JSPS, Japan; CNRST, Morocco; NWO, Netherlands; RCN, Norway; MNiSW and NCN, Poland; FCT, Portugal; MNE/IFA, Romania; MES of Russia and NRC KI, Russian Federation; JINR; MESTD, Serbia; MSSR, Slovakia; ARRS and MIZŠ, Slovenia; DST/NRF, South Africa; MINECO, Spain; SRC and Wallenberg Foundation, Sweden; SERI, SNSF and Cantons of Bern and Geneva, Switzerland; MOST, Taiwan; TAEK, Turkey; STFC, United Kingdom; DOE and NSF, United States of America. In addition, individual groups and members have received support from BCKDF, CANARIE, CRC and Compute Canada, Canada; COST, ERC, ERDF, Horizon 2020, and Marie Skłodowska-Curie Actions, European Union; Investissements d' Avenir Labex and Idex, ANR, France; DFG and AvH Foundation, Germany; Herakleitos, Thales and Aristeia programmes co-financed by EU-ESF and the Greek NSRF, Greece; BSF-NSF and GIF, Israel; CERCA Programme Generalitat de Catalunya, Spain; The Royal Society and Leverhulme Trust, United Kingdom.

JHEP06(2019)144

The crucial computing support from all WLCG partners is acknowledged gratefully, in particular from CERN, the ATLAS Tier-1 facilities at TRIUMF (Canada), NDGF (Denmark, Norway, Sweden), CC-IN2P3 (France), KIT/GridKA (Germany), INFN-CNAF (Italy), NL-T1 (Netherlands), PIC (Spain), ASGC (Taiwan), RAL (U.K.) and BNL (U.S.A.), the Tier-2 facilities worldwide and large non-WLCG resource providers. Major contributors of computing resources are listed in ref. [50].

JHEP06(2019)144

References

[1] S. Dimopoulos and L. Susskind, *Mass Without Scalars*, *Nucl. Phys.* **B 155** (1979) 237 [INSPIRE].

[2] S. Dimopoulos, *Technicolored Signatures*, *Nucl. Phys.* **B 168** (1980) 69 [INSPIRE].

[3] E. Eichten and K.D. Lane, *Dynamical Breaking of Weak Interaction Symmetries*, *Phys. Lett.* **90B** (1980) 125 [INSPIRE].

[4] V.D. Angelopoulos, J.R. Ellis, H. Kowalski, D.V. Nanopoulos, N.D. Tracas and F. Zwirner, *Search for New Quarks Suggested by the Superstring*, *Nucl. Phys.* **B 292** (1987) 59 [INSPIRE].

[5] W. Buchmüller and D. Wyler, *Constraints on* SU(5) *Type Leptoquarks*, *Phys. Lett.* **B 177** (1986) 377 [INSPIRE].

[6] J.C. Pati and A. Salam, *Lepton Number as the Fourth Color*, *Phys. Rev.* **D 10** (1974) 275 [*Erratum ibid.* **D 11** (1975) 703] [INSPIRE].

[7] H. Georgi and S.L. Glashow, *Unity of All Elementary Particle Forces*, *Phys. Rev. Lett.* **32** (1974) 438 [INSPIRE].

[8] G. Hiller and M. Schmaltz, R_K *and future* $b \to s\ell\ell$ *physics beyond the standard model opportunities*, *Phys. Rev.* **D 90** (2014) 054014 [arXiv:1408.1627] [INSPIRE].

[9] B. Gripaios, M. Nardecchia and S.A. Renner, *Composite leptoquarks and anomalies in B-meson decays*, *JHEP* **05** (2015) 006 [arXiv:1412.1791] [INSPIRE].

[10] M. Freytsis, Z. Ligeti and J.T. Ruderman, *Flavor models for* $\bar{B} \to D^{(*)}\tau\bar{\nu}$, *Phys. Rev.* **D 92** (2015) 054018 [arXiv:1506.08896] [INSPIRE].

[11] M. Bauer and M. Neubert, *Minimal Leptoquark Explanation for the* $R_{D^{(*)}}$, R_K *and* $(g-2)_g$ *Anomalies*, *Phys. Rev. Lett.* **116** (2016) 141802 [arXiv:1511.01900] [INSPIRE].

[12] L. Di Luzio and M. Nardecchia, *What is the scale of new physics behind the B-flavour anomalies?*, *Eur. Phys. J.* **C 77** (2017) 536 [arXiv:1706.01868] [INSPIRE].

[13] D. Buttazzo, A. Greljo, G. Isidori and D. Marzocca, *B-physics anomalies: a guide to combined explanations*, *JHEP* **11** (2017) 044 [arXiv:1706.07808] [INSPIRE].

[14] J.M. Cline, *B decay anomalies and dark matter from vectorlike confinement*, *Phys. Rev.* **D 97** (2018) 015013 [arXiv:1710.02140] [INSPIRE].

[15] W. Buchmüller, R. Ruckl and D. Wyler, *Leptoquarks in lepton-quark collisions*, *Phys. Lett.* **B 191** (1987) 442 [*Erratum ibid.* **B 448** (1999) 320] [INSPIRE].

[16] ATLAS collaboration, *Searches for scalar leptoquarks and differential cross-section measurements in dilepton-dijet events in proton-proton collisions at a centre-of-mass energy of* $\sqrt{s} = 13$ *TeV with the ATLAS experiment*, arXiv:1902.00377 [INSPIRE].

[17] ATLAS collaboration, *Searches for scalar leptoquarks in pp collisions at $\sqrt{s} = 8$ TeV with the ATLAS detector*, *Eur. Phys. J.* **C 76** (2016) 5 [arXiv:1508.04735] [INSPIRE].

[18] CMS collaboration, *Constraints on models of scalar and vector leptoquarks decaying to a quark and a neutrino at $\sqrt{s} = 13$ TeV*, *Phys. Rev.* **D 98** (2018) 032005 [arXiv:1805.10228] [INSPIRE].

[19] CMS collaboration, *Search for heavy neutrinos and third-generation leptoquarks in hadronic states of two τ leptons and two jets in proton-proton collisions at $\sqrt{s} = 13$ TeV*, *JHEP* **03** (2019) 170 [arXiv:1811.00806] [INSPIRE].

[20] CMS collaboration, *Search for third-generation scalar leptoquarks decaying to a top quark and a τ lepton at $\sqrt{s} = 13$ TeV*, *Eur. Phys. J.* **C 78** (2018) 707 [arXiv:1803.02864] [INSPIRE].

[21] ATLAS collaboration, *Search for resonant and non-resonant Higgs boson pair production in the $b\bar{b}\tau^+\tau^-$ decay channel in pp collisions at $\sqrt{s} = 13$ TeV with the ATLAS detector*, *Phys. Rev. Lett.* **121** (2018) 191801 [*Erratum ibid.* **122** (2019) 089901] [arXiv:1808.00336] [INSPIRE].

[22] ATLAS collaboration, *Search for top-squark pair production in final states with one lepton, jets and missing transverse momentum using 36 fb^{-1} of $\sqrt{s} = 13$ TeV pp collision data with the ATLAS detector*, *JHEP* **06** (2018) 108 [arXiv:1711.11520] [INSPIRE].

[23] ATLAS collaboration, *Search for a scalar partner of the top quark in the jets plus missing transverse momentum final state at $\sqrt{s} = 13$ TeV with the ATLAS detector*, *JHEP* **12** (2017) 085 [arXiv:1709.04183] [INSPIRE].

[24] ATLAS collaboration, *Search for supersymmetry in events with b-tagged jets and missing transverse momentum in pp collisions at $\sqrt{s} = 13$ TeV with the ATLAS detector*, *JHEP* **11** (2017) 195 [arXiv:1708.09266] [INSPIRE].

[25] ATLAS collaboration, *Search for top squarks decaying to tau sleptons in pp collisions at $\sqrt{s} = 13$ TeV with the ATLAS detector*, *Phys. Rev.* **D 98** (2018) 032008 [arXiv:1803.10178] [INSPIRE].

[26] ATLAS collaboration, *The ATLAS Experiment at the CERN Large Hadron Collider*, 2008 *JINST* **3** S08003 [INSPIRE].

[27] ATLAS collaboration, *ATLAS Insertable B-Layer Technical Design Report*, ATLAS-TDR-19 (2010).

[28] ATLAS collaboration, *ATLAS Insertable B-Layer Technical Design Report Addendum*, ATLAS-TDR-19-ADD-1 (2012).

[29] ATLAS collaboration, *Early Inner Detector Tracking Performance in the 2015 data at $\sqrt{s} = 13$ TeV*, ATL-PHYS-PUB-2015-051 (2015).

[30] ATLAS collaboration, *Performance of the ATLAS Trigger System in 2015*, *Eur. Phys. J.* **C 77** (2017) 317 [arXiv:1611.09661] [INSPIRE].

[31] J. Alwall et al., *The automated computation of tree-level and next-to-leading order differential cross sections and their matching to parton shower simulations*, *JHEP* **07** (2014) 079 [arXiv:1405.0301] [INSPIRE].

[32] T. Mandal, S. Mitra and S. Seth, *Pair Production of Scalar Leptoquarks at the LHC to NLO Parton Shower Accuracy*, *Phys. Rev.* **D 93** (2016) 035018 [arXiv:1506.07369] [INSPIRE].

[33] M. Krämer, T. Plehn, M. Spira and P.M. Zerwas, *Pair production of scalar leptoquarks at the CERN LHC*, *Phys. Rev.* **D 71** (2005) 057503 [hep-ph/0411038] [INSPIRE].

JHEP06(2019)144

[34] NNPDF collaboration, *Parton distributions for the LHC Run II*, *JHEP* **04** (2015) 040 [arXiv:1410.8849] [INSPIRE].

[35] T. Sjöstrand et al., *An Introduction to PYTHIA 8.2*, *Comput. Phys. Commun.* **191** (2015) 159 [arXiv:1410.3012] [INSPIRE].

[36] ATLAS collaboration, *ATLAS Run 1 PYTHIA8 tunes*, ATL-PHYS-PUB-2014-021 (2014).

[37] C. Borschensky et al., *Squark and gluino production cross sections in pp collisions at* $\sqrt{s} = 13$*,* 14*,* 33 *and* 100 *TeV*, *Eur. Phys. J.* **C 74** (2014) 3174 [arXiv:1407.5066] [INSPIRE].

[38] P. Artoisenet, R. Frederix, O. Mattelaer and R. Rietkerk, *Automatic spin-entangled decays of heavy resonances in Monte Carlo simulations*, *JHEP* **03** (2013) 015 [arXiv:1212.3460] [INSPIRE].

[39] A. Belyaev, C. Leroy, R. Mehdiyev and A. Pukhov, *Leptoquark single and pair production at LHC with CalcHEP/CompHEP in the complete model*, *JHEP* **09** (2005) 005 [hep-ph/0502067] [INSPIRE].

[40] ATLAS collaboration, *Electron reconstruction and identification efficiency measurements with the ATLAS detector using the 2011 LHC proton-proton collision data*, *Eur. Phys. J.* **C 74** (2014) 2941 [arXiv:1404.2240] [INSPIRE].

[41] ATLAS collaboration, *Muon reconstruction performance of the ATLAS detector in proton-proton collision data at* $\sqrt{s} = 13$ *TeV*, *Eur. Phys. J.* **C 76** (2016) 292 [arXiv:1603.05598] [INSPIRE].

[42] A.L. Read, *Modified frequentist analysis of search results (the* CL_s *method)*, CERN-OPEN-2000-205 (2000).

[43] P. Konar, K. Kong, K.T. Matchev and M. Park, *Dark Matter Particle Spectroscopy at the LHC: Generalizing* M_{T_2} *to Asymmetric Event Topologies*, *JHEP* **04** (2010) 086 [arXiv:0911.4126] [INSPIRE].

[44] M. Cacciari, G.P. Salam and G. Soyez, *The anti-*k_t *jet clustering algorithm*, *JHEP* **04** (2008) 063 [arXiv:0802.1189] [INSPIRE].

[45] G. Cowan, K. Cranmer, E. Gross and O. Vitells, *Asymptotic formulae for likelihood-based tests of new physics*, *Eur. Phys. J.* **C 71** (2011) 1554 [*Erratum ibid.* **C 73** (2013) 2501] [arXiv:1007.1727] [INSPIRE].

[46] C.G. Lester and D.J. Summers, *Measuring masses of semiinvisibly decaying particles pair produced at hadron colliders*, *Phys. Lett.* **B 463** (1999) 99 [hep-ph/9906349] [INSPIRE].

[47] A. Barr, C. Lester and P. Stephens, *A variable for measuring masses at hadron colliders when missing energy is expected;* m_{T2}*: the truth behind the glamour*, *J. Phys.* **G 29** (2003) 2343 [hep-ph/0304226] [INSPIRE].

[48] C.G. Lester and B. Nachman, *Bisection-based asymmetric* M_{T2} *computation: a higher precision calculator than existing symmetric methods*, *JHEP* **03** (2015) 100 [arXiv:1411.4312] [INSPIRE].

[49] D.R. Tovey, *On measuring the masses of pair-produced semi-invisibly decaying particles at hadron colliders*, *JHEP* **04** (2008) 034 [arXiv:0802.2879] [INSPIRE].

[50] ATLAS collaboration, *ATLAS Computing Acknowledgements*, ATL-GEN-PUB-2016-002 (2016).

JHEP06(2019)144

The ATLAS collaboration

M. Aaboud[34d], G. Aad[100], B. Abbott[126], D.C. Abbott[101], O. Abdinov[13,*], D.K. Abhayasinghe[92], S.H. Abidi[165], O.S. AbouZeid[39], N.L. Abraham[154], H. Abramowicz[159], H. Abreu[158], Y. Abulaiti[6], B.S. Acharya[65a,65b,o], S. Adachi[161], L. Adam[98], L. Adamczyk[82a], L. Adamek[165], J. Adelman[120], M. Adersberger[113], A. Adiguzel[12c,ah], T. Adye[142], A.A. Affolder[144], Y. Afik[158], C. Agapopoulou[130], M.N. Agaras[37], A. Aggarwal[118], C. Agheorghiesei[27c], J.A. Aguilar-Saavedra[138f,138a,ag], F. Ahmadov[78], G. Aielli[72a,72b], S. Akatsuka[84], T.P.A. Åkesson[95], E. Akilli[53], A.V. Akimov[109], K. Al Khoury[130], G.L. Alberghi[23b,23a], J. Albert[174], M.J. Alconada Verzini[87], S. Alderweireldt[118], M. Aleksa[35], I.N. Aleksandrov[78], C. Alexa[27b], D. Alexandre[19], T. Alexopoulos[10], M. Alhroob[126], B. Ali[140], G. Alimonti[67a], J. Alison[36], S.P. Alkire[146], C. Allaire[130], B.M.M. Allbrooke[154], B.W. Allen[129], P.P. Allport[21], A. Aloisio[68a,68b], A. Alonso[39], F. Alonso[87], C. Alpigiani[146], A.A. Alshehri[56], M.I. Alstaty[100], M. Alvarez Estevez[97], B. Alvarez Gonzalez[35], D. Álvarez Piqueras[172], M.G. Alviggi[68a,68b], Y. Amaral Coutinho[79b], A. Ambler[102], L. Ambroz[133], C. Amelung[26], D. Amidei[104], S.P. Amor Dos Santos[138a,138c], S. Amoroso[45], C.S. Amrouche[53], F. An[77], C. Anastopoulos[147], N. Andari[143], T. Andeen[11], C.F. Anders[60b], J.K. Anders[20], A. Andreazza[67a,67b], V. Andrei[60a], C.R. Anelli[174], S. Angelidakis[37], I. Angelozzi[119], A. Angerami[38], A.V. Anisenkov[121b,121a], A. Annovi[70a], C. Antel[60a], M.T. Anthony[147], M. Antonelli[50], D.J.A. Antrim[169], F. Anulli[71a], M. Aoki[80], J.A. Aparisi Pozo[172], L. Aperio Bella[35], G. Arabidze[105], J.P. Araque[138a], V. Araujo Ferraz[79b], R. Araujo Pereira[79b], A.T.H. Arce[48], F.A. Arduh[87], J-F. Arguin[108], S. Argyropoulos[76], J.-H. Arling[45], A.J. Armbruster[35], L.J. Armitage[91], A. Armstrong[169], O. Arnaez[165], H. Arnold[119], A. Artamonov[110,*], G. Artoni[133], S. Artz[98], S. Asai[161], N. Asbah[58], E.M. Asimakopoulou[170], L. Asquith[154], K. Assamagan[29], R. Astalos[28a], R.J. Atkin[32a], M. Atkinson[171], N.B. Atlay[149], K. Augsten[140], G. Avolio[35], R. Avramidou[59a], M.K. Ayoub[15a], A.M. Azoulay[166b], G. Azuelos[108,av], A.E. Baas[60a], M.J. Baca[21], H. Bachacou[143], K. Bachas[66a,66b], M. Backes[133], F. Backman[44a,44b], P. Bagnaia[71a,71b], M. Bahmani[83], H. Bahrasemani[150], A.J. Bailey[172], V.R. Bailey[171], J.T. Baines[142], M. Bajic[39], C. Bakalis[10], O.K. Baker[181], P.J. Bakker[119], D. Bakshi Gupta[8], S. Balaji[155], E.M. Baldin[121b,121a], P. Balek[178], F. Balli[143], W.K. Balunas[133], J. Balz[98], E. Banas[83], A. Bandyopadhyay[24], S. Banerjee[179,k], A.A.E. Bannoura[180], L. Barak[159], W.M. Barbe[37], E.L. Barberio[103], D. Barberis[54b,54a], M. Barbero[100], T. Barillari[114], M-S. Barisits[35], J. Barkeloo[129], T. Barklow[151], R. Barnea[158], S.L. Barnes[59c], B.M. Barnett[142], R.M. Barnett[18], Z. Barnovska-Blenessy[59a], A. Baroncelli[59a], G. Barone[29], A.J. Barr[133], L. Barranco Navarro[172], F. Barreiro[97], J. Barreiro Guimarães da Costa[15a], R. Bartoldus[151], A.E. Barton[88], P. Bartos[28a], A. Basalaev[45], A. Bassalat[130], R.L. Bates[56], S.J. Batista[165], S. Batlamous[34e], J.R. Batley[31], M. Battaglia[144], M. Bauce[71a,71b], F. Bauer[143], K.T. Bauer[169], H.S. Bawa[151], J.B. Beacham[124], T. Beau[134], P.H. Beauchemin[168], P. Bechtle[24], H.C. Beck[52], H.P. Beck[20,r], K. Becker[51], M. Becker[98], C. Becot[45], A. Beddall[12d], A.J. Beddall[12a], V.A. Bednyakov[78], M. Bedognetti[119], C.P. Bee[153], T.A. Beermann[75], M. Begalli[79b], M. Begel[29], A. Behera[153], J.K. Behr[45], F. Beisiegel[24], A.S. Bell[93], G. Bella[159], L. Bellagamba[23b], A. Bellerive[33], P. Bellos[9], K. Beloborodov[121b,121a], K. Belotskiy[111], N.L. Belyaev[111], O. Benary[159,*], D. Benchekroun[34a], N. Benekos[10], Y. Benhammou[159], D.P. Benjamin[6], M. Benoit[53], J.R. Bensinger[26], S. Bentvelsen[119], L. Beresford[133], M. Beretta[50], D. Berge[45], E. Bergeaas Kuutmann[170], N. Berger[5], B. Bergmann[140], L.J. Bergsten[26], J. Beringer[18], S. Berlendis[7], N.R. Bernard[101], G. Bernardi[134], C. Bernius[151], F.U. Bernlochner[24], T. Berry[92], P. Berta[98], C. Bertella[15a], G. Bertoli[44a,44b], I.A. Bertram[88], G.J. Besjes[39], O. Bessidskaia Bylund[180], N. Besson[143], A. Bethani[99], S. Bethke[114], A. Betti[24], A.J. Bevan[91], J. Beyer[114], R. Bi[137], R.M. Bianchi[137], O. Biebel[113],

JHEP06(2019)144

D. Biedermann[19], R. Bielski[35], K. Bierwagen[98], N.V. Biesuz[70a,70b], M. Biglietti[73a], T.R.V. Billoud[108], M. Bindi[52], A. Bingul[12d], C. Bini[71a,71b], S. Biondi[23b,23a], M. Birman[178], T. Bisanz[52], J.P. Biswal[159], A. Bitadze[99], C. Bittrich[47], D.M. Bjergaard[48], J.E. Black[151], K.M. Black[25], T. Blazek[28a], I. Bloch[45], C. Blocker[26], A. Blue[56], U. Blumenschein[91], Dr. Blunier[145a], G.J. Bobbink[119], V.S. Bobrovnikov[121b,121a], S.S. Bocchetta[95], A. Bocci[48], D. Boerner[45], D. Bogavac[113], A.G. Bogdanchikov[121b,121a], C. Bohm[44a], V. Boisvert[92], P. Bokan[52,170], T. Bold[82a], A.S. Boldyrev[112], A.E. Bolz[60b], M. Bomben[134], M. Bona[91], J.S. Bonilla[129], M. Boonekamp[143], H.M. Borecka-Bielska[89], A. Borisov[122], G. Borissov[88], J. Bortfeldt[35], D. Bortoletto[133], V. Bortolotto[72a,72b], D. Boscherini[23b], M. Bosman[14], J.D. Bossio Sola[30], K. Bouaouda[34a], J. Boudreau[137], E.V. Bouhova-Thacker[88], D. Boumediene[37], C. Bourdarios[130], S.K. Boutle[56], A. Boveia[124], J. Boyd[35], D. Boye[32b,ap], I.R. Boyko[78], A.J. Bozson[92], J. Bracinik[21], N. Brahimi[100], G. Brandt[180], O. Brandt[60a], F. Braren[45], U. Bratzler[162], B. Brau[101], J.E. Brau[129], W.D. Breaden Madden[56], K. Brendlinger[45], L. Brenner[45], R. Brenner[170], S. Bressler[178], B. Brickwedde[98], D.L. Briglin[21], D. Britton[56], D. Britzger[114], I. Brock[24], R. Brock[105], G. Brooijmans[38], T. Brooks[92], W.K. Brooks[145b], E. Brost[120], J.H Broughton[21], P.A. Bruckman de Renstrom[83], D. Bruncko[28b], A. Bruni[23b], G. Bruni[23b], L.S. Bruni[119], S. Bruno[72a,72b], B.H. Brunt[31], M. Bruschi[23b], N. Bruscino[137], P. Bryant[36], L. Bryngemark[95], T. Buanes[17], Q. Buat[35], P. Buchholz[149], A.G. Buckley[56], I.A. Budagov[78], M.K. Bugge[132], F. Bührer[51], O. Bulekov[111], T.J. Burch[120], S. Burdin[89], C.D. Burgard[119], A.M. Burger[127], B. Burghgrave[8], K. Burka[83], I. Burmeister[46], J.T.P. Burr[45], V. Büscher[98], E. Buschmann[52], P. Bussey[56], J.M. Butler[25], C.M. Buttar[56], J.M. Butterworth[93], P. Butti[35], W. Buttinger[35], A. Buzatu[156], A.R. Buzykaev[121b,121a], G. Cabras[23b,23a], S. Cabrera Urbán[172], D. Caforio[140], H. Cai[171], V.M.M. Cairo[2], O. Cakir[4a], N. Calace[35], P. Calafiura[18], A. Calandri[100], G. Calderini[134], P. Calfayan[64], G. Callea[56], L.P. Caloba[79b], S. Calvente Lopez[97], D. Calvet[37], S. Calvet[37], T.P. Calvet[153], M. Calvetti[70a,70b], R. Camacho Toro[134], S. Camarda[35], D. Camarero Munoz[97], P. Camarri[72a,72b], D. Cameron[132], R. Caminal Armadans[101], C. Camincher[35], S. Campana[35], M. Campanelli[93], A. Camplani[39], A. Campoverde[149], V. Canale[68a,68b], M. Cano Bret[59c], J. Cantero[127], T. Cao[159], Y. Cao[171], M.D.M. Capeans Garrido[35], M. Capua[40b,40a], R. Cardarelli[72a], F.C. Cardillo[147], I. Carli[141], T. Carli[35], G. Carlino[68a], B.T. Carlson[137], L. Carminati[67a,67b], R.M.D. Carney[44a,44b], S. Caron[118], E. Carquin[145b], S. Carrá[67a,67b], J.W.S. Carter[165], M.P. Casado[14,g], A.F. Casha[165], D.W. Casper[169], R. Castelijn[119], F.L. Castillo[172], V. Castillo Gimenez[172], N.F. Castro[138a,138e], A. Catinaccio[35], J.R. Catmore[132], A. Cattai[35], J. Caudron[24], V. Cavaliere[29], E. Cavallaro[14], D. Cavalli[67a], M. Cavalli-Sforza[14], V. Cavasinni[70a,70b], E. Celebi[12b], L. Cerda Alberich[172], A.S. Cerqueira[79a], A. Cerri[154], L. Cerrito[72a,72b], F. Cerutti[18], A. Cervelli[23b,23a], S.A. Cetin[12b], A. Chafaq[34a], D. Chakraborty[120], S.K. Chan[58], W.S. Chan[119], W.Y. Chan[89], J.D. Chapman[31], B. Chargeishvili[157b], D.G. Charlton[21], C.C. Chau[33], C.A. Chavez Barajas[154], S. Che[124], A. Chegwidden[105], S. Chekanov[6], S.V. Chekulaev[166a], G.A. Chelkov[78,au], M.A. Chelstowska[35], B. Chen[77], C. Chen[59a], C.H. Chen[77], H. Chen[29], J. Chen[59a], J. Chen[38], S. Chen[135], S.J. Chen[15c], X. Chen[15b,at], Y. Chen[81], Y-H. Chen[45], H.C. Cheng[62a], H.J. Cheng[15d], A. Cheplakov[78], E. Cheremushkina[122], R. Cherkaoui El Moursli[34e], E. Cheu[7], K. Cheung[63], T.J.A. Chevalérias[143], L. Chevalier[143], V. Chiarella[50], G. Chiarelli[70a], G. Chiodini[66a], A.S. Chisholm[35,21], A. Chitan[27b], I. Chiu[161], Y.H. Chiu[174], M.V. Chizhov[78], K. Choi[64], A.R. Chomont[130], S. Chouridou[160], Y.S. Chow[119], M.C. Chu[62a], J. Chudoba[139], A.J. Chuinard[102], J.J. Chwastowski[83], L. Chytka[128], D. Cinca[46], V. Cindro[90], I.A. Cioară[27b], A. Ciocio[18], F. Cirotto[68a,68b], Z.H. Citron[178], M. Citterio[67a], B.M. Ciungu[165], A. Clark[53], M.R. Clark[38], P.J. Clark[49], C. Clement[44a,44b], Y. Coadou[100], M. Cobal[65a,65c], A. Coccaro[54b], J. Cochran[77], H. Cohen[159], A.E.C. Coimbra[178], L. Colasurdo[118], B. Cole[38], A.P. Colijn[119], J. Collot[57], P. Conde Muiño[138a,h], E. Coniavitis[51],

JHEP06(2019)144

S.H. Connell[32b], I.A. Connelly[99], S. Constantinescu[27b], F. Conventi[68a,aw], A.M. Cooper-Sarkar[133], F. Cormier[173], K.J.R. Cormier[165], L.D. Corpe[93], M. Corradi[71a,71b], E.E. Corrigan[95], F. Corriveau[102,ac], A. Cortes-Gonzalez[35], M.J. Costa[172], F. Costanza[5], D. Costanzo[147], G. Cowan[92], J.W. Cowley[31], J. Crane[99], K. Cranmer[123], S.J. Crawley[56], R.A. Creager[135], S. Crépé-Renaudin[57], F. Crescioli[134], M. Cristinziani[24], V. Croft[123], G. Crosetti[40b,40a], A. Cueto[97], T. Cuhadar Donszelmann[147], A.R. Cukierman[151], S. Czekierda[83], P. Czodrowski[35], M.J. Da Cunha Sargedas De Sousa[59b], J.V. Da Fonseca Pinto[79b], C. Da Via[99], W. Dabrowski[82a], T. Dado[28a], S. Dahbi[34e], T. Dai[104], C. Dallapiccola[101], M. Dam[39], G. D'amen[23b,23a], J. Damp[98], J.R. Dandoy[135], M.F. Daneri[30], N.P. Dang[179,k], N.D Dann[99], M. Danninger[173], V. Dao[35], G. Darbo[54b], O. Dartsi[5], A. Dattagupta[129], T. Daubney[45], S. D'Auria[67a,67b], W. Davey[24], C. David[45], T. Davidek[141], D.R. Davis[48], E. Dawe[103], I. Dawson[147], K. De[8], R. De Asmundis[68a], A. De Benedetti[126], M. De Beurs[119], S. De Castro[23b,23a], S. De Cecco[71a,71b], N. De Groot[118], P. de Jong[119], H. De la Torre[105], A. De Maria[70a,70b], D. De Pedis[71a], A. De Salvo[71a], U. De Sanctis[72a,72b], M. De Santis[72a,72b], A. De Santo[154], K. De Vasconcelos Corga[100], J.B. De Vivie De Regie[130], C. Debenedetti[144], D.V. Dedovich[78], M. Del Gaudio[40b,40a], J. Del Peso[97], Y. Delabat Diaz[45], D. Delgove[130], F. Deliot[143], C.M. Delitzsch[7], M. Della Pietra[68a,68b], D. Della Volpe[53], A. Dell'Acqua[35], L. Dell'Asta[25], M. Delmastro[5], C. Delporte[130], P.A. Delsart[57], D.A. DeMarco[165], S. Demers[181], M. Demichev[78], S.P. Denisov[122], D. Denysiuk[119], L. D'Eramo[134], D. Derendarz[83], J.E. Derkaoui[34d], F. Derue[134], P. Dervan[89], K. Desch[24], C. Deterre[45], K. Dette[165], M.R. Devesa[30], P.O. Deviveiros[35], A. Dewhurst[142], S. Dhaliwal[26], F.A. Di Bello[53], A. Di Ciaccio[72a,72b], L. Di Ciaccio[5], W.K. Di Clemente[135], C. Di Donato[68a,68b], A. Di Girolamo[35], G. Di Gregorio[70a,70b], B. Di Micco[73a,73b], R. Di Nardo[101], K.F. Di Petrillo[58], R. Di Sipio[165], D. Di Valentino[33], C. Diaconu[100], F.A. Dias[39], T. Dias Do Vale[138a,138e], M.A. Diaz[145a], J. Dickinson[18], E.B. Diehl[104], J. Dietrich[19], S. Díez Cornell[45], A. Dimitrievska[18], J. Dingfelder[24], F. Dittus[35], F. Djama[100], T. Djobava[157b], J.I. Djuvsland[17], M.A.B. Do Vale[79c], M. Dobre[27b], D. Dodsworth[26], C. Doglioni[95], J. Dolejsi[141], Z. Dolezal[141], M. Donadelli[79d], J. Donini[37], A. D'onofrio[91], M. D'Onofrio[89], J. Dopke[142], A. Doria[68a], M.T. Dova[87], A.T. Doyle[56], E. Drechsler[150], E. Dreyer[150], T. Dreyer[52], Y. Du[59b], Y. Duan[59b], F. Dubinin[109], M. Dubovsky[28a], A. Dubreuil[53], E. Duchovni[178], G. Duckeck[113], A. Ducourthial[134], O.A. Ducu[108,w], D. Duda[114], A. Dudarev[35], A.C. Dudder[98], E.M. Duffield[18], L. Duflot[130], M. Dührssen[35], C. Dülsen[180], M. Dumancic[178], A.E. Dumitriu[27b], A.K. Duncan[56], M. Dunford[60a], A. Duperrin[100], H. Duran Yildiz[4a], M. Düren[55], A. Durglishvili[157b], D. Duschinger[47], B. Dutta[45], D. Duvnjak[1], G. Dyckes[135], M. Dyndal[45], S. Dysch[99], B.S. Dziedzic[83], K.M. Ecker[114], R.C. Edgar[104], T. Eifert[35], G. Eigen[17], K. Einsweiler[18], T. Ekelof[170], M. El Kacimi[34c], R. El Kosseifi[100], V. Ellajosyula[170], M. Ellert[170], F. Ellinghaus[180], A.A. Elliot[91], N. Ellis[35], J. Elmsheuser[29], M. Elsing[35], D. Emeliyanov[142], A. Emerman[38], Y. Enari[161], J.S. Ennis[176], M.B. Epland[48], J. Erdmann[46], A. Ereditato[20], M. Escalier[130], C. Escobar[172], O. Estrada Pastor[172], A.I. Etienvre[143], E. Etzion[159], H. Evans[64], A. Ezhilov[136], M. Ezzi[34e], F. Fabbri[56], L. Fabbri[23b,23a], V. Fabiani[118], G. Facini[93], R.M. Faisca Rodrigues Pereira[138a], R.M. Fakhrutdinov[122], S. Falciano[71a], P.J. Falke[5], S. Falke[5], J. Faltova[141], Y. Fang[15a], Y. Fang[15a], G. Fanourakis[43], M. Fanti[67a,67b], A. Farbin[8], A. Farilla[73a], E.M. Farina[69a,69b], T. Farooque[105], S. Farrell[18], S.M. Farrington[176], P. Farthouat[35], F. Fassi[34e], P. Fassnacht[35], D. Fassouliotis[9], M. Faucci Giannelli[49], W.J. Fawcett[31], L. Fayard[130], O.L. Fedin[136,p], W. Fedorko[173], M. Feickert[41], S. Feigl[132], L. Feligioni[100], C. Feng[59b], E.J. Feng[35], M. Feng[48], M.J. Fenton[56], A.B. Fenyuk[122], J. Ferrando[45], A. Ferrari[170], P. Ferrari[119], R. Ferrari[69a], D.E. Ferreira de Lima[60b], A. Ferrer[172], D. Ferrere[53], C. Ferretti[104], F. Fiedler[98], A. Filipčič[90], F. Filthaut[118], K.D. Finelli[25], M.C.N. Fiolhais[138a,138c,a], L. Fiorini[172], C. Fischer[14], W.C. Fisher[105], I. Fleck[149], P. Fleischmann[104], R.R.M. Fletcher[135], T. Flick[180], B.M. Flierl[113],

JHEP06(2019)144

L.M. Flores[135], L.R. Flores Castillo[62a], F.M. Follega[74a,74b], N. Fomin[17], G.T. Forcolin[74a,74b], A. Formica[143], F.A. Förster[14], A.C. Forti[99], A.G. Foster[21], D. Fournier[130], H. Fox[88], S. Fracchia[147], P. Francavilla[70a,70b], M. Franchini[23b,23a], S. Franchino[60a], D. Francis[35], L. Franconi[144], M. Franklin[58], M. Frate[169], A.N. Fray[91], B. Freund[108], W.S. Freund[79b], E.M. Freundlich[46], D.C. Frizzell[126], D. Froidevaux[35], J.A. Frost[133], C. Fukunaga[162], E. Fullana Torregrosa[172], E. Fumagalli[54b,54a], T. Fusayasu[115], J. Fuster[172], A. Gabrielli[23b,23a], A. Gabrielli[18], G.P. Gach[82a], S. Gadatsch[53], P. Gadow[114], G. Gagliardi[54b,54a], L.G. Gagnon[108], C. Galea[27b], B. Galhardo[138a,138c], E.J. Gallas[133], B.J. Gallop[142], P. Gallus[140], G. Galster[39], R. Gamboa Goni[91], K.K. Gan[124], S. Ganguly[178], J. Gao[59a], Y. Gao[89], Y.S. Gao[151,m], C. García[172], J.E. García Navarro[172], J.A. García Pascual[15a], C. Garcia-Argos[51], M. Garcia-Sciveres[18], R.W. Gardner[36], N. Garelli[151], S. Gargiulo[51], V. Garonne[132], A. Gaudiello[54b,54a], G. Gaudio[69a], I.L. Gavrilenko[109], A. Gavrilyuk[110], C. Gay[173], G. Gaycken[24], E.N. Gazis[10], C.N.P. Gee[142], J. Geisen[52], M. Geisen[98], M.P. Geisler[60a], C. Gemme[54b], M.H. Genest[57], C. Geng[104], S. Gentile[71a,71b], S. George[92], T. Geralis[43], D. Gerbaudo[14], G. Gessner[46], S. Ghasemi[149], M. Ghasemi Bostanabad[174], M. Ghneimat[24], A. Ghosh[76], B. Giacobbe[23b], S. Giagu[71a,71b], N. Giangiacomi[23b,23a], P. Giannetti[70a], A. Giannini[68a,68b], S.M. Gibson[92], M. Gignac[144], D. Gillberg[33], G. Gilles[180], D.M. Gingrich[3,av], M.P. Giordani[65a,65c], F.M. Giorgi[23b], P.F. Giraud[143], G. Giugliarelli[65a,65c], D. Giugni[67a], F. Giuli[133], M. Giulini[60b], S. Gkaitatzis[160], I. Gkialas[9,j], E.L. Gkougkousis[14], P. Gkountoumis[10], L.K. Gladilin[112], C. Glasman[97], J. Glatzer[14], P.C.F. Glaysher[45], A. Glazov[45], M. Goblirsch-Kolb[26], S. Goldfarb[103], T. Golling[53], D. Golubkov[122], A. Gomes[138a,138b], R. Goncalves Gama[52], R. Gonçalo[138a,138b], G. Gonella[51], L. Gonella[21], A. Gongadze[78], F. Gonnella[21], J.L. Gonski[58], S. González de la Hoz[172], S. Gonzalez-Sevilla[53], G.R. Gonzalvo Rodriguez[172], L. Goossens[35], P.A. Gorbounov[110], H.A. Gordon[29], B. Gorini[35], E. Gorini[66a,66b], A. Gorišek[90], A.T. Goshaw[48], C. Gössling[46], M.I. Gostkin[78], C.A. Gottardo[24], C.R. Goudet[130], D. Goujdami[34c], A.G. Goussiou[146], N. Govender[32b,c], C. Goy[5], E. Gozani[158], I. Grabowska-Bold[82a], P.O.J. Gradin[170], E.C. Graham[89], J. Gramling[169], E. Gramstad[132], S. Grancagnolo[19], M. Grandi[154], V. Gratchev[136], P.M. Gravila[27f], F.G. Gravili[66a,66b], C. Gray[56], H.M. Gray[18], C. Grefe[24], K. Gregersen[95], I.M. Gregor[45], P. Grenier[151], K. Grevtsov[45], N.A. Grieser[126], J. Griffiths[8], A.A. Grillo[144], K. Grimm[151,b], S. Grinstein[14,x], J.-F. Grivaz[130], S. Groh[98], E. Gross[178], J. Grosse-Knetter[52], Z.J. Grout[93], C. Grud[104], A. Grummer[117], L. Guan[104], W. Guan[179], J. Guenther[35], A. Guerguichon[130], F. Guescini[166a], D. Guest[169], R. Gugel[51], B. Gui[124], T. Guillemin[5], S. Guindon[35], U. Gul[56], J. Guo[59c], W. Guo[104], Y. Guo[59a,s], Z. Guo[100], R. Gupta[45], S. Gurbuz[12c], G. Gustavino[126], P. Gutierrez[126], C. Gutschow[93], C. Guyot[143], M.P. Guzik[82a], C. Gwenlan[133], C.B. Gwilliam[89], A. Haas[123], C. Haber[18], H.K. Hadavand[8], N. Haddad[34e], A. Hadef[59a], S. Hageböck[35], M. Hagihara[167], M. Haleem[175], J. Haley[127], G. Halladjian[105], G.D. Hallewell[100], K. Hamacher[180], P. Hamal[128], K. Hamano[174], H. Hamdaoui[34e], G.N. Hamity[147], K. Han[59a,aj], L. Han[59a], S. Han[15d], K. Hanagaki[80,u], M. Hance[144], D.M. Handl[113], B. Haney[135], R. Hankache[134], P. Hanke[60a], E. Hansen[95], J.B. Hansen[39], J.D. Hansen[39], M.C. Hansen[24], P.H. Hansen[39], E.C. Hanson[99], K. Hara[167], A.S. Hard[179], T. Harenberg[180], S. Harkusha[106], P.F. Harrison[176], N.M. Hartmann[113], Y. Hasegawa[148], A. Hasib[49], S. Hassani[143], S. Haug[20], R. Hauser[105], L. Hauswald[47], L.B. Havener[38], M. Havranek[140], C.M. Hawkes[21], R.J. Hawkings[35], D. Hayden[105], C. Hayes[153], R.L. Hayes[173], C.P. Hays[133], J.M. Hays[91], H.S. Hayward[89], S.J. Haywood[142], F. He[59a], M.P. Heath[49], V. Hedberg[95], L. Heelan[8], S. Heer[24], K.K. Heidegger[51], J. Heilman[33], S. Heim[45], T. Heim[18], B. Heinemann[45,aq], J.J. Heinrich[113], L. Heinrich[123], C. Heinz[55], J. Hejbal[139], L. Helary[60b], A. Held[173], S. Hellesund[132], C.M. Helling[144], S. Hellman[44a,44b], C. Helsens[35], R.C.W. Henderson[88], Y. Heng[179], S. Henkelmann[173], A.M. Henriques Correia[35], G.H. Herbert[19],

JHEP06(2019)144

H. Herde[26], V. Herget[175], Y. Hernández Jiménez[32c], H. Herr[98], M.G. Herrmann[113], T. Herrmann[47], G. Herten[51], R. Hertenberger[113], L. Hervas[35], T.C. Herwig[135], G.G. Hesketh[93], N.P. Hessey[166a], A. Higashida[161], S. Higashino[80], E. Higón-Rodriguez[172], K. Hildebrand[36], E. Hill[174], J.C. Hill[31], K.K. Hill[29], K.H. Hiller[45], S.J. Hillier[21], M. Hils[47], I. Hinchliffe[18], F. Hinterkeuser[24], M. Hirose[131], D. Hirschbuehl[180], B. Hiti[90], O. Hladik[139], D.R. Hlaluku[32c], X. Hoad[49], J. Hobbs[153], N. Hod[178], M.C. Hodgkinson[147], A. Hoecker[35], F. Hoenig[113], D. Hohn[51], D. Hohov[130], T.R. Holmes[36], M. Holzbock[113], L.B.A.H Hommels[31], S. Honda[167], T. Honda[80], T.M. Hong[137], A. Hönle[114], B.H. Hooberman[171], W.H. Hopkins[6], Y. Horii[116], P. Horn[47], A.J. Horton[150], L.A. Horyn[36], J-Y. Hostachy[57], A. Hostiuc[146], S. Hou[156], A. Hoummada[34a], J. Howarth[99], J. Hoya[87], M. Hrabovsky[128], J. Hrdinka[35], I. Hristova[19], J. Hrivnac[130], A. Hrynevich[107], T. Hryn'ova[5], P.J. Hsu[63], S.-C. Hsu[146], Q. Hu[29], S. Hu[59c], Y. Huang[15a], Z. Hubacek[140], F. Hubaut[100], M. Huebner[24], F. Huegging[24], T.B. Huffman[133], M. Huhtinen[35], R.F.H. Hunter[33], P. Huo[153], A.M. Hupe[33], N. Huseynov[78,ae], J. Huston[105], J. Huth[58], R. Hyneman[104], G. Iacobucci[53], G. Iakovidis[29], I. Ibragimov[149], L. Iconomidou-Fayard[130], Z. Idrissi[34e], P. Iengo[35], R. Ignazzi[39], O. Igonkina[119,z], R. Iguchi[161], T. Iizawa[53], Y. Ikegami[80], M. Ikeno[80], D. Iliadis[160], N. Ilic[118], F. Iltzsche[47], G. Introzzi[69a,69b], M. Iodice[73a], K. Iordanidou[38], V. Ippolito[71a,71b], M.F. Isacson[170], N. Ishijima[131], M. Ishino[161], M. Ishitsuka[163], W. Islam[127], C. Issever[133], S. Istin[158], F. Ito[167], J.M. Iturbe Ponce[62a], R. Iuppa[74a,74b], A. Ivina[178], H. Iwasaki[80], J.M. Izen[42], V. Izzo[68a], P. Jacka[139], P. Jackson[1], R.M. Jacobs[24], V. Jain[2], G. Jäkel[180], K.B. Jakobi[98], K. Jakobs[51], S. Jakobsen[75], T. Jakoubek[139], D.O. Jamin[127], R. Jansky[53], J. Janssen[24], M. Janus[52], P.A. Janus[82a], G. Jarlskog[95], N. Javadov[78,ae], T. Javůrek[35], M. Javurkova[51], F. Jeanneau[143], L. Jeanty[129], J. Jejelava[157a,af], A. Jelinskas[176], P. Jenni[51,d], J. Jeong[45], N. Jeong[45], S. Jézéquel[5], H. Ji[179], J. Jia[153], H. Jiang[77], Y. Jiang[59a], Z. Jiang[151,q], S. Jiggins[51], F.A. Jimenez Morales[37], J. Jimenez Pena[172], S. Jin[15c], A. Jinaru[27b], O. Jinnouchi[163], H. Jivan[32c], P. Johansson[147], K.A. Johns[7], C.A. Johnson[64], K. Jon-And[44a,44b], R.W.L. Jones[88], S.D. Jones[154], S. Jones[7], T.J. Jones[89], J. Jongmanns[60a], P.M. Jorge[138a,138b], J. Jovicevic[166a], X. Ju[18], J.J. Junggeburth[114], A. Juste Rozas[14,x], A. Kaczmarska[83], M. Kado[130], H. Kagan[124], M. Kagan[151], T. Kaji[177], E. Kajomovitz[158], C.W. Kalderon[95], A. Kaluza[98], A. Kamenshchikov[122], L. Kanjir[90], Y. Kano[161], V.A. Kantserov[111], J. Kanzaki[80], L.S. Kaplan[179], D. Kar[32c], M.J. Kareem[166b], E. Karentzos[10], S.N. Karpov[78], Z.M. Karpova[78], V. Kartvelishvili[88], A.N. Karyukhin[122], L. Kashif[179], R.D. Kass[124], A. Kastanas[44a,44b], Y. Kataoka[161], C. Kato[59d,59c], J. Katzy[45], K. Kawade[81], K. Kawagoe[86], T. Kawaguchi[116], T. Kawamoto[161], G. Kawamura[52], E.F. Kay[174], V.F. Kazanin[121b,121a], R. Keeler[174], R. Kehoe[41], J.S. Keller[33], E. Kellermann[95], J.J. Kempster[21], J. Kendrick[21], O. Kepka[139], S. Kersten[180], B.P. Kerševan[90], S. Ketabchi Haghighat[165], R.A. Keyes[102], M. Khader[171], F. Khalil-Zada[13], A. Khanov[127], A.G. Kharlamov[121b,121a], T. Kharlamova[121b,121a], E.E. Khoda[173], A. Khodinov[164], T.J. Khoo[53], E. Khramov[78], J. Khubua[157b], S. Kido[81], M. Kiehn[53], C.R. Kilby[92], Y.K. Kim[36], N. Kimura[65a,65c], O.M. Kind[19], B.T. King[89], D. Kirchmeier[47], J. Kirk[142], A.E. Kiryunin[114], T. Kishimoto[161], V. Kitali[45], O. Kivernyk[5], E. Kladiva[28b,*], T. Klapdor-Kleingrothaus[51], M.H. Klein[104], M. Klein[89], U. Klein[89], K. Kleinknecht[98], P. Klimek[120], A. Klimentov[29], T. Klingl[24], T. Klioutchnikova[35], F.F. Klitzner[113], P. Kluit[119], S. Kluth[114], E. Kneringer[75], E.B.F.G. Knoops[100], A. Knue[51], D. Kobayashi[86], T. Kobayashi[161], M. Kobel[47], M. Kocian[151], P. Kodys[141], P.T. Koenig[24], T. Koffas[33], N.M. Köhler[114], T. Koi[151], M. Kolb[60b], I. Koletsou[5], T. Kondo[80], N. Kondrashova[59c], K. Köneke[51], A.C. König[118], T. Kono[80], R. Konoplich[123,am], V. Konstantinides[93], N. Konstantinidis[93], B. Konya[95], R. Kopeliansky[64], S. Koperny[82a], K. Korcyl[83], K. Kordas[160], G. Koren[159], A. Korn[93], I. Korolkov[14], E.V. Korolkova[147], N. Korotkova[112], O. Kortner[114], S. Kortner[114], T. Kosek[141], V.V. Kostyukhin[24], A. Kotwal[48], A. Koulouris[10], A. Kourkoumeli-Charalampidi[69a,69b], C. Kourkoumelis[9], E. Kourlitis[147],

JHEP06(2019)144

V. Kouskoura[29], A.B. Kowalewska[83], R. Kowalewski[174], C. Kozakai[161], W. Kozanecki[143], A.S. Kozhin[122], V.A. Kramarenko[112], G. Kramberger[90], D. Krasnopevtsev[59a], M.W. Krasny[134], A. Krasznahorkay[35], D. Krauss[114], J.A. Kremer[82a], J. Kretzschmar[89], P. Krieger[165], K. Krizka[18], K. Kroeninger[46], H. Kroha[114], J. Kroll[139], J. Kroll[135], J. Krstic[16], U. Kruchonak[78], H. Krüger[24], N. Krumnack[77], M.C. Kruse[48], T. Kubota[103], S. Kuday[4b], J.T. Kuechler[45], S. Kuehn[35], A. Kugel[60a], T. Kuhl[45], V. Kukhtin[78], R. Kukla[100], Y. Kulchitsky[106,ai], S. Kuleshov[145b], Y.P. Kulinich[171], M. Kuna[57], T. Kunigo[84], A. Kupco[139], T. Kupfer[46], O. Kuprash[51], H. Kurashige[81], L.L. Kurchaninov[166a], Y.A. Kurochkin[106], A. Kurova[111], M.G. Kurth[15d], E.S. Kuwertz[35], M. Kuze[163], J. Kvita[128], T. Kwan[102], A. La Rosa[114], J.L. La Rosa Navarro[79d], L. La Rotonda[40b,40a], F. La Ruffa[40b,40a], C. Lacasta[172], F. Lacava[71a,71b], D.P.J. Lack[99], H. Lacker[19], D. Lacour[134], E. Ladygin[78], R. Lafaye[5], B. Laforge[134], T. Lagouri[32c], S. Lai[52], S. Lammers[64], W. Lampl[7], E. Lançon[29], U. Landgraf[51], M.P.J. Landon[91], M.C. Lanfermann[53], V.S. Lang[45], J.C. Lange[52], R.J. Langenberg[35], A.J. Lankford[169], F. Lanni[29], K. Lantzsch[24], A. Lanza[69a], A. Lapertosa[54b,54a], S. Laplace[134], J.F. Laporte[143], T. Lari[67a], F. Lasagni Manghi[23b,23a], M. Lassnig[35], T.S. Lau[62a], A. Laudrain[130], A. Laurier[33], M. Lavorgna[68a,68b], M. Lazzaroni[67a,67b], B. Le[103], O. Le Dortz[134], E. Le Guirriec[100], M. LeBlanc[7], T. LeCompte[6], F. Ledroit-Guillon[57], C.A. Lee[29], G.R. Lee[145a], L. Lee[58], S.C. Lee[156], S.J. Lee[33], B. Lefebvre[102], M. Lefebvre[174], F. Legger[113], C. Leggett[18], K. Lehmann[150], N. Lehmann[180], G. Lehmann Miotto[35], W.A. Leight[45], A. Leisos[160,v], M.A.L. Leite[79d], R. Leitner[141], D. Lellouch[178], K.J.C. Leney[41], T. Lenz[24], B. Lenzi[35], R. Leone[7], S. Leone[70a], C. Leonidopoulos[49], A. Leopold[134], G. Lerner[154], C. Leroy[108], R. Les[165], C.G. Lester[31], M. Levchenko[136], J. Levêque[5], D. Levin[104], L.J. Levinson[178], B. Li[15b], B. Li[104], C-Q. Li[59a,al], H. Li[59a], H. Li[59b], K. Li[151], L. Li[59c], M. Li[15a], Q. Li[15d], Q.Y. Li[59a], S. Li[59d,59c], X. Li[59c], Y. Li[45], Z. Liang[15a], B. Liberti[72a], A. Liblong[165], K. Lie[62c], S. Liem[119], C.Y. Lin[31], K. Lin[105], T.H. Lin[98], R.A. Linck[64], J.H. Lindon[21], A.L. Lionti[53], E. Lipeles[135], A. Lipniacka[17], M. Lisovyi[60b], T.M. Liss[171,as], A. Lister[173], A.M. Litke[144], J.D. Little[8], B. Liu[77], B.L Liu[6], H.B. Liu[29], H. Liu[104], J.B. Liu[59a], J.K.K. Liu[133], K. Liu[134], M. Liu[59a], P. Liu[18], Y. Liu[15d], Y.L. Liu[59a], Y.W. Liu[59a], M. Livan[69a,69b], A. Lleres[57], J. Llorente Merino[15a], S.L. Lloyd[91], C.Y. Lo[62b], F. Lo Sterzo[41], E.M. Lobodzinska[45], P. Loch[7], T. Lohse[19], K. Lohwasser[147], M. Lokajicek[139], J.D. Long[171], R.E. Long[88], L. Longo[35], K.A. Looper[124], J.A. Lopez[145b], I. Lopez Paz[99], A. Lopez Solis[147], J. Lorenz[113], N. Lorenzo Martinez[5], A.M. Lory[113], M. Losada[22], P.J. Lösel[113], A. Lösle[51], X. Lou[45], X. Lou[15a], A. Lounis[130], J. Love[6], P.A. Love[88], J.J. Lozano Bahilo[172], H. Lu[62a], M. Lu[59a], Y.J. Lu[63], H.J. Lubatti[146], C. Luci[71a,71b], A. Lucotte[57], C. Luedtke[51], F. Luehring[64], I. Luise[134], L. Luminari[71a], B. Lund-Jensen[152], M.S. Lutz[101], D. Lynn[29], R. Lysak[139], E. Lytken[95], F. Lyu[15a], V. Lyubushkin[78], T. Lyubushkina[78], H. Ma[29], L.L. Ma[59b], Y. Ma[59b], G. Maccarrone[50], A. Macchiolo[114], C.M. Macdonald[147], J. Machado Miguens[135,138b], D. Madaffari[172], R. Madar[37], W.F. Mader[47], N. Madysa[47], J. Maeda[81], K. Maekawa[161], S. Maeland[17], T. Maeno[29], M. Maerker[47], A.S. Maevskiy[112], V. Magerl[51], N. Magini[77], D.J. Mahon[38], C. Maidantchik[79b], T. Maier[113], A. Maio[138a,138b,138d], O. Majersky[28a], S. Majewski[129], Y. Makida[80], N. Makovec[130], B. Malaescu[134], Pa. Malecki[83], V.P. Maleev[136], F. Malek[57], U. Mallik[76], D. Malon[6], C. Malone[31], S. Maltezos[10], S. Malyukov[35], J. Mamuzic[172], G. Mancini[50], I. Mandić[90], L. Manhaes de Andrade Filho[79a], I.M. Maniatis[160], J. Manjarres Ramos[47], K.H. Mankinen[95], A. Mann[113], A. Manousos[75], B. Mansoulie[143], I. Manthos[160], S. Manzoni[119], A. Marantis[160], G. Marceca[30], L. Marchese[133], G. Marchiori[134], M. Marcisovsky[139], C. Marcon[95], C.A. Marin Tobon[35], M. Marjanovic[37], F. Marroquim[79b], Z. Marshall[18], M.U.F Martensson[170], S. Marti-Garcia[172], C.B. Martin[124], T.A. Martin[176], V.J. Martin[49], B. Martin dit Latour[17], M. Martinez[14,x], V.I. Martinez Outschoorn[101], S. Martin-Haugh[142], V.S. Martoiu[27b],

JHEP06(2019)144

A.C. Martyniuk[93], A. Marzin[35], L. Masetti[98], T. Mashimo[161], R. Mashinistov[109], J. Masik[99], A.L. Maslennikov[121b,121a], L.H. Mason[103], L. Massa[72a,72b], P. Massarotti[68a,68b], P. Mastrandrea[70a,70b], A. Mastroberardino[40b,40a], T. Masubuchi[161], A. Matic[113], P. Mättig[24], J. Maurer[27b], B. Maček[90], S.J. Maxfield[89], D.A. Maximov[121b,121a], R. Mazini[156], I. Maznas[160], S.M. Mazza[144], S.P. Mc Kee[104], A. McCarn, Deiana[41], T.G. McCarthy[114], L.I. McClymont[93], W.P. McCormack[18], E.F. McDonald[103], J.A. Mcfayden[35], G. Mchedlidze[52], M.A. McKay[41], K.D. McLean[174], S.J. McMahon[142], P.C. McNamara[103], C.J. McNicol[176], R.A. McPherson[174,ac], J.E. Mdhluli[32c], Z.A. Meadows[101], S. Meehan[146], T.M. Megy[51], S. Mehlhase[113], A. Mehta[89], T. Meideck[57], B. Meirose[42], D. Melini[172], B.R. Mellado Garcia[32c], J.D. Mellenthin[52], M. Melo[28a], F. Meloni[45], A. Melzer[24], S.B. Menary[99], E.D. Mendes Gouveia[138a,138e], L. Meng[35], X.T. Meng[104], S. Menke[114], E. Meoni[40b,40a], S. Mergelmeyer[19], S.A.M. Merkt[137], C. Merlassino[20], P. Mermod[53], L. Merola[68a,68b], C. Meroni[67a], J.K.R. Meshreki[149], A. Messina[71a,71b], J. Metcalfe[6], A.S. Mete[169], C. Meyer[64], J. Meyer[158], J-P. Meyer[143], H. Meyer Zu Theenhausen[60a], F. Miano[154], R.P. Middleton[142], L. Mijović[49], G. Mikenberg[178], M. Mikestikova[139], M. Mikuž[90], M. Milesi[103], A. Milic[165], D.A. Millar[91], D.W. Miller[36], A. Milov[178], D.A. Milstead[44a,44b], R.A. Mina[151,q], A.A. Minaenko[122], M. Miñano Moya[172], I.A. Minashvili[157b], A.I. Mincer[123], B. Mindur[82a], M. Mineev[78], Y. Minegishi[161], Y. Ming[179], L.M. Mir[14], A. Mirto[66a,66b], K.P. Mistry[135], T. Mitani[177], J. Mitrevski[113], V.A. Mitsou[172], M. Mittal[59c], A. Miucci[20], P.S. Miyagawa[147], A. Mizukami[80], J.U. Mjörnmark[95], T. Mkrtchyan[182], M. Mlynarikova[141], T. Moa[44a,44b], K. Mochizuki[108], P. Mogg[51], S. Mohapatra[38], R. Moles-Valls[24], M.C. Mondragon[105], K. Mönig[45], J. Monk[39], E. Monnier[100], A. Montalbano[150], J. Montejo Berlingen[35], M. Montella[93], F. Monticelli[87], S. Monzani[67a], N. Morange[130], D. Moreno[22], M. Moreno Llácer[35], P. Morettini[54b], M. Morgenstern[119], S. Morgenstern[47], D. Mori[150], M. Morii[58], M. Morinaga[177], V. Morisbak[132], A.K. Morley[35], G. Mornacchi[35], A.P. Morris[93], L. Morvaj[153], P. Moschovakos[10], M. Mosidze[157b], H.J. Moss[147], J. Moss[151,n], K. Motohashi[163], E. Mountricha[35], E.J.W. Moyse[101], S. Muanza[100], F. Mueller[114], J. Mueller[137], R.S.P. Mueller[113], D. Muenstermann[88], G.A. Mullier[95], F.J. Munoz Sanchez[99], P. Murin[28b], W.J. Murray[176,142], A. Murrone[67a,67b], M. Muškinja[90], C. Mwewa[32a], A.G. Myagkov[122,an], J. Myers[129], M. Myska[140], B.P. Nachman[18], O. Nackenhorst[46], K. Nagai[133], K. Nagano[80], Y. Nagasaka[61], M. Nagel[51], E. Nagy[100], A.M. Nairz[35], Y. Nakahama[116], K. Nakamura[80], T. Nakamura[161], I. Nakano[125], H. Nanjo[131], F. Napolitano[60a], R.F. Naranjo Garcia[45], R. Narayan[11], D.I. Narrias Villar[60a], I. Naryshkin[136], T. Naumann[45], G. Navarro[22], H.A. Neal[104,*], P.Y. Nechaeva[109], F. Nechansky[45], T.J. Neep[143], A. Negri[69a,69b], M. Negrini[23b], S. Nektarijevic[118], C. Nellist[52], M.E. Nelson[133], S. Nemecek[139], P. Nemethy[123], M. Nessi[35,f], M.S. Neubauer[171], M. Neumann[180], P.R. Newman[21], T.Y. Ng[62c], Y.S. Ng[19], Y.W.Y. Ng[169], H.D.N. Nguyen[100], T. Nguyen Manh[108], E. Nibigira[37], R.B. Nickerson[133], R. Nicolaidou[143], D.S. Nielsen[39], J. Nielsen[144], N. Nikiforou[11], V. Nikolaenko[122,an], I. Nikolic-Audit[134], K. Nikolopoulos[21], P. Nilsson[29], H.R. Nindhito[53], Y. Ninomiya[80], A. Nisati[71a], N. Nishu[59c], R. Nisius[114], I. Nitsche[46], T. Nitta[177], T. Nobe[161], Y. Noguchi[84], M. Nomachi[131], I. Nomidis[134], M.A. Nomura[29], M. Nordberg[35], N. Norjoharuddeen[133], T. Novak[90], O. Novgorodova[47], R. Novotny[140], L. Nozka[128], K. Ntekas[169], E. Nurse[93], F. Nuti[103], F.G. Oakham[33,av], H. Oberlack[114], J. Ocariz[134], A. Ochi[81], I. Ochoa[38], J.P. Ochoa-Ricoux[145a], K. O'Connor[26], S. Oda[86], S. Odaka[80], S. Oerdek[52], A. Ogrodnik[82a], A. Oh[99], S.H. Oh[48], C.C. Ohm[152], H. Oide[54b,54a], M.L. Ojeda[165], H. Okawa[167], Y. Okazaki[84], Y. Okumura[161], T. Okuyama[80], A. Olariu[27b], L.F. Oleiro Seabra[138a], S.A. Olivares Pino[145a], D. Oliveira Damazio[29], J.L. Oliver[1], M.J.R. Olsson[36], A. Olszewski[83], J. Olszowska[83], D.C. O'Neil[150], A. Onofre[138a,138e], K. Onogi[116], P.U.E. Onyisi[11], H. Oppen[132], M.J. Oreglia[36], G.E. Orellana[87], Y. Oren[159], D. Orestano[73a,73b], N. Orlando[14], R.S. Orr[165], B. Osculati[54b,54a,*], V. O'Shea[56], R. Ospanov[59a], G. Otero y Garzon[30], H. Otono[86], M. Ouchrif[34d], F. Ould-Saada[132],

JHEP06(2019)144

A. Ouraou[143], Q. Ouyang[15a], M. Owen[56], R.E. Owen[21], V.E. Ozcan[12c], N. Ozturk[8], J. Pacalt[128], H.A. Pacey[31], K. Pachal[48], A. Pacheco Pages[14], C. Padilla Aranda[14], S. Pagan Griso[18], M. Paganini[181], G. Palacino[64], S. Palazzo[49], S. Palestini[35], M. Palka[82b], D. Pallin[37], I. Panagoulias[10], C.E. Pandini[35], J.G. Panduro Vazquez[92], P. Pani[45], G. Panizzo[65a,65c], L. Paolozzi[53], K. Papageorgiou[9,j], A. Paramonov[6], D. Paredes Hernandez[62b], S.R. Paredes Saenz[133], B. Parida[164], T.H. Park[165], A.J. Parker[88], M.A. Parker[31], F. Parodi[54b,54a], E.W.P. Parrish[120], J.A. Parsons[38], U. Parzefall[51], L. Pascual Dominguez[134], V.R. Pascuzzi[165], J.M.P. Pasner[144], E. Pasqualucci[71a], S. Passaggio[54b], F. Pastore[92], P. Pasuwan[44a,44b], S. Pataraia[98], J.R. Pater[99], A. Pathak[179,k], T. Pauly[35], B. Pearson[114], M. Pedersen[132], L. Pedraza Diaz[118], R. Pedro[138a,138b], S.V. Peleganchuk[121b,121a], O. Penc[139], C. Peng[15a], H. Peng[59a], B.S. Peralva[79a], M.M. Perego[130], A.P. Pereira Peixoto[138a,138e], D.V. Perepelitsa[29], F. Peri[19], L. Perini[67a,67b], H. Pernegger[35], S. Perrella[68a,68b], V.D. Peshekhonov[78,*], K. Peters[45], R.F.Y. Peters[99], B.A. Petersen[35], T.C. Petersen[39], E. Petit[57], A. Petridis[1], C. Petridou[160], P. Petroff[130], M. Petrov[133], F. Petrucci[73a,73b], M. Pettee[181], N.E. Pettersson[101], K. Petukhova[141], A. Peyaud[143], R. Pezoa[145b], T. Pham[103], F.H. Phillips[105], P.W. Phillips[142], M.W. Phipps[171], G. Piacquadio[153], E. Pianori[18], A. Picazio[101], R.H. Pickles[99], R. Piegaia[30], J.E. Pilcher[36], A.D. Pilkington[99], M. Pinamonti[72a,72b], J.L. Pinfold[3], M. Pitt[178], L. Pizzimento[72a,72b], M.-A. Pleier[29], V. Pleskot[141], E. Plotnikova[78], D. Pluth[77], P. Podberezko[121b,121a], R. Poettgen[95], R. Poggi[53], L. Poggioli[130], I. Pogrebnyak[105], D. Pohl[24], I. Pokharel[52], G. Polesello[69a], A. Poley[18], A. Policicchio[71a,71b], R. Polifka[35], A. Polini[23b], C.S. Pollard[45], V. Polychronakos[29], D. Ponomarenko[111], L. Pontecorvo[35], G.A. Popeneciu[27d], D.M. Portillo Quintero[134], S. Pospisil[140], K. Potamianos[45], I.N. Potrap[78], C.J. Potter[31], H. Potti[11], T. Poulsen[95], J. Poveda[35], T.D. Powell[147], M.E. Pozo Astigarraga[35], P. Pralavorio[100], S. Prell[77], D. Price[99], M. Primavera[66a], S. Prince[102], M.L. Proffitt[146], N. Proklova[111], K. Prokofiev[62c], F. Prokoshin[145b], S. Protopopescu[29], J. Proudfoot[6], M. Przybycien[82a], A. Puri[171], P. Puzo[130], J. Qian[104], Y. Qin[99], A. Quadt[52], M. Queitsch-Maitland[45], A. Qureshi[1], P. Rados[103], F. Ragusa[67a,67b], G. Rahal[96], J.A. Raine[53], S. Rajagopalan[29], A. Ramirez Morales[91], K. Ran[15d], T. Rashid[130], S. Raspopov[5], M.G. Ratti[67a,67b], D.M. Rauch[45], F. Rauscher[113], S. Rave[98], B. Ravina[147], I. Ravinovich[178], J.H. Rawling[99], M. Raymond[35], A.L. Read[132], N.P. Readioff[57], M. Reale[66a,66b], D.M. Rebuzzi[69a,69b], A. Redelbach[175], G. Redlinger[29], R.G. Reed[32c], K. Reeves[42], L. Rehnisch[19], J. Reichert[135], D. Reikher[159], A. Reiss[98], A. Rej[149], C. Rembser[35], H. Ren[15a], M. Rescigno[71a], S. Resconi[67a], E.D. Resseguie[135], S. Rettie[173], E. Reynolds[21], O.L. Rezanova[121b,121a], P. Reznicek[141], E. Ricci[74a,74b], R. Richter[114], S. Richter[45], E. Richter-Was[82b], O. Ricken[24], M. Ridel[134], P. Rieck[114], C.J. Riegel[180], O. Rifki[45], M. Rijssenbeek[153], A. Rimoldi[69a,69b], M. Rimoldi[20], L. Rinaldi[23b], G. Ripellino[152], B. Ristić[88], E. Ritsch[35], I. Riu[14], J.C. Rivera Vergara[145a], F. Rizatdinova[127], E. Rizvi[91], C. Rizzi[14], R.T. Roberts[99], S.H. Robertson[102,ac], D. Robinson[31], J.E.M. Robinson[45], A. Robson[56], E. Rocco[98], C. Roda[70a,70b], Y. Rodina[100], S. Rodriguez Bosca[172], A. Rodriguez Perez[14], D. Rodriguez Rodriguez[172], A.M. Rodríguez Vera[166b], S. Roe[35], J. Roggel[180], O. Røhne[132], R. Röhrig[114], C.P.A. Roland[64], J. Roloff[58], A. Romaniouk[111], M. Romano[23b,23a], N. Rompotis[89], M. Ronzani[123], L. Roos[134], S. Rosati[71a], K. Rosbach[51], N-A. Rosien[52], B.J. Rosser[135], E. Rossi[45], E. Rossi[73a,73b], E. Rossi[68a,68b], L.P. Rossi[54b], L. Rossini[67a,67b], J.H.N. Rosten[31], R. Rosten[14], M. Rotaru[27b], J. Rothberg[146], D. Rousseau[130], D. Roy[32c], A. Rozanov[100], Y. Rozen[158], X. Ruan[32c], F. Rubbo[151], F. Rühr[51], A. Ruiz-Martinez[172], Z. Rurikova[51], N.A. Rusakovich[78], H.L. Russell[102], L. Rustige[37,46], J.P. Rutherfoord[7], E.M. Rüttinger[45,l], Y.F. Ryabov[136], M. Rybar[38], G. Rybkin[130], S. Ryu[6], A. Ryzhov[122], G.F. Rzehorz[52], P. Sabatini[52], G. Sabato[119], S. Sacerdoti[130], H.F-W. Sadrozinski[144], R. Sadykov[78], F. Safai Tehrani[71a], P. Saha[120], M. Sahinsoy[60a], A. Sahu[180], M. Saimpert[45], M. Saito[161], T. Saito[161], H. Sakamoto[161],

JHEP06(2019)144

A. Sakharov[123,am], D. Salamani[53], G. Salamanna[73a,73b], J.E. Salazar Loyola[145b], P.H. Sales De Bruin[170], D. Salihagic[114,*], A. Salnikov[151], J. Salt[172], D. Salvatore[40b,40a], F. Salvatore[154], A. Salvucci[62a,62b,62c], A. Salzburger[35], J. Samarati[35], D. Sammel[51], D. Sampsonidis[160], D. Sampsonidou[160], J. Sánchez[172], A. Sanchez Pineda[65a,65c], H. Sandaker[132], C.O. Sander[45], M. Sandhoff[180], C. Sandoval[22], D.P.C. Sankey[142], M. Sannino[54b,54a], Y. Sano[116], A. Sansoni[50], C. Santoni[37], H. Santos[138a,138b], S.N. Santpur[18], A. Santra[172], A. Sapronov[78], J.G. Saraiva[138a,138d], O. Sasaki[80], K. Sato[167], E. Sauvan[5], P. Savard[165,av], N. Savic[114], R. Sawada[161], C. Sawyer[142], L. Sawyer[94,ak], C. Sbarra[23b], A. Sbrizzi[23a], T. Scanlon[93], J. Schaarschmidt[146], P. Schacht[114], B.M. Schachtner[113], D. Schaefer[36], L. Schaefer[135], J. Schaeffer[98], S. Schaepe[35], U. Schäfer[98], A.C. Schaffer[130], D. Schaile[113], R.D. Schamberger[153], N. Scharmberg[99], V.A. Schegelsky[136], D. Scheirich[141], F. Schenck[19], M. Schernau[169], C. Schiavi[54b,54a], S. Schier[144], L.K. Schildgen[24], Z.M. Schillaci[26], E.J. Schioppa[35], M. Schioppa[40b,40a], K.E. Schleicher[51], S. Schlenker[35], K.R. Schmidt-Sommerfeld[114], K. Schmieden[35], C. Schmitt[98], S. Schmitt[45], S. Schmitz[98], J.C. Schmoeckel[45], U. Schnoor[51], L. Schoeffel[143], A. Schoening[60b], E. Schopf[133], M. Schott[98], J.F.P. Schouwenberg[118], J. Schovancova[35], S. Schramm[53], A. Schulte[98], H-C. Schultz-Coulon[60a], M. Schumacher[51], B.A. Schumm[144], Ph. Schune[143], A. Schwartzman[151], T.A. Schwarz[104], Ph. Schwemling[143], R. Schwienhorst[105], A. Sciandra[24], G. Sciolla[26], M. Scornajenghi[40b,40a], F. Scuri[70a], F. Scutti[103], L.M. Scyboz[114], C.D. Sebastiani[71a,71b], P. Seema[19], S.C. Seidel[117], A. Seiden[144], T. Seiss[36], J.M. Seixas[79b], G. Sekhniaidze[68a], K. Sekhon[104], S.J. Sekula[41], N. Semprini-Cesari[23b,23a], S. Sen[48], S. Senkin[37], C. Serfon[75], L. Serin[130], L. Serkin[65a,65b], M. Sessa[59a], H. Severini[126], F. Sforza[168], A. Sfyrla[53], E. Shabalina[52], J.D. Shahinian[144], N.W. Shaikh[44a,44b], D. Shaked Renous[178], L.Y. Shan[15a], R. Shang[171], J.T. Shank[25], M. Shapiro[18], A.S. Sharma[1], A. Sharma[133], P.B. Shatalov[110], K. Shaw[154], S.M. Shaw[99], A. Shcherbakova[136], Y. Shen[126], N. Sherafati[33], A.D. Sherman[25], P. Sherwood[93], L. Shi[156,ar], S. Shimizu[80], C.O. Shimmin[181], Y. Shimogama[177], M. Shimojima[115], I.P.J. Shipsey[133], S. Shirabe[86], M. Shiyakova[78,aa], J. Shlomi[178], A. Shmeleva[109], M.J. Shochet[36], S. Shojaii[103], D.R. Shope[126], S. Shrestha[124], E. Shulga[111], P. Sicho[139], A.M. Sickles[171], P.E. Sidebo[152], E. Sideras Haddad[32c], O. Sidiropoulou[35], A. Sidoti[23b,23a], F. Siegert[47], Dj. Sijacki[16], J. Silva[138a], M. Silva Jr.[179], M.V. Silva Oliveira[79a], S.B. Silverstein[44a], S. Simion[130], E. Simioni[98], M. Simon[98], R. Simoniello[98], P. Sinervo[165], N.B. Sinev[129], M. Sioli[23b,23a], I. Siral[104], S.Yu. Sivoklokov[112], J. Sjölin[44a,44b], E. Skorda[95], P. Skubic[126], M. Slawinska[83], K. Sliwa[168], R. Slovak[141], V. Smakhtin[178], B.H. Smart[5], J. Smiesko[28a], N. Smirnov[111], S.Yu. Smirnov[111], Y. Smirnov[111], L.N. Smirnova[112], O. Smirnova[95], J.W. Smith[52], M. Smizanska[88], K. Smolek[140], A. Smykiewicz[83], A.A. Snesarev[109], I.M. Snyder[129], S. Snyder[29], R. Sobie[174,ac], A.M. Soffa[169], A. Soffer[159], A. Søgaard[49], F. Sohns[52], G. Sokhrannyi[90], C.A. Solans Sanchez[35], E.Yu. Soldatov[111], U. Soldevila[172], A.A. Solodkov[122], A. Soloshenko[78], O.V. Solovyanov[122], V. Solovyev[136], P. Sommer[147], H. Son[168], W. Song[142], W.Y. Song[166b], A. Sopczak[140], F. Sopkova[28b], C.L. Sotiropoulou[70a,70b], S. Sottocornola[69a,69b], R. Soualah[65a,65c,i], A.M. Soukharev[121b,121a], D. South[45], S. Spagnolo[66a,66b], M. Spalla[114], M. Spangenberg[176], F. Spanò[92], D. Sperlich[19], T.M. Spieker[60a], R. Spighi[23b], G. Spigo[35], L.A. Spiller[103], D.P. Spiteri[56], M. Spousta[141], A. Stabile[67a,67b], B.L. Stamas[120], R. Stamen[60a], M. Stamenkovic[119], S. Stamm[19], E. Stanecka[83], R.W. Stanek[6], B. Stanislaus[133], M.M. Stanitzki[45], B. Stapf[119], E.A. Starchenko[122], G.H. Stark[144], J. Stark[57], S.H Stark[39], P. Staroba[139], P. Starovoitov[60a], S. Stärz[102], R. Staszewski[83], G. Stavropoulos[43], M. Stegler[45], P. Steinberg[29], B. Stelzer[150], H.J. Stelzer[35], O. Stelzer-Chilton[166a], H. Stenzel[55], T.J. Stevenson[154], G.A. Stewart[35], M.C. Stockton[35], G. Stoicea[27b], M. Stolarski[138a], P. Stolte[52], S. Stonjek[114], A. Straessner[47], J. Strandberg[152], S. Strandberg[44a,44b], M. Strauss[126], P. Strizenec[28b], R. Ströhmer[175], D.M. Strom[129],

JHEP06(2019)144

R. Stroynowski[41], A. Strubig[49], S.A. Stucci[29], B. Stugu[17], J. Stupak[126], N.A. Styles[45], D. Su[151], S. Suchek[60a], Y. Sugaya[131], V.V. Sulin[109], M.J. Sullivan[89], D.M.S. Sultan[53], S. Sultansoy[4c], T. Sumida[84], S. Sun[104], X. Sun[3], K. Suruliz[154], C.J.E. Suster[155], M.R. Sutton[154], S. Suzuki[80], M. Svatos[139], M. Swiatlowski[36], S.P. Swift[2], A. Sydorenko[98], I. Sykora[28a], M. Sykora[141], T. Sykora[141], D. Ta[98], K. Tackmann[45,y], J. Taenzer[159], A. Taffard[169], R. Tafirout[166a], E. Tahirovic[91], H. Takai[29], R. Takashima[85], K. Takeda[81], T. Takeshita[148], Y. Takubo[80], M. Talby[100], A.A. Talyshev[121b,121a], J. Tanaka[161], M. Tanaka[163], R. Tanaka[130], B.B. Tannenwald[124], S. Tapia Araya[171], S. Tapprogge[98], A. Tarek Abouelfadl Mohamed[134], S. Tarem[158], G. Tarna[27b,e], G.F. Tartarelli[67a], P. Tas[141], M. Tasevsky[139], T. Tashiro[84], E. Tassi[40b,40a], A. Tavares Delgado[138a,138b], Y. Tayalati[34e], A.J. Taylor[49], G.N. Taylor[103], P.T.E. Taylor[103], W. Taylor[166b], A.S. Tee[88], R. Teixeira De Lima[151], P. Teixeira-Dias[92], H. Ten Kate[35], J.J. Teoh[119], S. Terada[80], K. Terashi[161], J. Terron[97], S. Terzo[14], M. Testa[50], R.J. Teuscher[165,ac], S.J. Thais[181], T. Theveneaux-Pelzer[45], F. Thiele[39], D.W. Thomas[92], J.P. Thomas[21], A.S. Thompson[56], P.D. Thompson[21], L.A. Thomsen[181], E. Thomson[135], Y. Tian[38], R.E. Ticse Torres[52], V.O. Tikhomirov[109,ao], Yu.A. Tikhonov[121b,121a], S. Timoshenko[111], P. Tipton[181], S. Tisserant[100], K. Todome[163], S. Todorova-Nova[5], S. Todt[47], J. Tojo[86], S. Tokár[28a], K. Tokushuku[80], E. Tolley[124], K.G. Tomiwa[32c], M. Tomoto[116], L. Tompkins[151,q], K. Toms[117], B. Tong[58], P. Tornambe[51], E. Torrence[129], H. Torres[47], E. Torró Pastor[146], C. Tosciri[133], J. Toth[100,ab], D.R. Tovey[147], C.J. Treado[123], T. Trefzger[175], F. Tresoldi[154], A. Tricoli[29], I.M. Trigger[166a], S. Trincaz-Duvoid[134], W. Trischuk[165], B. Trocmé[57], A. Trofymov[130], C. Troncon[67a], M. Trovatelli[174], F. Trovato[154], L. Truong[32b], M. Trzebinski[83], A. Trzupek[83], F. Tsai[45], J.C-L. Tseng[133], P.V. Tsiareshka[106,ai], A. Tsirigotis[160], N. Tsirintanis[9], V. Tsiskaridze[153], E.G. Tskhadadze[157a], M. Tsopoulou[160], I.I. Tsukerman[110], V. Tsulaia[18], S. Tsuno[80], D. Tsybychev[153,164], Y. Tu[62b], A. Tudorache[27b], V. Tudorache[27b], T.T. Tulbure[27a], A.N. Tuna[58], S. Turchikhin[78], D. Turgeman[178], I. Turk Cakir[4b,t], R.J. Turner[21], R.T. Turra[67a], P.M. Tuts[38], S Tzamarias[160], E. Tzovara[98], G. Ucchielli[46], I. Ueda[80], M. Ughetto[44a,44b], F. Ukegawa[167], G. Unal[35], A. Undrus[29], G. Unel[169], F.C. Ungaro[103], Y. Unno[80], K. Uno[161], J. Urban[28b], P. Urquijo[103], G. Usai[8], J. Usui[80], L. Vacavant[100], V. Vacek[140], B. Vachon[102], K.O.H. Vadla[132], A. Vaidya[93], C. Valderanis[113], E. Valdes Santurio[44a,44b], M. Valente[53], S. Valentinetti[23b,23a], A. Valero[172], L. Valéry[45], R.A. Vallance[21], A. Vallier[5], J.A. Valls Ferrer[172], T.R. Van Daalen[14], P. Van Gemmeren[6], I. Van Vulpen[119], M. Vanadia[72a,72b], W. Vandelli[35], A. Vaniachine[164], R. Vari[71a], E.W. Varnes[7], C. Varni[54b,54a], T. Varol[41], D. Varouchas[130], K.E. Varvell[155], G.A. Vasquez[145b], J.G. Vasquez[181], F. Vazeille[37], D. Vazquez Furelos[14], T. Vazquez Schroeder[35], J. Veatch[52], V. Vecchio[73a,73b], L.M. Veloce[165], F. Veloso[138a,138c], S. Veneziano[71a], A. Ventura[66a,66b], N. Venturi[35], A. Verbytskyi[114], V. Vercesi[69a], M. Verducci[73a,73b], C.M. Vergel Infante[77], C. Vergis[24], W. Verkerke[119], A.T. Vermeulen[119], J.C. Vermeulen[119], M.C. Vetterli[150,av], N. Viaux Maira[145b], M. Vicente Barreto Pinto[53], I. Vichou[171,*], T. Vickey[147], O.E. Vickey Boeriu[147], G.H.A. Viehhauser[133], L. Vigani[133], M. Villa[23b,23a], M. Villaplana Perez[67a,67b], E. Vilucchi[50], M.G. Vincter[33], V.B. Vinogradov[78], A. Vishwakarma[45], C. Vittori[23b,23a], I. Vivarelli[154], M. Vogel[180], P. Vokac[140], G. Volpi[14], S.E. von Buddenbrock[32c], E. Von Toerne[24], V. Vorobel[141], K. Vorobev[111], M. Vos[172], J.H. Vossebeld[89], N. Vranjes[16], M. Vranjes Milosavljevic[16], V. Vrba[140], M. Vreeswijk[119], T. Šfiligoj[90], R. Vuillermet[35], I. Vukotic[36], T. Ženiš[28a], L. Živković[16], P. Wagner[24], W. Wagner[180], J. Wagner-Kuhr[113], H. Wahlberg[87], S. Wahrmund[47], K. Wakamiya[81], V.M. Walbrecht[114], J. Walder[88], R. Walker[113], S.D. Walker[92], W. Walkowiak[149], V. Wallangen[44a,44b], A.M. Wang[58], C. Wang[59b], F. Wang[179], H. Wang[18], H. Wang[3], J. Wang[155], J. Wang[60b], P. Wang[41], Q. Wang[126], R.-J. Wang[134], R. Wang[59a], R. Wang[6], S.M. Wang[156], W.T. Wang[59a], W. Wang[15c,ad], W.X. Wang[59a,ad], Y. Wang[59a,al], Z. Wang[59c], C. Wanotayaroj[45],

JHEP06(2019)144

A. Warburton[102], C.P. Ward[31], D.R. Wardrope[93], A. Washbrook[49], A.T. Watson[21], M.F. Watson[21], G. Watts[146], B.M. Waugh[93], A.F. Webb[11], S. Webb[98], C. Weber[181], M.S. Weber[20], S.A. Weber[33], S.M. Weber[60a], A.R. Weidberg[133], J. Weingarten[46], M. Weirich[98], C. Weiser[51], P.S. Wells[35], T. Wenaus[29], T. Wengler[35], S. Wenig[35], N. Wermes[24], M.D. Werner[77], P. Werner[35], M. Wessels[60a], T.D. Weston[20], K. Whalen[129], N.L. Whallon[146], A.M. Wharton[88], A.S. White[104], A. White[8], M.J. White[1], R. White[145b], D. Whiteson[169], B.W. Whitmore[88], F.J. Wickens[142], W. Wiedenmann[179], M. Wielers[142], C. Wiglesworth[39], L.A.M. Wiik-Fuchs[51], F. Wilk[99], H.G. Wilkens[35], L.J. Wilkins[92], H.H. Williams[135], S. Williams[31], C. Willis[105], S. Willocq[101], J.A. Wilson[21], I. Wingerter-Seez[5], E. Winkels[154], F. Winklmeier[129], O.J. Winston[154], B.T. Winter[51], M. Wittgen[151], M. Wobisch[94], A. Wolf[98], T.M.H. Wolf[119], R. Wolff[100], J. Wollrath[51], M.W. Wolter[83], H. Wolters[138a,138c], V.W.S. Wong[173], N.L. Woods[144], S.D. Worm[21], B.K. Wosiek[83], K.W. Woźniak[83], K. Wraight[56], S.L. Wu[179], X. Wu[53], Y. Wu[59a], T.R. Wyatt[99], B.M. Wynne[49], S. Xella[39], Z. Xi[104], L. Xia[176], D. Xu[15a], H. Xu[59a,e], L. Xu[29], T. Xu[143], W. Xu[104], Z. Xu[151], B. Yabsley[155], S. Yacoob[32a], K. Yajima[131], D.P. Yallup[93], D. Yamaguchi[163], Y. Yamaguchi[163], A. Yamamoto[80], T. Yamanaka[161], F. Yamane[81], M. Yamatani[161], T. Yamazaki[161], Y. Yamazaki[81], Z. Yan[25], H.J. Yang[59c,59d], H.T. Yang[18], S. Yang[76], Y. Yang[161], Z. Yang[17], W-M. Yao[18], Y.C. Yap[45], Y. Yasu[80], E. Yatsenko[59c,59d], J. Ye[41], S. Ye[29], I. Yeletskikh[78], E. Yigitbasi[25], E. Yildirim[98], K. Yorita[177], K. Yoshihara[135], C.J.S. Young[35], C. Young[151], J. Yu[77], X. Yue[60a], S.P.Y. Yuen[24], B. Zabinski[83], G. Zacharis[10], E. Zaffaroni[53], R. Zaidan[14], A.M. Zaitsev[122,an], T. Zakareishvili[157b], N. Zakharchuk[33], S. Zambito[58], D. Zanzi[35], D.R. Zaripovas[56], S.V. Zeißner[46], C. Zeitnitz[180], G. Zemaityte[133], J.C. Zeng[171], O. Zenin[122], D. Zerwas[130], M. Zgubič[133], D.F. Zhang[15b], F. Zhang[179], G. Zhang[59a], G. Zhang[15b], H. Zhang[15c], J. Zhang[6], L. Zhang[15c], L. Zhang[59a], M. Zhang[171], R. Zhang[59a], R. Zhang[24], X. Zhang[59b], Y. Zhang[15d], Z. Zhang[62a], Z. Zhang[130], P. Zhao[48], Y. Zhao[59b], Z. Zhao[59a], A. Zhemchugov[78], Z. Zheng[104], D. Zhong[171], B. Zhou[104], C. Zhou[179], M.S. Zhou[15d], M. Zhou[153], N. Zhou[59c], Y. Zhou[7], C.G. Zhu[59b], H.L. Zhu[59a], H. Zhu[15a], J. Zhu[104], Y. Zhu[59a], X. Zhuang[15a], K. Zhukov[109], V. Zhulanov[121b,121a], D. Zieminska[64], N.I. Zimine[78], S. Zimmermann[51], Z. Zinonos[114], M. Ziolkowski[149], G. Zobernig[179], A. Zoccoli[23b,23a], K. Zoch[52], T.G. Zorbas[147], R. Zou[36], L. Zwalinski[35]

[1] *Department of Physics, University of Adelaide, Adelaide; Australia*
[2] *Physics Department, SUNY Albany, Albany NY; United States of America*
[3] *Department of Physics, University of Alberta, Edmonton AB; Canada*
[4] [(a)] *Department of Physics, Ankara University, Ankara;* [(b)] *Istanbul Aydin University, Istanbul;* [(c)] *Division of Physics, TOBB University of Economics and Technology, Ankara; Turkey*
[5] *LAPP, Université Grenoble Alpes, Université Savoie Mont Blanc, CNRS/IN2P3, Annecy; France*
[6] *High Energy Physics Division, Argonne National Laboratory, Argonne IL; United States of America*
[7] *Department of Physics, University of Arizona, Tucson AZ; United States of America*
[8] *Department of Physics, University of Texas at Arlington, Arlington TX; United States of America*
[9] *Physics Department, National and Kapodistrian University of Athens, Athens; Greece*
[10] *Physics Department, National Technical University of Athens, Zografou; Greece*
[11] *Department of Physics, University of Texas at Austin, Austin TX; United States of America*
[12] [(a)] *Bahcesehir University, Faculty of Engineering and Natural Sciences, Istanbul;* [(b)] *Istanbul Bilgi University, Faculty of Engineering and Natural Sciences, Istanbul;* [(c)] *Department of Physics, Bogazici University, Istanbul;* [(d)] *Department of Physics Engineering, Gaziantep University, Gaziantep; Turkey*
[13] *Institute of Physics, Azerbaijan Academy of Sciences, Baku; Azerbaijan*
[14] *Institut de Física d'Altes Energies (IFAE), Barcelona Institute of Science and Technology, Barcelona; Spain*

JHEP06(2019)144

[15] [(a)] Institute of High Energy Physics, Chinese Academy of Sciences, Beijing;[(b)] Physics Department, Tsinghua University, Beijing;[(c)] Department of Physics, Nanjing University, Nanjing;[(d)] University of Chinese Academy of Science (UCAS), Beijing; China
[16] Institute of Physics, University of Belgrade, Belgrade; Serbia
[17] Department for Physics and Technology, University of Bergen, Bergen; Norway
[18] Physics Division, Lawrence Berkeley National Laboratory and University of California, Berkeley CA; United States of America
[19] Institut für Physik, Humboldt Universität zu Berlin, Berlin; Germany
[20] Albert Einstein Center for Fundamental Physics and Laboratory for High Energy Physics, University of Bern, Bern; Switzerland
[21] School of Physics and Astronomy, University of Birmingham, Birmingham; United Kingdom
[22] Facultad de Ciencias y Centro de Investigaciónes, Universidad Antonio Nariño, Bogota; Colombia
[23] [(a)] INFN Bologna and Universita' di Bologna, Dipartimento di Fisica;[(b)] INFN Sezione di Bologna; Italy
[24] Physikalisches Institut, Universität Bonn, Bonn; Germany
[25] Department of Physics, Boston University, Boston MA; United States of America
[26] Department of Physics, Brandeis University, Waltham MA; United States of America
[27] [(a)] Transilvania University of Brasov, Brasov;[(b)] Horia Hulubei National Institute of Physics and Nuclear Engineering, Bucharest;[(c)] Department of Physics, Alexandru Ioan Cuza University of Iasi, Iasi;[(d)] National Institute for Research and Development of Isotopic and Molecular Technologies, Physics Department, Cluj-Napoca;[(e)] University Politehnica Bucharest, Bucharest;[(f)] West University in Timisoara, Timisoara; Romania
[28] [(a)] Faculty of Mathematics, Physics and Informatics, Comenius University, Bratislava;[(b)] Department of Subnuclear Physics, Institute of Experimental Physics of the Slovak Academy of Sciences, Kosice; Slovak Republic
[29] Physics Department, Brookhaven National Laboratory, Upton NY; United States of America
[30] Departamento de Física, Universidad de Buenos Aires, Buenos Aires; Argentina
[31] Cavendish Laboratory, University of Cambridge, Cambridge; United Kingdom
[32] [(a)] Department of Physics, University of Cape Town, Cape Town;[(b)] Department of Mechanical Engineering Science, University of Johannesburg, Johannesburg;[(c)] School of Physics, University of the Witwatersrand, Johannesburg; South Africa
[33] Department of Physics, Carleton University, Ottawa ON; Canada
[34] [(a)] Faculté des Sciences Ain Chock, Réseau Universitaire de Physique des Hautes Energies — Université Hassan II, Casablanca;[(b)] Centre National de l'Energie des Sciences Techniques Nucleaires (CNESTEN), Rabat;[(c)] Faculté des Sciences Semlalia, Université Cadi Ayyad, LPHEA-Marrakech;[(d)] Faculté des Sciences, Université Mohamed Premier and LPTPM, Oujda;[(e)] Faculté des sciences, Université Mohammed V, Rabat; Morocco
[35] CERN, Geneva; Switzerland
[36] Enrico Fermi Institute, University of Chicago, Chicago IL; United States of America
[37] LPC, Université Clermont Auvergne, CNRS/IN2P3, Clermont-Ferrand; France
[38] Nevis Laboratory, Columbia University, Irvington NY; United States of America
[39] Niels Bohr Institute, University of Copenhagen, Copenhagen; Denmark
[40] [(a)] Dipartimento di Fisica, Università della Calabria, Rende;[(b)] INFN Gruppo Collegato di Cosenza, Laboratori Nazionali di Frascati; Italy
[41] Physics Department, Southern Methodist University, Dallas TX; United States of America
[42] Physics Department, University of Texas at Dallas, Richardson TX; United States of America
[43] National Centre for Scientific Research "Demokritos", Agia Paraskevi; Greece
[44] [(a)] Department of Physics, Stockholm University;[(b)] Oskar Klein Centre, Stockholm; Sweden
[45] Deutsches Elektronen-Synchrotron DESY, Hamburg and Zeuthen; Germany
[46] Lehrstuhl für Experimentelle Physik IV, Technische Universität Dortmund, Dortmund; Germany
[47] Institut für Kern- und Teilchenphysik, Technische Universität Dresden, Dresden; Germany
[48] Department of Physics, Duke University, Durham NC; United States of America

JHEP06(2019)144

[49] SUPA — School of Physics and Astronomy, University of Edinburgh, Edinburgh; United Kingdom
[50] INFN e Laboratori Nazionali di Frascati, Frascati; Italy
[51] Physikalisches Institut, Albert-Ludwigs-Universität Freiburg, Freiburg; Germany
[52] II. Physikalisches Institut, Georg-August-Universität Göttingen, Göttingen; Germany
[53] Département de Physique Nucléaire et Corpusculaire, Université de Genève, Genève; Switzerland
[54] [(a)] Dipartimento di Fisica, Università di Genova, Genova; [(b)] INFN Sezione di Genova; Italy
[55] II. Physikalisches Institut, Justus-Liebig-Universität Giessen, Giessen; Germany
[56] SUPA — School of Physics and Astronomy, University of Glasgow, Glasgow; United Kingdom
[57] LPSC, Université Grenoble Alpes, CNRS/IN2P3, Grenoble INP, Grenoble; France
[58] Laboratory for Particle Physics and Cosmology, Harvard University, Cambridge MA; United States of America
[59] [(a)] Department of Modern Physics and State Key Laboratory of Particle Detection and Electronics, University of Science and Technology of China, Hefei; [(b)] Institute of Frontier and Interdisciplinary Science and Key Laboratory of Particle Physics and Particle Irradiation (MOE), Shandong University, Qingdao; [(c)] School of Physics and Astronomy, Shanghai Jiao Tong University, KLPPAC-MoE, SKLPPC, Shanghai; [(d)] Tsung-Dao Lee Institute, Shanghai; China
[60] [(a)] Kirchhoff-Institut für Physik, Ruprecht-Karls-Universität Heidelberg, Heidelberg; [(b)] Physikalisches Institut, Ruprecht-Karls-Universität Heidelberg, Heidelberg; Germany
[61] Faculty of Applied Information Science, Hiroshima Institute of Technology, Hiroshima; Japan
[62] [(a)] Department of Physics, Chinese University of Hong Kong, Shatin, N.T., Hong Kong; [(b)] Department of Physics, University of Hong Kong, Hong Kong; [(c)] Department of Physics and Institute for Advanced Study, Hong Kong University of Science and Technology, Clear Water Bay, Kowloon, Hong Kong; China
[63] Department of Physics, National Tsing Hua University, Hsinchu; Taiwan
[64] Department of Physics, Indiana University, Bloomington IN; United States of America
[65] [(a)] INFN Gruppo Collegato di Udine, Sezione di Trieste, Udine; [(b)] ICTP, Trieste; [(c)] Dipartimento Politecnico di Ingegneria e Architettura, Università di Udine, Udine; Italy
[66] [(a)] INFN Sezione di Lecce; [(b)] Dipartimento di Matematica e Fisica, Università del Salento, Lecce; Italy
[67] [(a)] INFN Sezione di Milano; [(b)] Dipartimento di Fisica, Università di Milano, Milano; Italy
[68] [(a)] INFN Sezione di Napoli; [(b)] Dipartimento di Fisica, Università di Napoli, Napoli; Italy
[69] [(a)] INFN Sezione di Pavia; [(b)] Dipartimento di Fisica, Università di Pavia, Pavia; Italy
[70] [(a)] INFN Sezione di Pisa; [(b)] Dipartimento di Fisica E. Fermi, Università di Pisa, Pisa; Italy
[71] [(a)] INFN Sezione di Roma; [(b)] Dipartimento di Fisica, Sapienza Università di Roma, Roma; Italy
[72] [(a)] INFN Sezione di Roma Tor Vergata; [(b)] Dipartimento di Fisica, Università di Roma Tor Vergata, Roma; Italy
[73] [(a)] INFN Sezione di Roma Tre; [(b)] Dipartimento di Matematica e Fisica, Università Roma Tre, Roma; Italy
[74] [(a)] INFN-TIFPA; [(b)] Università degli Studi di Trento, Trento; Italy
[75] Institut für Astro- und Teilchenphysik, Leopold-Franzens-Universität, Innsbruck; Austria
[76] University of Iowa, Iowa City IA; United States of America
[77] Department of Physics and Astronomy, Iowa State University, Ames IA; United States of America
[78] Joint Institute for Nuclear Research, Dubna; Russia
[79] [(a)] Departamento de Engenharia Elétrica, Universidade Federal de Juiz de Fora (UFJF), Juiz de Fora; [(b)] Universidade Federal do Rio De Janeiro COPPE/EE/IF, Rio de Janeiro; [(c)] Universidade Federal de São João del Rei (UFSJ), São João del Rei; [(d)] Instituto de Física, Universidade de São Paulo, São Paulo; Brazil
[80] KEK, High Energy Accelerator Research Organization, Tsukuba; Japan
[81] Graduate School of Science, Kobe University, Kobe; Japan
[82] [(a)] AGH University of Science and Technology, Faculty of Physics and Applied Computer Science, Krakow; [(b)] Marian Smoluchowski Institute of Physics, Jagiellonian University, Krakow; Poland
[83] Institute of Nuclear Physics Polish Academy of Sciences, Krakow; Poland

JHEP06(2019)144

[84] Faculty of Science, Kyoto University, Kyoto; Japan
[85] Kyoto University of Education, Kyoto; Japan
[86] Research Center for Advanced Particle Physics and Department of Physics, Kyushu University, Fukuoka; Japan
[87] Instituto de Física La Plata, Universidad Nacional de La Plata and CONICET, La Plata; Argentina
[88] Physics Department, Lancaster University, Lancaster; United Kingdom
[89] Oliver Lodge Laboratory, University of Liverpool, Liverpool; United Kingdom
[90] Department of Experimental Particle Physics, Jožef Stefan Institute and Department of Physics, University of Ljubljana, Ljubljana; Slovenia
[91] School of Physics and Astronomy, Queen Mary University of London, London; United Kingdom
[92] Department of Physics, Royal Holloway University of London, Egham; United Kingdom
[93] Department of Physics and Astronomy, University College London, London; United Kingdom
[94] Louisiana Tech University, Ruston LA; United States of America
[95] Fysiska institutionen, Lunds universitet, Lund; Sweden
[96] Centre de Calcul de l'Institut National de Physique Nucléaire et de Physique des Particules (IN2P3), Villeurbanne; France
[97] Departamento de Física Teorica C-15 and CIAFF, Universidad Autónoma de Madrid, Madrid; Spain
[98] Institut für Physik, Universität Mainz, Mainz; Germany
[99] School of Physics and Astronomy, University of Manchester, Manchester; United Kingdom
[100] CPPM, Aix-Marseille Université, CNRS/IN2P3, Marseille; France
[101] Department of Physics, University of Massachusetts, Amherst MA; United States of America
[102] Department of Physics, McGill University, Montreal QC; Canada
[103] School of Physics, University of Melbourne, Victoria; Australia
[104] Department of Physics, University of Michigan, Ann Arbor MI; United States of America
[105] Department of Physics and Astronomy, Michigan State University, East Lansing MI; United States of America
[106] B.I. Stepanov Institute of Physics, National Academy of Sciences of Belarus, Minsk; Belarus
[107] Research Institute for Nuclear Problems of Byelorussian State University, Minsk; Belarus
[108] Group of Particle Physics, University of Montreal, Montreal QC; Canada
[109] P.N. Lebedev Physical Institute of the Russian Academy of Sciences, Moscow; Russia
[110] Institute for Theoretical and Experimental Physics of the National Research Centre Kurchatov Institute, Moscow; Russia
[111] National Research Nuclear University MEPhI, Moscow; Russia
[112] D.V. Skobeltsyn Institute of Nuclear Physics, M.V. Lomonosov Moscow State University, Moscow; Russia
[113] Fakultät für Physik, Ludwig-Maximilians-Universität München, München; Germany
[114] Max-Planck-Institut für Physik (Werner-Heisenberg-Institut), München; Germany
[115] Nagasaki Institute of Applied Science, Nagasaki; Japan
[116] Graduate School of Science and Kobayashi-Maskawa Institute, Nagoya University, Nagoya; Japan
[117] Department of Physics and Astronomy, University of New Mexico, Albuquerque NM; United States of America
[118] Institute for Mathematics, Astrophysics and Particle Physics, Radboud University Nijmegen/Nikhef, Nijmegen; Netherlands
[119] Nikhef National Institute for Subatomic Physics and University of Amsterdam, Amsterdam; Netherlands
[120] Department of Physics, Northern Illinois University, DeKalb IL; United States of America
[121] [(a)] Budker Institute of Nuclear Physics and NSU, SB RAS, Novosibirsk;[(b)] Novosibirsk State University Novosibirsk; Russia
[122] Institute for High Energy Physics of the National Research Centre Kurchatov Institute, Protvino; Russia
[123] Department of Physics, New York University, New York NY; United States of America

JHEP06(2019)144

[124] Ohio State University, Columbus OH; United States of America
[125] Faculty of Science, Okayama University, Okayama; Japan
[126] Homer L. Dodge Department of Physics and Astronomy, University of Oklahoma, Norman OK; United States of America
[127] Department of Physics, Oklahoma State University, Stillwater OK; United States of America
[128] Palacký University, RCPTM, Joint Laboratory of Optics, Olomouc; Czech Republic
[129] Center for High Energy Physics, University of Oregon, Eugene OR; United States of America
[130] LAL, Université Paris-Sud, CNRS/IN2P3, Université Paris-Saclay, Orsay; France
[131] Graduate School of Science, Osaka University, Osaka; Japan
[132] Department of Physics, University of Oslo, Oslo; Norway
[133] Department of Physics, Oxford University, Oxford; United Kingdom
[134] LPNHE, Sorbonne Université, Paris Diderot Sorbonne Paris Cité, CNRS/IN2P3, Paris; France
[135] Department of Physics, University of Pennsylvania, Philadelphia PA; United States of America
[136] Konstantinov Nuclear Physics Institute of National Research Centre "Kurchatov Institute", PNPI, St. Petersburg; Russia
[137] Department of Physics and Astronomy, University of Pittsburgh, Pittsburgh PA; United States of America
[138] [(a)] Laboratório de Instrumentação e Física Experimental de Partículas — LIP;[(b)] Departamento de Física, Faculdade de Ciências, Universidade de Lisboa, Lisboa;[(c)] Departamento de Física, Universidade de Coimbra, Coimbra;[(d)] Centro de Física Nuclear da Universidade de Lisboa, Lisboa;[(e)] Departamento de Física, Universidade do Minho, Braga;[(f)] Universidad de Granada, Granada (Spain);[(g)] Dep Física and CEFITEC of Faculdade de Ciências e Tecnologia, Universidade Nova de Lisboa, Caparica; Portugal
[139] Institute of Physics of the Czech Academy of Sciences, Prague; Czech Republic
[140] Czech Technical University in Prague, Prague; Czech Republic
[141] Charles University, Faculty of Mathematics and Physics, Prague; Czech Republic
[142] Particle Physics Department, Rutherford Appleton Laboratory, Didcot; United Kingdom
[143] IRFU, CEA, Université Paris-Saclay, Gif-sur-Yvette; France
[144] Santa Cruz Institute for Particle Physics, University of California Santa Cruz, Santa Cruz CA; United States of America
[145] [(a)] Departamento de Física, Pontificia Universidad Católica de Chile, Santiago;[(b)] Departamento de Física, Universidad Técnica Federico Santa María, Valparaíso; Chile
[146] Department of Physics, University of Washington, Seattle WA; United States of America
[147] Department of Physics and Astronomy, University of Sheffield, Sheffield; United Kingdom
[148] Department of Physics, Shinshu University, Nagano; Japan
[149] Department Physik, Universität Siegen, Siegen; Germany
[150] Department of Physics, Simon Fraser University, Burnaby BC; Canada
[151] SLAC National Accelerator Laboratory, Stanford CA; United States of America
[152] Physics Department, Royal Institute of Technology, Stockholm; Sweden
[153] Departments of Physics and Astronomy, Stony Brook University, Stony Brook NY; United States of America
[154] Department of Physics and Astronomy, University of Sussex, Brighton; United Kingdom
[155] School of Physics, University of Sydney, Sydney; Australia
[156] Institute of Physics, Academia Sinica, Taipei; Taiwan
[157] [(a)] E. Andronikashvili Institute of Physics, Iv. Javakhishvili Tbilisi State University, Tbilisi;[(b)] High Energy Physics Institute, Tbilisi State University, Tbilisi; Georgia
[158] Department of Physics, Technion, Israel Institute of Technology, Haifa; Israel
[159] Raymond and Beverly Sackler School of Physics and Astronomy, Tel Aviv University, Tel Aviv; Israel
[160] Department of Physics, Aristotle University of Thessaloniki, Thessaloniki; Greece
[161] International Center for Elementary Particle Physics and Department of Physics, University of Tokyo, Tokyo; Japan

JHEP06(2019)144

[162] Graduate School of Science and Technology, Tokyo Metropolitan University, Tokyo; Japan
[163] Department of Physics, Tokyo Institute of Technology, Tokyo; Japan
[164] Tomsk State University, Tomsk; Russia
[165] Department of Physics, University of Toronto, Toronto ON; Canada
[166] [(a)] TRIUMF, Vancouver BC; [(b)] Department of Physics and Astronomy, York University, Toronto ON; Canada
[167] Division of Physics and Tomonaga Center for the History of the Universe, Faculty of Pure and Applied Sciences, University of Tsukuba, Tsukuba; Japan
[168] Department of Physics and Astronomy, Tufts University, Medford MA; United States of America
[169] Department of Physics and Astronomy, University of California Irvine, Irvine CA; United States of America
[170] Department of Physics and Astronomy, University of Uppsala, Uppsala; Sweden
[171] Department of Physics, University of Illinois, Urbana IL; United States of America
[172] Instituto de Física Corpuscular (IFIC), Centro Mixto Universidad de Valencia — CSIC, Valencia; Spain
[173] Department of Physics, University of British Columbia, Vancouver BC; Canada
[174] Department of Physics and Astronomy, University of Victoria, Victoria BC; Canada
[175] Fakultät für Physik und Astronomie, Julius-Maximilians-Universität Würzburg, Würzburg; Germany
[176] Department of Physics, University of Warwick, Coventry; United Kingdom
[177] Waseda University, Tokyo; Japan
[178] Department of Particle Physics, Weizmann Institute of Science, Rehovot; Israel
[179] Department of Physics, University of Wisconsin, Madison WI; United States of America
[180] Fakultät für Mathematik und Naturwissenschaften, Fachgruppe Physik, Bergische Universität Wuppertal, Wuppertal; Germany
[181] Department of Physics, Yale University, New Haven CT; United States of America
[182] Yerevan Physics Institute, Yerevan; Armenia

[a] Also at Borough of Manhattan Community College, City University of New York, NY; United States of America
[b] Also at California State University, East Bay; United States of America
[c] Also at Centre for High Performance Computing, CSIR Campus, Rosebank, Cape Town; South Africa
[d] Also at CERN, Geneva; Switzerland
[e] Also at CPPM, Aix-Marseille Université, CNRS/IN2P3, Marseille; France
[f] Also at Département de Physique Nucléaire et Corpusculaire, Université de Genève, Genève; Switzerland
[g] Also at Departament de Fisica de la Universitat Autonoma de Barcelona, Barcelona; Spain
[h] Also at Departamento de Física, Instituto Superior Técnico, Universidade de Lisboa, Lisboa; Portugal
[i] Also at Department of Applied Physics and Astronomy, University of Sharjah, Sharjah; United Arab Emirates
[j] Also at Department of Financial and Management Engineering, University of the Aegean, Chios; Greece
[k] Also at Department of Physics and Astronomy, University of Louisville, Louisville, KY; United States of America
[l] Also at Department of Physics and Astronomy, University of Sheffield, Sheffield; United Kingdom
[m] Also at Department of Physics, California State University, Fresno CA; United States of America
[n] Also at Department of Physics, California State University, Sacramento CA; United States of America
[o] Also at Department of Physics, King's College London, London; United Kingdom
[p] Also at Department of Physics, St. Petersburg State Polytechnical University, St. Petersburg; Russia

JHEP06(2019)144

[q] Also at Department of Physics, Stanford University, Stanford CA; United States of America
[r] Also at Department of Physics, University of Fribourg, Fribourg; Switzerland
[s] Also at Department of Physics, University of Michigan, Ann Arbor MI; United States of America
[t] Also at Giresun University, Faculty of Engineering, Giresun; Turkey
[u] Also at Graduate School of Science, Osaka University, Osaka; Japan
[v] Also at Hellenic Open University, Patras; Greece
[w] Also at Horia Hulubei National Institute of Physics and Nuclear Engineering, Bucharest; Romania
[x] Also at Institucio Catalana de Recerca i Estudis Avancats, ICREA, Barcelona; Spain
[y] Also at Institut für Experimentalphysik, Universität Hamburg, Hamburg; Germany
[z] Also at Institute for Mathematics, Astrophysics and Particle Physics, Radboud University Nijmegen/Nikhef, Nijmegen; Netherlands
[aa] Also at Institute for Nuclear Research and Nuclear Energy (INRNE) of the Bulgarian Academy of Sciences, Sofia; Bulgaria
[ab] Also at Institute for Particle and Nuclear Physics, Wigner Research Centre for Physics, Budapest; Hungary
[ac] Also at Institute of Particle Physics (IPP); Canada
[ad] Also at Institute of Physics, Academia Sinica, Taipei; Taiwan
[ae] Also at Institute of Physics, Azerbaijan Academy of Sciences, Baku; Azerbaijan
[af] Also at Institute of Theoretical Physics, Ilia State University, Tbilisi; Georgia
[ag] Also at Instituto de Física Teórica de la Universidad Autónoma de Madrid; Spain
[ah] Also at Istanbul University, Dept. of Physics, Istanbul; Turkey
[ai] Also at Joint Institute for Nuclear Research, Dubna; Russia
[aj] Also at LAL, Université Paris-Sud, CNRS/IN2P3, Université Paris-Saclay, Orsay; France
[ak] Also at Louisiana Tech University, Ruston LA; United States of America
[al] Also at LPNHE, Sorbonne Université, Paris Diderot Sorbonne Paris Cité, CNRS/IN2P3, Paris; France
[am] Also at Manhattan College, New York NY; United States of America
[an] Also at Moscow Institute of Physics and Technology State University, Dolgoprudny; Russia
[ao] Also at National Research Nuclear University MEPhI, Moscow; Russia
[ap] Also at Physics Dept, University of South Africa, Pretoria; South Africa
[aq] Also at Physikalisches Institut, Albert-Ludwigs-Universität Freiburg, Freiburg; Germany
[ar] Also at School of Physics, Sun Yat-sen University, Guangzhou; China
[as] Also at The City College of New York, New York NY; United States of America
[at] Also at The Collaborative Innovation Center of Quantum Matter (CICQM), Beijing; China
[au] Also at Tomsk State University, Tomsk, and Moscow Institute of Physics and Technology State University, Dolgoprudny; Russia
[av] Also at TRIUMF, Vancouver BC; Canada
[aw] Also at Universita di Napoli Parthenope, Napoli; Italy
[*] Deceased

JHEP06(2019)144